Diffusivity Studies in Fe-Cr alloys by Molecular Dynamics Simulations

A thesis submitted in partial fulfillment of the requirement for the degree of

Master of Technology

in

Mechanical Engineering

With specialization

STEEL TECHNOLOGY

By

NAVRATAN KUMAR

(Roll No- 212MM2338)

Department Metallurgical & Materials Engineering

National Institute of Technology

Rourkela-769008

May 2014

Diffusivity Studies in Fe- Cr alloys by Molecular Dynamics Simulations

A thesis submitted in partial fulfillment of the requirements for the degree of

Master of Technology

in

Mechanical Engineering

With specialization

STEEL TECHNOLOGY

By

NAVRATAN KUMAR

(212MM2338)

Under the guidance and supervision of

Dr. Natraj Yedla

Assistant Professor

Department of Metallurgical & Materials Engineering

National Institute of Technology

Rourkela-769008

May 2014

DEDICATED

TO

MY PARENTS

&

LORD MAHADEV

National Institute of Technology

Rourkela, Odisha

INDIA

CERTIFICATE

This is to certify that the thesis entitle "**Diffusivity studies in Fe-Cr alloys by Molecular dynamics simulations**" submitted by **Mr. NAVRATAN KUMAR (212MM2338)** in partial fulfillment of the requirements for the award of **Master of Technology** in specialization **Steel Technology** in the Department of **Mechanical Engineering** hostage in **Metallurgical & Materials Engineering** at **National Institute of Technology**, **Rourkela** is an authentic and bona fide work carried out by him under my guidance and supervision.

To the best of my knowledge, the research work assimilated in this thesis is based on candidate's own work and has not been submitted to any other university / institute for the award of any degree or diploma.

Date: ……..

Place: …….

Dr. Natraj Yedla

Dept. of Metallurgical and Materials Engineering

National Institute of Technology, Rourkela- 769008

ACKNOWLEDMENT

I take this opportunity to record our sincere thanks to **NIT Rourkela** for great support throughout my M. tech studies and providing its resources to me to work in such challenging environment.

Most likely, I expressed my heartiest obligation to my supervisor **Dr. N. Yedla** for their humble support, who given their valuable time and great attention toward my research work. I am great thankful to them who given me infantile knowledge of magnificent world of simulation and modeling. It was their great encouragement and effort that I am able to embarked upon career in academia. I would like to thanks them for all the time as they have spent with me explaining the concept and guide me in most prominent way. I would like to work with a person like him in coming future.

I place on record, my sincere gratitude to **Prof. B. C. Ray, HOD, Metallurgical & Materials engineering** for allowing us to use the department's facilities and for his valuable suggestion and encouragements extended to me.

I take this opportunity to record our sincere thanks to all the faculty members of the Department of Metallurgical & Materials engineering for their help and encouragement. I would like to thanks to all the staff members of department too. I also want to thanks my friends who have always encourage and helping in doing our work.

Finally, I would like to express my heartiest and deepest gratitude to my parents and my younger brothers for their unconditional love and encouragement. I would not rise up so high without their well wishes on my head.

Navratan Kumar (212MM2338)

Steel Technology

NIT Rourkela

ABSTRACT

Point-defect concentration and diffusivities are obtained from molecular dynamics (MD) simulations. It is found that self-diffusion in BCC-Fe is controlled by vacancy mechanism at all temperatures. The results obtained is due to the fact that the equilibrium vacancy concentration is always much larger than the equilibrium interstitial concentration. Molecular dynamics simulation is performed to study the self-diffusivities of BCC-Fe and Fe-Cr alloys with composition variation from 5%, 10%, 15%, 20% and 25% Cr respectively at temperature 50 K,100 K, 300 K, 500 K, 700 K, and 1000 K in box size of dimension $50\times50\times50$ $Å^3$. The temperature range has been divided into three parts: below room temperature (50 K and 100 K), above room temperature (300 K, 500 K, and 700 K) and 1000 K. This temperature range will describe better diffusivities of BCC Fe and Fe-Cr alloys system. Mean square displacement method is employed to calculate the diffusivity values of BCC-Fe and Fe-Cr alloy system. Slope of the MSD vs. timestep in the diffusive region gives the self-diffusivity values of the elements. The calculated diffusivity value is in good agreement with other MD simulation and experimental data.

Keywords: point- defect, mean square displacement, molecular dynamics simulation, embedded-atom-method, LAMMPS, pure Fe, Fe-Cr alloys

CONTENTS

LIST OF FIGURES

LIST OF TABLES

NOMENCLATURE

Symbols

K	Kelvin
Å	Angstrom
k	Boltzmann constant
Ps	picoseconds
T	Temperature
N	Total number of atomic site per mole
ΔE	Activation energy for formation of vacancy
n	Number of atomic site per mole
t	Simulation time
E_a	Activation energy
m^2	Square meter
c m^2	Square centimeter
s^{-1}	Per second
D_0	Pre-exponential constant
$D_A(T)$	Diffusion coefficient
H_f^V	Vacancy formation enthalpy
S_f^V	Vacancy formation entropy
F_i	Force acting on particle ‘i’
m_i	Mass of atom ‘i’
r_i	Position vector of atom ‘i’
E_i	Potential energy of an atom ‘i’

r_{ij}	Distance between atoms i and j
ρ_{β}	Electron charge density from atom j of β type at location of atom i
$\phi_{\alpha\beta}$	Pair-wise potential function
F	Embedding function

CHAPTER 1

Introduction

1. Introduction

1.1 Background

Fe-Cr alloys play an important role as a main constituent's element for the stainless steel. From the era of manufacturing and development of steel, stainless steel is classified into four major types: ferritic, martensitic, austenitic, and precipitation-hardened stainless steels. The main objectives for the invention of stainless steel to manufacture corrosion free steel. In 1912, two major types of stainless steel were discovered accidently just because of their corrosive behavior came into light [1]. H. Brearely discovered the ferritic stainless steel when he found difficulty in trying to etch gun barrels made from chromium steel. Secondly, austenitic stainless steel was discovered by E. Maurer in Germany when he noticed that certain chromium-nickel steels did not corroded even after placed in acid fumes environment. Steel considered as stainless must contain minimum under 12% Cr [2]. All the above four types of stainless steel have some amount of carbon content in their composition which is not desirable for binary Fe-Cr alloys as far Fe-Cr phase diagram [3] indicates.

In the present scenario Fe-Cr alloy preferred as a structural building material in the field of nuclear power generation. In this regards, diffusion plays an important role in the kinetics of many materials processes [4]. Experimental measurements of diffusion coefficients are expensive, difficult and in some cases nearly impossible. A complimentary approach is to determine diffusivities in materials by molecular dynamics (MD) simulations [5]. In addition to predicting diffusion coefficients, MD simulations can provide insights into atomic mechanisms of diffusion processes, creating a fundamental framework for materials design strategies through control of diffusion rates.

However much interest from both engineering and physical point of view, to know what kind of defects play major roles in phenomena related to radiation damage in materials. In particular, radiation-induced interstitial atoms, which have been reported to move very fast [6-7] will greatly affect the mechanical properties of materials by changing the growth and annihilation rates of radiation-induced defect clusters. Unfortunately only a few indirect methods such as measuring stress and magnetic relaxation as well as monitoring changes in residual resistivity and hardness have been available to estimate the behavior of defects that play roles at annealing stages after irradiation, and it is impossible to directly observe such small defects as self-interstitial atoms (SIAs) and vacancies in irradiated materials. Most promising methods overcoming this difficulty are theoretical calculations and atomistic simulations using proper interatomic potentials [8]. Using molecular-dynamics simulations, the present work aim is to measuring the diffusion coefficient of pure Fe and in Fe-Cr alloys under various temperatures.

1.2 Motivation for present studies

Since nuclear power plant is good source of power generation all over the world. However, radiation damage causes a serious factor in this field. So Fe-Cr alloy considered as a suitable material in designing the parts of fluid flowing system and pressure vessel where radiation damage mostly occurs. In literature survey, many works were carried out experimentally and computer simulation has been done related to these alloys. This work adds a link to whatever work has been done till now.

1.3 Research objective

- To study the self-diffusion in pure Fe and effect of temperature on diffusivity value.
- To study the effect of temperature and increasing Cr content on the diffusion in Fe-Cr alloys.

CHAPTER 2

Literature Review

2. Literature review

2.1. Introduction

In this section, material and terminology used in research is explained. The topics which are discuss as: Solid solution, alloys, Fe-Cr alloys system, point defects, diffusion, and mean square displacement (MSD). This chapter also takes an overview of different individual's work done on pure Fe and Fe-Cr system.

2.1.1. Solid solutions, Alloys and Fe-Cr alloys system

A solid solution is the solid state similar as liquid solution. Solid solution form when solute atoms are dissolved to a solvent. Solid solution is depending on the size of alloying elements. The dissolution may occur either substitutional solid solution or interstitial solid solution. Solute can be "substitute" as solvent atoms on lattice sites if the solute atoms are similar to the solvent (according to Hume-Rothery rules discuss below). If solute atoms are different (i.e. atomic radii differ by more than 15%, electro-negativities, coordination numbers are different) from the solvent, then an interstitial incorporation of solute atoms can occur where solute atoms occupies in between lattice sites, such as carbon atoms in steel. If solubility between solute and solvent is not present, then solute atoms may have a tendency to form cluster and trapped at defects within solvent (such as at grain boundaries and dislocations). If solubility is very low, then cluster behavior is predominated thermodynamically.

The currently steels (such as 304 stainless steel) used in reactors are incapable in handling the increased irradiation over long period of time, and at elevated temperature. They shows considerable swelling under higher temperature and radiation dose therefore new steels are required to build next generation nuclear reactor. The composition of present steel used in reactor is given below:

Table 2.1: Composition of 304 stainless steel [9]

Composition of SURV 304 Stainless Steel (given in weight percent)										
Material	C	Cr	Cu	Fe	Mn	Mo	Ni	P	S	Si
wt%	.08	18.38	.18	Bal.	.89	.21	10.0	.018	.020	.68

The noticeable factor to choose Fe-Cr alloys system is that the actual steel used have 10 alloying elements and modeling such a complex system is impossible in present time. Fe –Cr system will be faithful and easy to model that can add information about the behavior of Fe-Cr based steels useful for next generation reactor.

On the other way, elements in alloy can mix with base lattice matrix (α-Fe lattice in case of Fe-Cr system) in many ways. One common way that alloys elements can mix when alloying element occupies at lattice sites of host lattice. This is known as substitutional alloy since alloying

element is substituted to the original lattice atoms sites. The rule which describing whether two elements will form a substitutional alloy or not are called Hume-Rothery rules. These rule state as:

1. The radii of the host lattice atom and alloying element atom could not differ by more than 15%

2. The crystal structure of both elements must be same

3. The number of bonds of each element must be same

4. The electronegativity of each element must be similar

All the above rule of Hume-Rothery rules are satisfied by Fe and Cr in every aspect. Thus Fe-Cr system forms a substitutional alloy. The atomic radii of Fe and Cr are 1.27 Å and 1.28 Å, respectively. Both have body-centered cubic (bcc) crystal structure, and due to close appearance in periodic table, they have same valencies and electronegativities. The phase diagram of Fe-Cr alloys system is given below in Fig. 1. Here α phase of Fe-Cr system shows bcc crystal structure like α-Fe. The γ phase has a fcc structure which is more ductile and softer than bcc phase. Alternating layer of Cr and Fe are distinguished through σ phase [10]. This phase diagram show in units of mass (or weight) percent, and since Fe and Cr are so close in term of mass, mass percent and atomic percent that they may interchanged with minor error. The sigma (σ) phase located at bottom center is not having bcc structure. It has some different structure that turns out to be quit brittle, and consequently avoided because of higher Cr wt%, that is not under this investigation. The atomic percent used in this research work range from 0at% Cr (pure α-Fe) to 25at% Cr in the temperature range of 50 K-1000 K. 50 K and 100 K temperature are examined to check the diffusion behavior of Fe-Cr system. Apart from this temperature, 300 K-1000 K temperature have only bcc α phase. With 0wt% Cr to 15wt% Cr, γ phase appear only after ~850°C till ~1400°C. The melting temperature of Fe and Cr are 1538°C and 1907°C respectively.

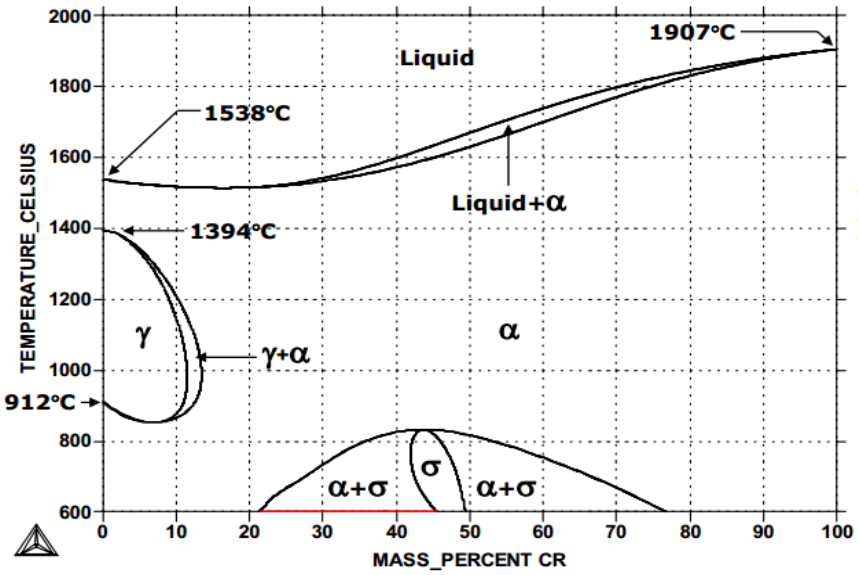

Fig.2.1 Iron –Chromium Phase diagram [11]

2.1.2. Point Defects

Point defects are lattice imperfection that occurs to the lattice site. These defects are classified as vacancies, interstitial, or substitutional. When point defects get introduced in crystal lattice, internal energy of the crystal increases. At equilibrium, the fraction of lattice that are vacant at a given temperature is given approximately by the Eq.

$$\frac{n}{N} = e^{-\Delta E/kT}$$

Where n= number of vacancies per mole

N= total number of atomic site per mole

ΔE = activation energy for formation of vacancy

K =Boltzmann constant

T = Temperature

When a lattice atom is removed from its position, the empty lattice position left behind is called a vacancy. Vacancies play a great role in diffusion of atoms in crystal lattice. They help in transport of atoms. Vacancies arise from thermal vibrations. The activation energy responsible for diffusion is the sum of the energy required to form a vacancy and the energy to move the vacancy. They also introduced during solidification. There is slight distortion in lattice planes due to vacancy because atoms surrounding a vacancy have tendency to come closer.

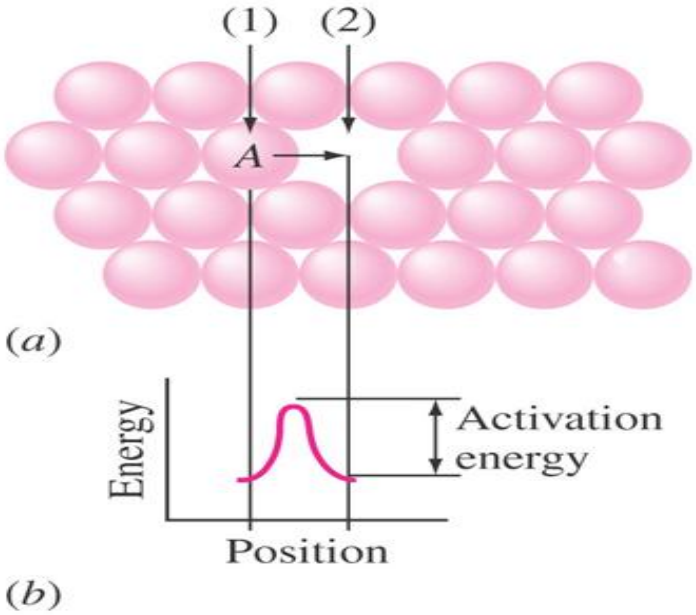

Fig.2.2 show vacancy mechanism helps in diffusion

Substitutional defects are former to the vacancies that have been occupied by non-lattice atoms. For example Cr atom is attracted to the vacancies in Fe-Cr system and tries to occupy vacant site whenever possible. Thus substitutional diffusion rate depends on number of vacancies, temperature, and activation energy to exchange. Substitutional defect may occur by small or larger atom than the original lattice atom.

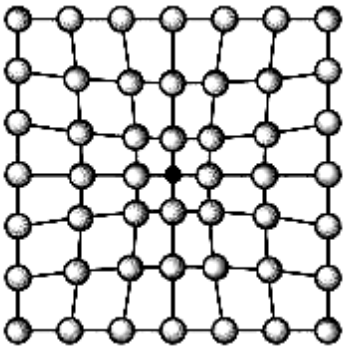

Fig.2.3 (a) Small substitutional atom

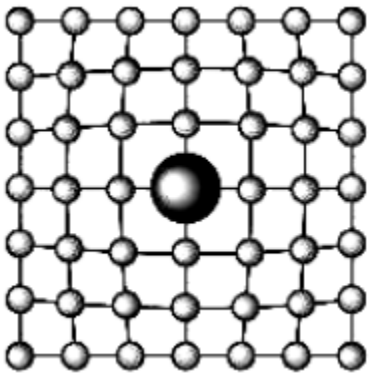

Fig.2.3 (b) Larger substitutional atom

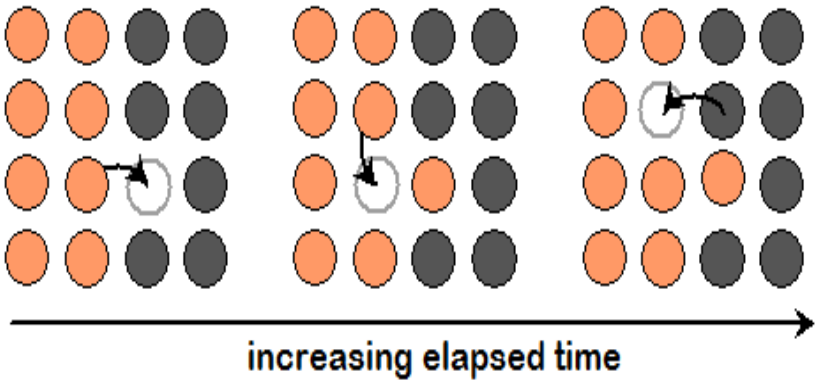

Fig.2.3 (c) show substitutional defect mechanism in diffusion

A point defect produced when an atom is placed into the crystal at a site that is normally not a lattice point. Also an "alien" atom (such as C) in one of the interstitials in a structure. An interstitial view of an foreign atom is shown in figure.

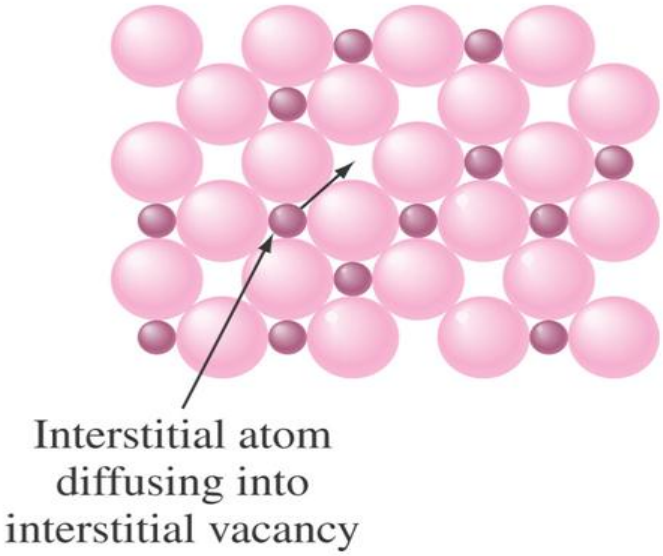

Fig.2.4 Show the interstitial atom diffusing into interstitial site

2.1.3. Calculation of diffusivity in point defects

The diffusivity D_A^* of an atom A in a virtual specimen of alloy can be calculated by Einstein's random-walk law [12]:

$$D_A^*(T) = \frac{\langle R^2(t) \rangle (T)}{6t} \quad \ldots\ldots\ldots\ldots\ldots\ldots (1)$$

Where t is the simulation time and $\langle R^2(t)\rangle(T)$ is the time increasing mean square displacement (MSD) of diffusing A atoms, that is calculated from MD simulation after running the code equilibrated at certain temperature T. vacancy concentration used in simulation, C_V^* is assured higher as comparable to equilibrium concentration at T, $D_A(T) = D_O \bullet e^{\frac{-E_a}{kT}}$. Hence, the diffusion coefficient $D_A(T)$ can be compared with experimental data, $D_A^*(T)$ has to be corrected by a factor $C_V^{eq}(T)/C_V^*$. Here $C_V^{eq}(T) = \exp[-(H_f^V - TS_f^V)K_S T]$, where K_S is Boltzmann constant and H_f^V, S_f^V are, respectively the vacancy formation enthalpy and entropy. By repeating the calculation symbolized by Eq. (1) at different temperature (to which atom block was equilibrated) and applying the correction factor, the Arrhenius plot of the diffusion coefficient is obtained and, by interpolating with expression [13]

$$D_A(T) = D_O \bullet e^{\frac{-E_a}{kT}} \quad \ldots\ldots\ldots\ldots\ldots\ldots\ldots\ldots (2)$$

both prefactor D_o and E_a as predicted by potential can be determined and compared with experimental data.

2.1.4. EAM potential used for Fe and Fe-Cr alloys to calculate diffusivity value

Mikhail I. Mendelev et al. [14] studied about interatomic interactions in bcc Fe through semi empirical interatomic potential developed as mention by G. J.Ackland et al. [15]. They study by calculating the equilibrium lattice parameter as a function of temperature. Simulation box contains 2,000 atom and periodic boundary conditions were employed. At a given temperature, NVT (constant number of atoms, volume, and temperature) ensembles selected to run MD code at several densities. After system equilibration with 20,000 MD steps (1 MD step= 2fs), statistics of pressure was collected in next 20,000 steps. In their work, diffusivity value calculated in bcc Fe through two different mechanisms of self-diffusion: one mediated by migration of vacancies and other by migration of self-interstitials. They found that self-diffusion in bcc Fe is controlled by vacancy mechanism at all temperatures.

Katsuyuki et al. [16] worked on α-Fe. They employed an embedded-atom-method (EAM) interatomic potential that was proposed by Haftel et al. [17] for the construction of non-magnetic α-Fe crystals. In order to obtained diffusion coefficient of SIA in α-Fe crystal, crystals sized 223 (21296 atoms contained) in a units of lattice parameter, were annealed for about 10 ns at fixed temperatures from 250 K to 1300 K. The interatomic potential used in the calculation was developed to reproduce only the properties of non-magnetic bcc iron.

H. Chamati *et al* [18] The EAM potential was used to determine Fe properties at finite temperatures. They performed MD simulations in the canonical ensemble (NVT), using a system

of 4500 atoms arranged on BCC or FCC lattices. The simulation boxes contained 20 layers with 225 atoms each, with periodic boundary conditions in all three directions. They performed MD runs of 10–50 ns (depending on the temperature) in the temperature range of 600–950 K. Below 600 K the number of diffusion events is too small to obtain any realistic statistics. The temperature dependence of the diffusion coefficients for three diffusion mechanisms (hopping and two exchange processes) follows the Arrhenius behavior. The most important result is that the diagonal exchange diffusion process is energetically favored over the direct hopping mechanism. Finally, they found that the diffusivity by the diagonal exchange mechanism is about an order of magnitude higher than that by the direct jump mechanism and by the non-diagonal exchange mechanism.

So far, self-diffusion in Fe-Cr binary alloys have been considered it is limited to Fe rich solid solution range that must be less than 20at%Cr[19] because higher Cr content are considerably brittle. For RAFM steels, the chromium content mainly range from 10 to 20 %. Molecular dynamics (MD) simulations employing two different Fe-Cr potentials are used to study the effect of 10% Cr on self interstitial and small interstitial cluster migration. Studies of the effect of Cr on displacement cascade evolution in Fe-Cr alloys have observed no effect on defect production [20, 21]. Although no differences were observed in the absolute number of defect formed, Cr may have an influence on the migration properties of point defect clusters that can influence eventual defect fate and produce a large effect on microstructural properties. Two different Fe-Cr interaction potentials [21] were used, which show different size effects of Cr in body-centered cubic (BCC) Fe matrix. In this work, MD simulations on the effect of Cr on single, di-, and tri-interstitial diffusion in Fe-10%Cr alloys was done. Simulations were also performed for Fe-1%Cr alloys; however effect of Cr at 1% concentration was minimal.
Resent work by Terentyev [22] has demonstrated decreased interstitial diffusivity in Fe-12%Cr based on EAM Fe-Cr potentials. Fe-Cr alloys of different concentrations (5%, 10%, and 20%) have been produced and validated [23,24]. In this work, their validation is extended by computing, via MD, the diffusivity of Fe and Cr atoms in a Fe-12%Cr alloy. This composition was chosen as the closest Cr concentration to RAFM steels for which experimental data of Cr diffusivity are available [25].
Ivanov and Ivanchev [26] studied in 1958 the diffusion of Cr51 and Fe59 in Fe-26-82.5 mass% Cr alloys in temperature range from 1313 to 1523 K .The objective of report is to (i) investigate the effect of Cr on point defect properties and microstructural evoluation in irradiated Fe-Cr alloys. The initial focus was on single interstitial and small interstitial cluster transport using MD simulations, (ii) to determine the tracer self-diffusion coefficient of Cr51 and Fe59 in the high purity Fe-50 mass% Cr alloy in a wide temperature range across 1103 K.

Table 2.2: shows the diffusivity values of 12%, 10%, 1% Chromium content based on MD simulation and experimental work has been observed from literature listed in column given.

Alloy composition	Potential	study	Activation energy E_a (eV)	Diffusivity value D_0 (cm^2/s)	Paper
Fe-12% Cr	5.16	a)atomic diffusion via vacancy mechanism b)interstitial diffusion	Cr 2.39 Fe 2.54 0.063	1.117 2.117 3.03×10^{-4}	[27]
Fe-10%C	Fe-Cr I Fe-Cr II	Single interstitial Di-interstitial Tri-interstitial Single interstitial Di-interstitial Tri-interstitial	0.22 0.11 0.12 0.24 0.10 0.10	9.4×10^{-5} 6.5×10^{-3} 6.3×10^{-4} 9.6×10^{-3} 6.0×10^{-4} 7.3×10^{-4}	[28]
Fe-1%Cr	Fe-Cr I Fe-Cr II	Single interstitial Di-interstitial Tri-interstitial Single interstitial Di-interstitial Tri-interstitial	0.06 0.06 0.05 0.11 0.16 0.03	1.1×10^{-3} 9.6×10^{-4} 2.5×10^{-4} 2.4×10^{-3} 5.7×10^{-3} 5.6×10^{-3}	[28]

Table 2.3: self-diffusion coefficient of Cr51 and Fe59 in Fe-50mass%Cr [29]

T (K)	t (ks)	D_{Cr} ($m^2\ s^{-1}$)	D_{Fe} ($m^2\ s^{-1}$)
1273	3.0	3.36×10^{-15}	3.30×10^{-15}
1223	3.6	8.78×10^{-16}	—
1173	3.6	2.93×10^{-16}	4.59×10^{-16}
1123	7.2	1.12×10^{-16}	1.71×10^{-16}
1073	27	3.51×10^{-17}	4.41×10^{-17}
1023	171	9.30×10^{-18}	—
973	325.8	1.75×10^{-18}	—
923	422.6	3.26×10^{-19}	—

CHAPTER 3

Theory & Computational Methodology

3. Theory & Computational Methodology

3.1. Introduction to Classical Molecular Dynamics Simulation

Classical Molecular dynamics (MD) is a computer simulation technique which give an idea about the time evolution of a group of interacting atoms and molecules organized in a system is followed by integrating their equation of motion. The word "classical" itself indicate that the core motion of the constituent particles obeys the laws of classical mechanics. The paths followed by interacting particles are solely determined by solving Newton's equation of motion where forces acting between the particles and potential energy are defined by molecular mechanics force field. MD simulations generate information at the microscopic level i.e. atomic position, velocities, and forces. As far history concern about Classical Molecular dynamics method as it was first introduced by Alder and Wainwright in the late 1950's and it was the first molecular dynamics study about the interaction of 500 hard sphere [30]. Many important insights concerning the behavior of simple liquids emerged from their studies. However, in 1964 , Rahman carried out the first simulation using a realistic potential for liquid argon in which investigation done on the particles motion of individual atoms [31]. Now a day MD simulation focusing towards biophysics problems, fracture, deformation studies of nano-composite material and many more area is routine. MD simulation is an effective way to investigate various properties of elements incorporated in a system at macroscopic level [32]. This is what we can say that objective of MD simulation of atomic & molecular system is to conversion of microscopic interaction to macroscopic behavior like pressure, stress tensor, strain tensor, energy etc. Some of the main strengths of MD simulation [33] which stand it better in position other than experimental work as (1) it is relatively easy to implement (2) exact dynamics for the chosen interatomic potential (no assumption of on-lattice behavior, known mechanisms, or thermal behavior) (3) very accurate compared to experiment, if potential is accurate, after the thermal spike stage (> ~1ps) (4) can probe behavior that is unavailable from experiment (5) some properties are relatively insensitive to the material, and hence are insensitive to errors in potential. For these properties, MD can provide meaningful, general results even with a cheap potential. Some limitation are also held with molecular simulation and modeling [33] i.e.(1) Time scale – currently limited to nanoseconds (2) it is only as good as interatomic potential (3) Thermal transport are not properly treated for metallic system (4) Electronic stopping are not directly treated. The main things in the MD simulation are assumption, approximations and simplifications of the model and computational procedure such that they contribute minimum inaccuracy means not affect significantly the property of interests [34].

3.2. Basic Principles

The MD simulation method is based on Newton's equation of motion, which described dynamics of atoms. The classical equation is written as [35].

$$m_i \ddot{r}_i = f_i \qquad f_i = -\frac{\delta}{\delta r_i} u \text{ .... (1)}$$

In this equation, forces f_i acting on the existing atom are to be calculated from a potential energy $u(r_N)$, where $r_N = (r_1, r_2, r_{3,} ....r_N)$ is the set of 3N atomic coordinate. Potential energy u is calculated from above equation in two way (1) non-bonded interactions (2) bonding potential

(1) Non-bounded Interactions: Potential energy u $_{\text{non-bounded}}$ indicates non-bounded interaction of atoms divided into 1-body,2-body, 3-body…..term

$$U_{\text{non-bounded}} = \sum_i u(r_i) + \sum_i \sum_{j>i} v(r_i, r_j) \quad \text{.....(2)}$$

Where $u(r)$ represents externally applied potential field or the effects of the container walls. Now, we concentrate over pair potential and neglect the 3-body and higher order interactions. Most commonly used Lenard- Jones potential is as follows

$$V^{lj}(r) = 4\varepsilon\left[\left(\frac{\sigma}{r}\right)^{12} - \left(\frac{\sigma}{r}\right)^{6}\right] \text{ .... (3)}$$

Here, σ is a diameter and ϵ is well depth.

If electrostatic charges are presents then appropriate coulomb potentials are added as

$$V^{coulomb}(r) = \frac{Q_1 Q_2}{4\pi r \varepsilon_0} \text{ .... (4)}$$

Where Q_1, Q_2 are charges and ε_0 is the permittivity of free space.

(2) Bonding Pontentials

For molecular system, we simply build the molecules out of site-by-site potentials of the form of Eq. (3) or similar. Thus it is not much important for study.

Force calculation

After determination of potential energy u(r^N), next step is to calculate the atomic forces through following Eq.

$$f_i = -\frac{\partial}{\partial r_i} u(r^N) \text{ .... (5)}$$

3.3. The velocity verlet algorithm [36]

Velocity verlet integrator is a numerical method used to integrate the Newton's equation of motion. It is used to calculate trajectories of particles in MD simulation. Let us we consider N number of particles in their 3D representation of position, velocity, and acceleration at time t given as $r_i(t), v_i(t)$ and $a_i(t)$ respectively. Where i(1,2,….N) is the particle index .

We known that $v = dr/dt$ and $a = dv/dt$, then Newton's Eq. for the system of 6N 1st order differential equation become

$$\dot{r}_i = \frac{d}{dt} r_i = V_i \quad \text{..... (6)}$$

$$\dot{V}_i = \frac{d}{dt} V_i = a_i = \frac{F_i}{m_i} \quad \text{..... (7)}$$

In the above equation, mass m_i and force f_i is acting on particle i. acceleration a_i is the time dependent function of all the particles position and their velocities.

Most popular velocity verlet algorithms for MD simulation to solve the 1st order differential equation can be written as

$$r(t+\Delta t) = r(t) + \Delta t V(t) + \frac{1}{2}(\Delta t)^2 a(t) + o\left((\Delta t^3)\right) \text{..... (8)}$$

$$a(t+\Delta t) = a\left(r_1(t+\Delta t)\right), ..., r_N(t+\Delta t);\ V_1(t+\Delta t) ....., V_N(t+\Delta t); t+\Delta t) \text{.... (9)}$$

$$V(t+\Delta t) = V(t) + \frac{1}{2}\Delta t\left[a(t) + a(t+\Delta t)\right] + o\left((\Delta t^3)\right) \text{..... (10)}$$

In simple MD problem without external magnetic fields, the particles acceleration doesn't depend on their velocity, so Eq. (9) can be change by following equation

$$a(t+\Delta t) = a\left(r_1(t+\Delta t)\right), ..., r_N(t+\Delta t); t+\Delta t) \text{..... (11)}$$

Eq. (8) can be helpful in calculation of $r(t+\Delta t)$ at time t and from Eq. (11) we can find $a(t+\Delta t)$ finally to get $V(t+\Delta t)$ using Eq. (10).

The advantages of this algorithm are (i) it is straightforward, and (ii) the storage requirements are modest. There is no compromise on precision.

3.4. Interatomic potential

It is possible to model a few thousands to millions of particles in classical MD using phenomenological interatomic and intermolecular potentials. They are obtained by using the phenomenological approach of selecting a parameterized mathematical form for the interaction between atoms, and fitting its unknown parameters to various experimental or higher-level theoretical (e.g. ab initio quantum mechanics simulation) properties. In general, the flexibility, accuracy, transferability, and computational efficiency of the interatomic potentials each have to be carefully considered.

3.4.1. Embedded atom method (EAM) [37]

Embedded atom method is an approximate description of energy between two atoms. The energy is a function of a sum of function of the separation between an atom and its neighbors. In 1984 EAM method was developed by Murray Daw and Mike Baskes in which they described the latter functions as the electron density. EAM is very closed to the second moment approximation to tight binding theory, also known as the Finnis-Sinclair model. These model are particularly appropriate for metallic system. EAM is widely used in MD simulations.

In a simulation, the potential energy of an atom i, is given by

$$E_i = F_\alpha \left(\sum_{i \neq j} \rho_\beta \left(r_{ij} \right) \right) + \frac{1}{2} \sum_{i \neq j} \phi_{\alpha\beta} \left(r_{ij} \right)$$

Where r_{ij} is the distance between atoms i and j.

$\phi_{\alpha\beta}$ is a pair-wise potential function

ρ_β is the contribution to the electron charge density from atom j of type β at the location of atom i and F is an embedding function that represents the energy required to place atom i of type α into the electron cloud.

Since the electron cloud density is a summation over many atoms, generally estimated by a cutoff radius, the EAM potential is described as a multi body potential. For a single element system of atoms, three scalar functions must be specified:

i) The embedding function

ii) a pair-wise interaction

iii) an electron cloud contribution function

For a binary alloy, EAM potential requires seven functions:

a) three pair-wise interaction (A-A, A-B, B-B)

b) two embedding function

c) two electron cloud contribution functions.

3.4.2. Pair wise potential and multi-body potential

Pair-wise interaction and the multi-body are related to the EAM potential. A pair-wise potential (primarily repulsive in nature) shows the interaction of the positively charged metal core ions with one another [38] where as multi- body potential (attractive interaction) models refers to "embedding" a positively charged pseudo-atom core into "sea" of free electrons created by the surrounding atoms

3.5 Periodic boundary condition

In MD simulation, Periodic boundary condition (PBC) is a set of boundary conditions that used for simulating a large system by modeling a small part that is far from its edge. During simulation the atom present inside the simulation box moved towards one edge, it reappears from the opposite edge with same velocity. This phenomenon behaves like tiling of the system [39].

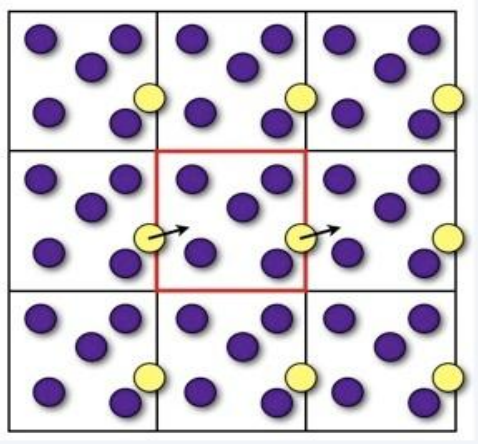

Fig. 3.1 shows 2D- representation of periodic boundary condition

3.5.1 Limitation of Periodic boundary condition

- The box size should larger than the double of cutoff distance (R_{cut}) of the interaction potential, if not so molecule may interact with its own image in a neighboring box
- PBC doesn't conserved angular momentum because it is not rotational symmetric, so it conserved only linear momentum

3.7 Mean Square Displacement

For the calculation of diffusivity value of pure Fe and Fe-Cr alloys system, mean square displacement (MSD) model was used. In general, MSD is defining as a measure of the average distance a molecules travels. Mathematically it is expressed as [40, 41]

$$MSD(t) = \left\langle \Delta r_i(t)^2 \right\rangle = \left\langle \left| r_i(t) - r_i(0) \right|^2 \right\rangle$$

In this equation, $r_i(t) - r_i(0)$ is the (vector) distance travelled by molecule / atoms I over time interval of length t, and the squared magnitude of this vector is averaged over many such time intervals. Often this quantity is averaged also over all molecules in the system, summing from 1 to N and dividing by N. The MSD also contain information on atomic diffusion. If the molecules doesn't encountered with other molecules that means they traveled in a trajectory called ballistic region, then the distance travelled would be proportional to the time interval distance equals velocity-times, time and the MSD would be increases quadratically with time t. In denser phases, quadratic behavior holds only for a very short time interval, of the order of mean collision time. Beyond this time the motion is better described as a random walk, for which the MSD increases only linearly with time. The rate of growth of the mean square displacement depends on how often the molecules suffer collisions. At higher density, it will take longer to diffuse a given distance, as other molecules continually impede its progress.
The limiting slope of MSD (t), considered for time intervals sufficient long for it to be in the linear regime, is related to the self-diffusion constant D.

$$D = \lim_{t \to \infty} \frac{1}{6} \left\langle \left| r(t) - r(0) \right| \right\rangle$$

The graph has shown below as an example how diffusivity value calculated.

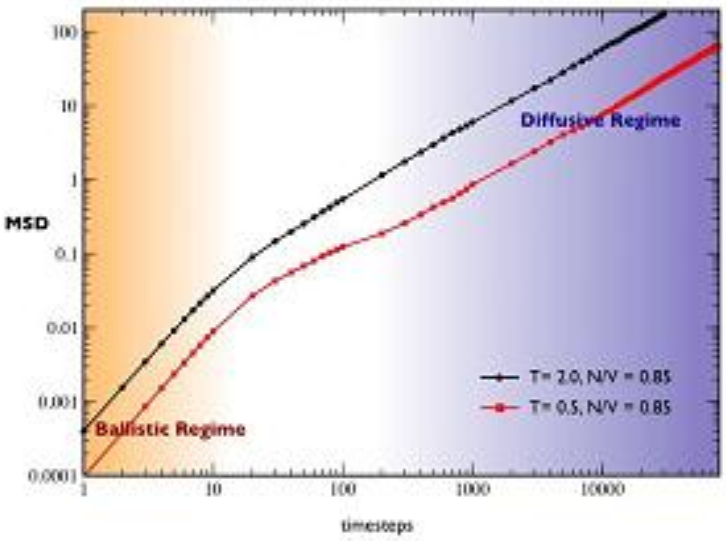

Fig.3.2 MSD vs. timestep [42]

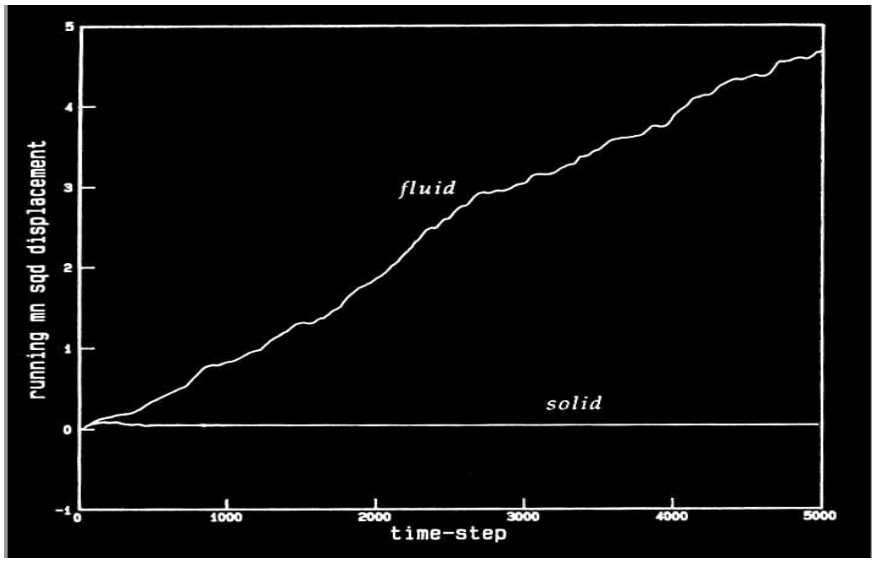

Fig.3.3 represents temporal variation of MSD for solid and fluid [43]

3.8 Introduction to LAMMPS (Large-scale Atomic/ Molecular Massively Parallel Simulator)

3.8.1 Background and Features

LAMMPS stands for Large-scale Atomic/Molecular Massively Parallel Simulator is a classical MD simulation code designed to run effectively on parallel computer and desktop or laptop also. It was originally developed under US Department of Energy CRADA (Cooperative Research and

Development Agreement) with two DOE labs and three companies [44]. Later on this software is distributed by Sandia National Laboratory under general public license (GPL). Software has open-source code and can be modify with new capabilities. It is easy to operate by code and current version LAMMPS is written in C++. Some of the important features of LAMMPS are described as below:

- runs on single processor or in parallel
- distributed –memory message-passing parallelism(MPI)
- open-source distribution
- spatial-decomposition of simulation domain for parallelism
- optional libraries used: MPI and single-processor FFT
- runs from an input script
- highly portable C++
- runs one or multiple simulations simultaneously (in parallel) from one script
- syntax for defining and using variables and formulas
- syntax for looping over runs and breaking out of loops
- easy to extend with new features and functionality

LAMMPS is very easy to be use as it is compiled in a specific computational language. Three basic files are needed to run the MD code on LAMMPS platform: input script, a potential file and an exe. File. LAMMPS input script has basically four parts;

1.) Initialization

2.) Atom definition

3.) Setting

4.) Run a simulation

3.8.2 Force field

Force fields are useful for analysis and running the input script. It is come under initialization part of LAMMPS. Some of them used in LAMMPS are as follows:

- pairwise potential: Lennard-Jones, Buckingham, Morse, Born-Mayer-Huggins, Yukawa

- Charged pairwise potential: coulombic, point-dipole.
- Many body potentials: EAM, Finnis/Sinclair EAM, modified EAM(MEAM)

3.8.3 Atoms creation

This section defines atoms in a simulation box. The code used in this work to create atom in simulation as given below:

```
create_box          1 box
lattice             bcc 2.851
region              Fe block 0 50 0 50  0 50 units box
create_atoms        1 region Fe units box
create_box          1 box
```

3.8.4 Ensembles and boundary condition

In LAMMPS, three basic ensembles are used. They are:

1) NPT (number of atom, pressure, temperature)
2) NVE (number of atom, volume, energy)
3) NVT (number of atom, volume, temperature)

Boundary condition used in LAMMPS is:

- p p p
- p p f
- s f f_m

Where 'p' is periodic, 'f' is non-periodic and fixed, 's' is non-periodic and shrink-wrapped, and m is non-periodic and shrink-wrapped with minimum value.

By default boundary condition used in MD code is p p p, where p shows box is periodic, so that atoms should interact across the boundary.

3.8.5 Integrators

The integrator that are used in LAMMPS as given below:

- Velocity-verlet integrator
- Energy minimization via conjugate
- Rigid body integration
- Brownian dynamics

3.8.6 Energy minimization

Syntax used for energy minimization is

minimize etol ftol maxiter maxeval

where

etol = stopping tolerance for energy (unit less)

ftol = stopping tolerance for force (force units)

maxiter = max interation of minimize

maxeval= max number of force or energy evaluations

Energy minimization is done for the system by interatively adjusting atom coordinates. When one of the stopping criteria satisfied interation is terminated. At that point the configuration will be in local potential energy minimum.

3.8.7 Output

Output file is generated after completion of running the MD code. There is three file generated in this research work.

1) DUMP file: this file gives the atoms position in all three direction and respective their velocity.
2) Log file: This file contents the thermodynamic information of atoms like temperature, pressure, volume, and total energy.
3) Log. lammps file

3.8.8 Computing MSD via LAMMPS

MSD is calculated by using the syntax:

compute 1 Fe msd

The above syntax is used for calculating MSD of pure Fe atom. Whereas syntax for MSD calculation of Fe-Cr alloys given as:

```
compute     1 Fe msd

compute     2 Cr msd
```

3.8.9 Visual Molecular dynamics (VMD)

For display, animation, and analyzing large atoms or molecules in 3-D graphical mode VMD (molecular visualization package) is used that is built-in scripting. In this work the entire atomic snapshots are taken by VMD software [45].

CHAPTER 4

Simulation Results

&

Discussions

4. Simulation Results & Discussion

4.1. Creation of Pure Fe crystal at temperature 50 K & 100 K

Simulation box size of dimension 50 $Å^3$ containing 11,643 atoms were generated by running MD code. The code described the formation of sample equilibrated at temperature 50 K and movement of the atoms written in a infile. This infile is written in appendix I.

4.1.1. VMD snap shots

After running the MD code VMD snapshots of Fe-lattice has been taken as shown in following figures.

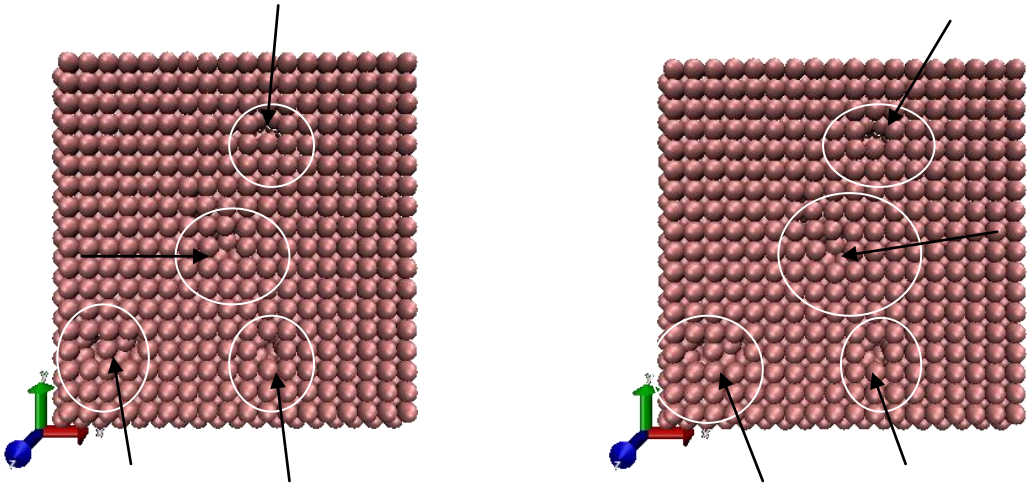

Fig. 4.1.1 (a) & (b) shows VMD snapshot of Fe-lattice at temperature 50 K

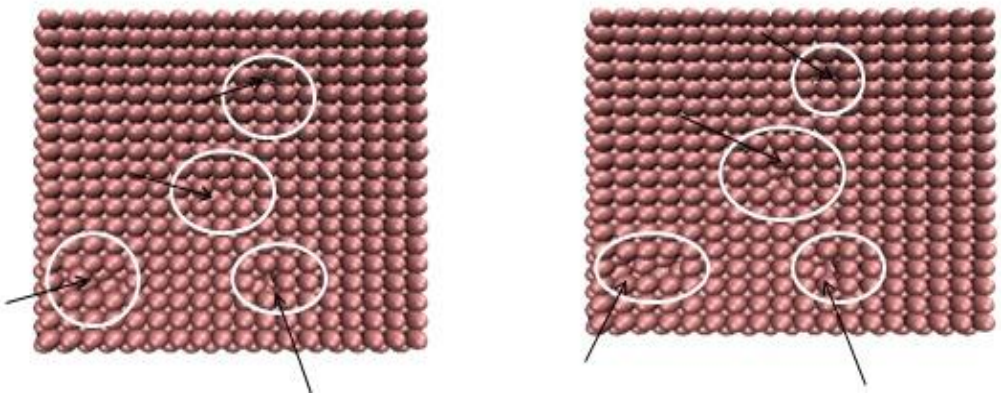

Fig.4.1.1 (c) & (d) shows VMD snapshots of Fe-lattice at 100 K

In the above VMD snapshots circle region show the vacancy created by MD code and arrow indicates the movement of atoms during running the MD code. Purple color indicates Fe atoms.

4.1.2. MSD calculation

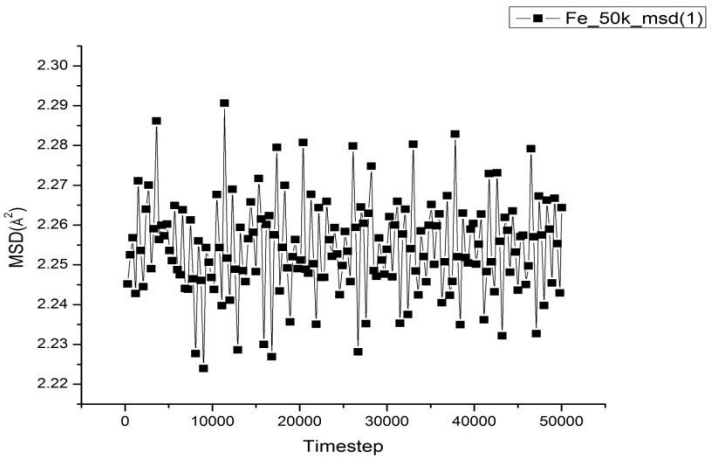

Fig.4.1.2. (a) MSD vs. Time step plot of Fe-lattice at temperature 50 K

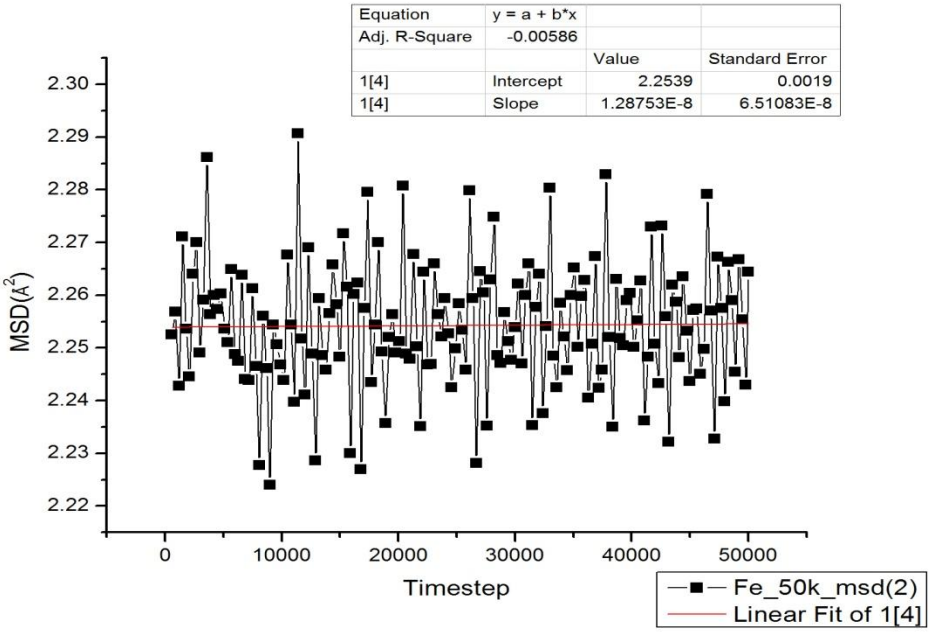

Fig.4.1.2 (b) MSD vs. Time step (self-diffusivity value of Fe-lattice at 50 K)

Self diffusivity of Fe has been calculated from MSD vs. time step plots at temperature 50 K & 100 K. Fig.4.1.2 (a) and Fig.4.1.2 (c) shows MSD vs. time step. The value of self diffusivity calculated from the diffusive region of the plot is shown in Fig. 4.1.2. (b) & Fig. 4.1.2 (d)

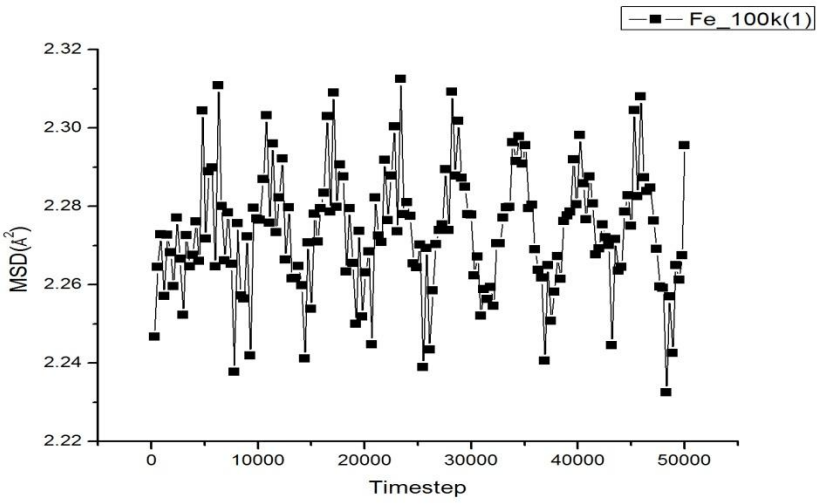

Fig.4.1.2. (c) MSD vs. Time step plot of Fe-lattice at temperature 100 K

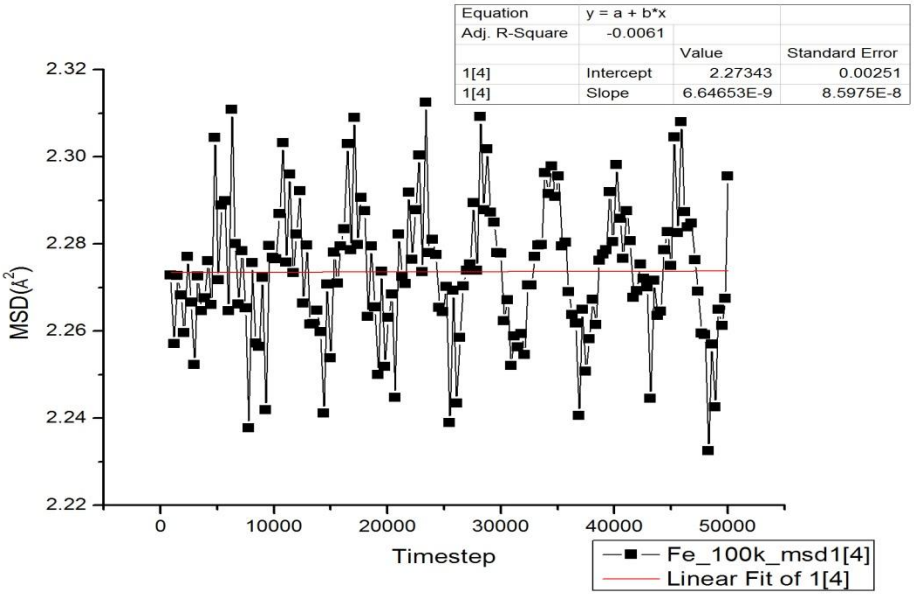

Fig.4.1.2. (d) MSD vs. Time step (self-diffusivity value of Fe-lattice at 100 K)

4.2. Creation of Pure Fe crystal at temperature 300 K, 500 K, and 700 K

Simulation box size of dimension 50 $Å^3$ containing 11,600 atoms were generated by running MD code. The pattern of writing the code for creating Fe-lattice is same as code written for Fe-lattice equilibrated at 50k.

4.2.1. VMD snapshots

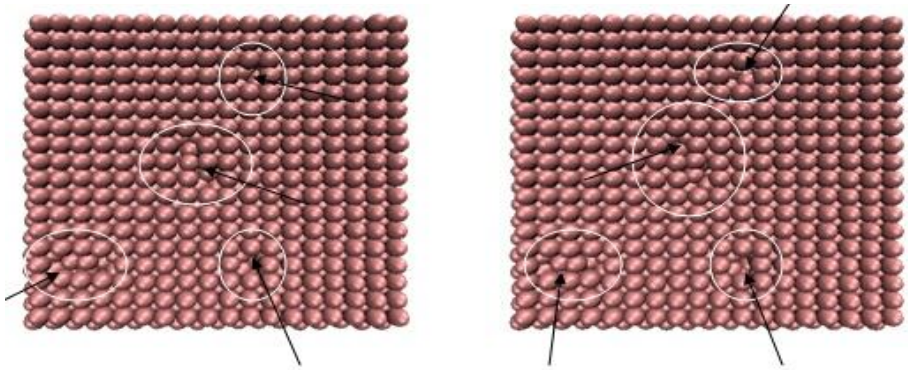

Fig.4.2.1 (a)

Fig.4.2.1 (b)

Fig. 4.2.1 (a) & Fig.4.2.1 (b) shows VMD snapshots of Fe-lattice at 300 k

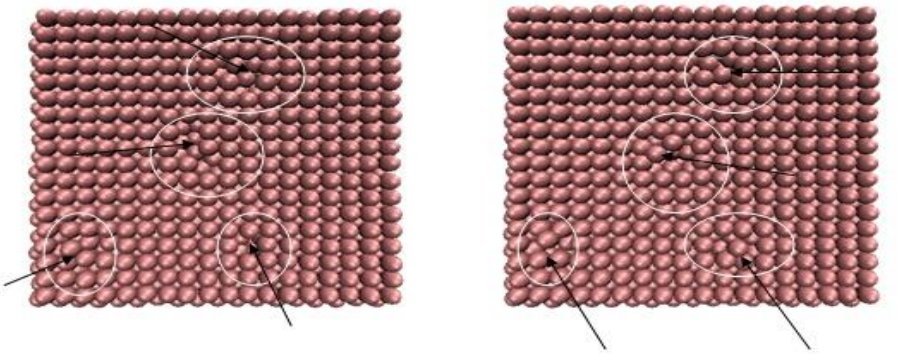

Fig.4.2.1 (c)

Fig.4.2.1 (d)

Fig.4.2.1 (c) & Fig.4.2.1 (d) shows VMD snapshots of Fe-lattice at 500 k

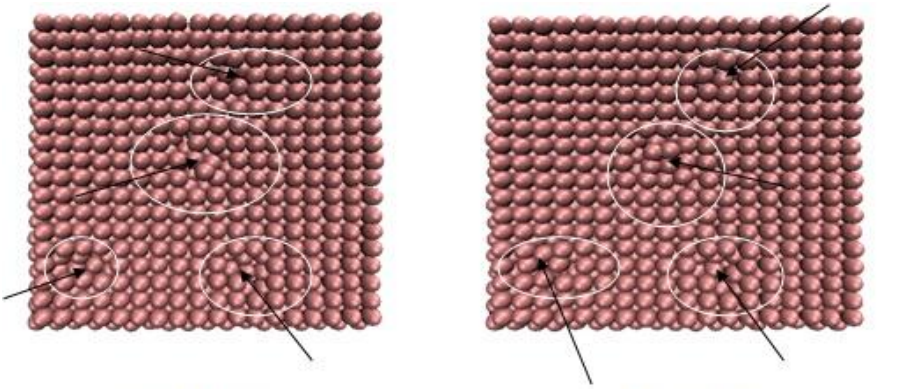

Fig.4.2.1 (e)

Fig.4.2.1 (f)

Fig.4.2.1 (e) & Fig.4.2.1 (f) shows VMD snapshots of Fe-lattice at 700 k

In all the above VMD snapshots circle region show the vacancy created by MD code and arrow indicates the movement of atoms during running the MD code. Purple color indicates Fe atoms.

4.2.2. MSD calculation

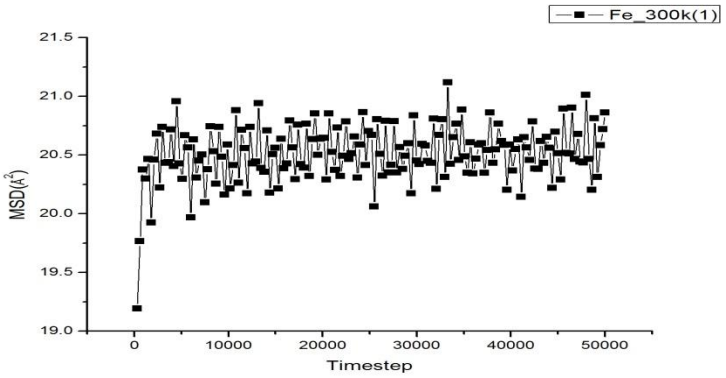

Fig.4.2.2 (a) MSD vs. Time step plot of Fe-lattice at temperature 300 K

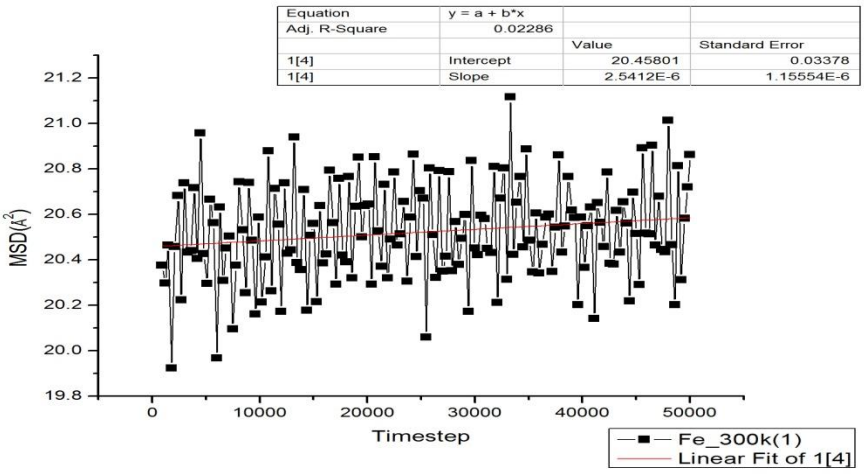

Fig.4.2.2 (b) MSD vs. Time step (self-diffusivity value of Fe-lattice at 300 K)

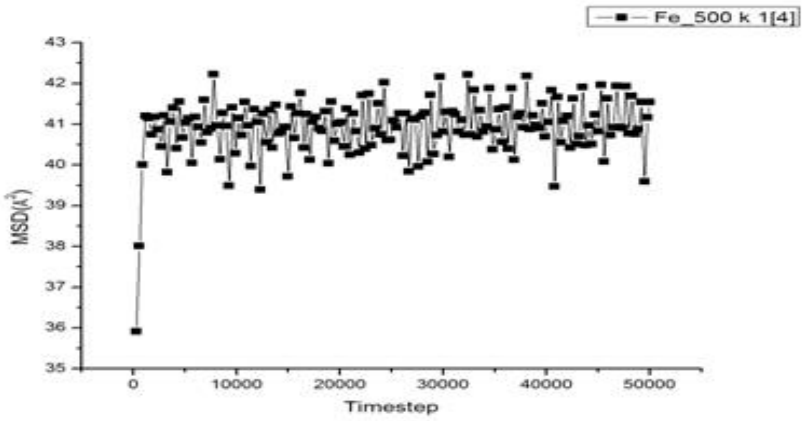

Fig.4.2.2 (c) MSD vs. Time step plot of Fe-lattice at temperature 500 K

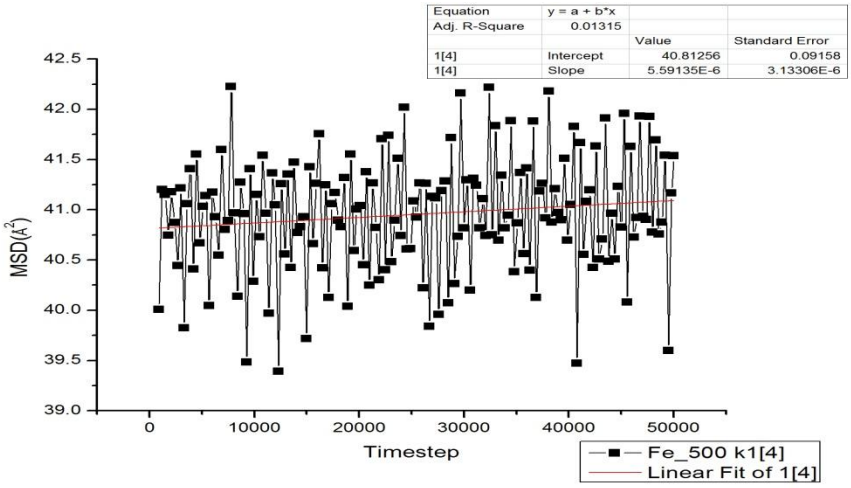

Fig.4.2.2 (d) MSD vs. Time step (self-diffusivity value of Fe-lattice at 500 K)

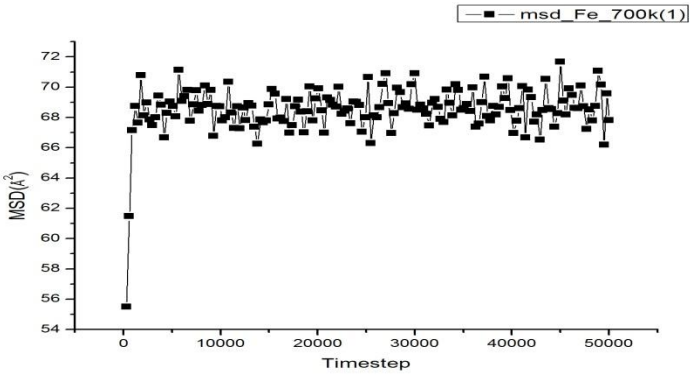

Fig.4.2.2 (e) MSD vs. Time step plot of Fe-lattice at temperature 700 K

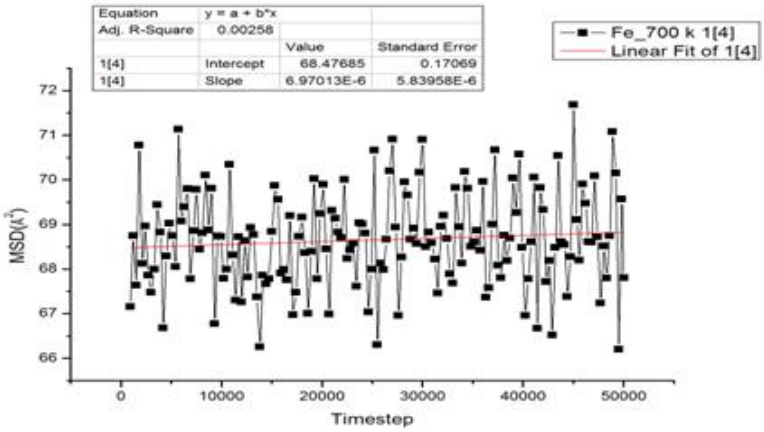

Fig.4.2.2 (f) MSD vs. Time step (self-diffusivity value of Fe-lattice at 700 K)

Self diffusivity of Fe has been calculated from MSD vs. time step plots at temperature 300 K, 500 K & 700 K. Fig.4.2.2 (a), Fig.4.2.2 (c) and Fig4.2.2 (e) shows MSD vs. time step. The value of self diffusivity calculated from the diffusive region of the plot is shown in Fig. 4.2.2. (b), Fig. 4.2.2 (d) & Fig.4.2.2 (f)

4.3 Creation of Pure Fe crystal at temperature 1000 K

Simulation box size of dimension 50 $Å^3$ containing 11,600 atoms were generated by running MD code. The pattern of writing the code for creating Fe-lattice is same as code written for Fe-lattice equilibrated at 50k.

4.3.1 VMD snapshots

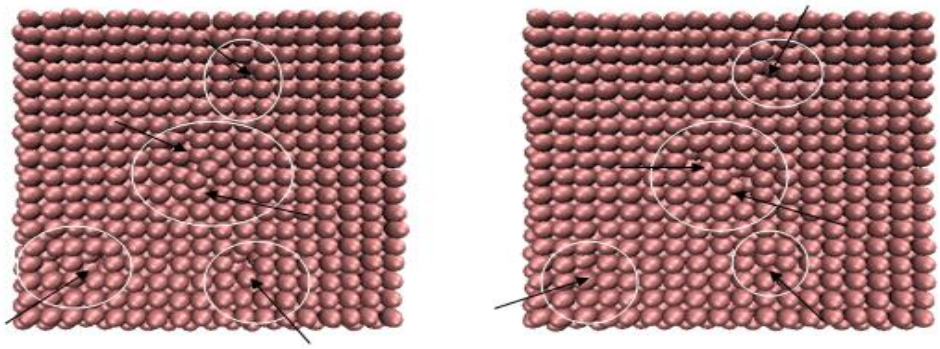

Fig.4.3.1 (a)

Fig.4.3.1 (b)

Fig.4.3.1 (a) & Fig.4.3.1 (b) shows the VMD snapshots of Fe- lattice at temp. 1000 K

In the above VMD snapshots circle region show the vacancy created by MD code and arrow indicates the movement of atoms during running the MD code. Purple color indicates Fe atoms.

4.3.2. MSD calculation

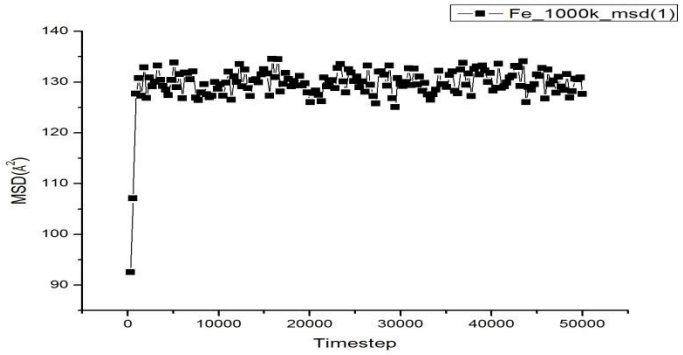

Fig.4.3.2 (a) MSD vs. Time step plot of Fe-lattice at temperature 1000 K

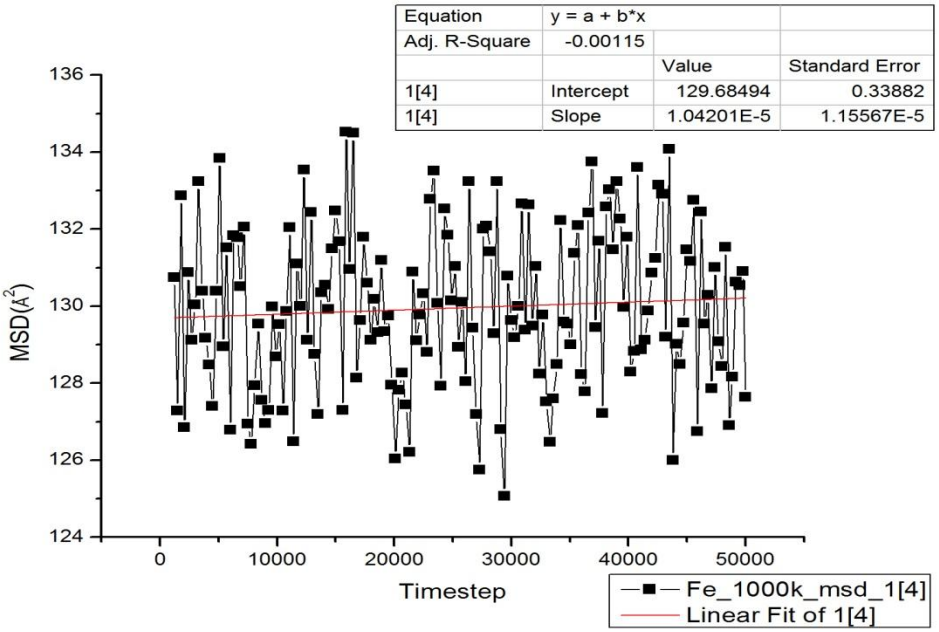

Fig.4.3.2 (b) MSD vs. Time step (self-diffusivity value of Fe-lattice at 1000 K)

Self diffusivity of Fe has been calculated from MSD vs. time step plots at temperature 1000 K. Fig.4.3.2 (a) shows MSD vs. time step. The value of self diffusivity calculated from the diffusive region of the plot is shown in Fig. 4.3.2. (b).

4.4 comparisons of MSD values of Fe- lattice

Table 4.1: Diffusivity values of BCC-Fe at different temperature

Temperature (K)	**Diffusivity ($Å^2$/Ps)**	**Diffusivity (m^2/s)**
50	1.28753×10^{-8}	1.28753×10^{-16}
100	6.64653×10^{-9}	6.64653×10^{-17}
300	2.5412×10^{-6}	2.5412×10^{-14}
500	5.59135×10^{-6}	5.59135×10^{-14}
700	6.97013×10^{-6}	6.97013×10^{-14}
1000	1.04201×10^{-5}	1.04201×10^{-13}

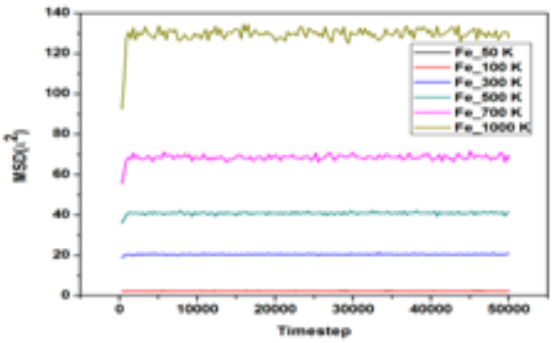

Fig.4.4 (a) Comparison of MSD vs Time step plotted at given temperature

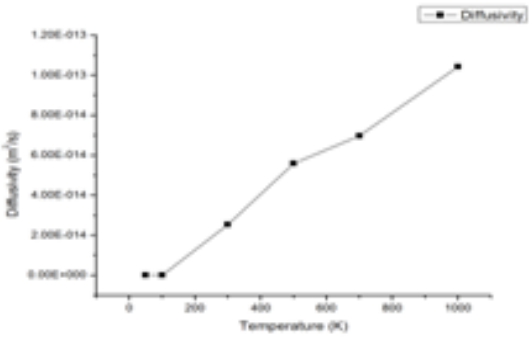

Fig.4.4 (b) shows diffusivity changes with increase in temperature

Table 1 shows the diffusivity value of Fe atoms. Diffusivity value of pure Fe is lower at lower temperature (50 K, 100 K), but diffusivity value increases linearly above 100 K temperature. It also shown graphically in Fig.4.3 (b) that diffusivity increases with increase in temperature. Fig.4.3 (a) shows a comparative increase of diffusivity in term of MSD plot.

4.5. Effect of Temperature

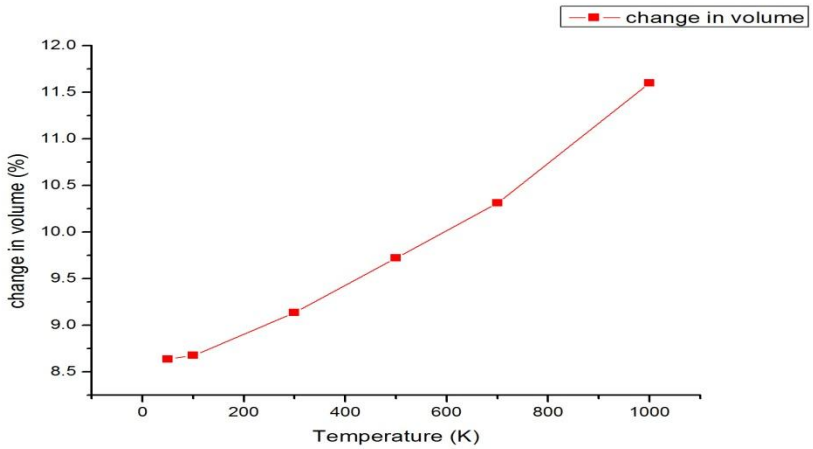

Fig.4.5 shows the increase in volume with increase in temperature

Volume increases with increase in temperature, it is due to reason that increasing the temperature atoms collision gets faster because of higher activation energy.

4.6 Creation of Fe-5%Cr alloys

4.6.1 Creation of Fe-5%Cr alloys at temperature 50 K

Simulation box size of dimension 50 $Å^3$ containing 11,600 atoms were generated by running MD code. The pattern of writing the code for creating Fe-5%Cr alloys sample is same as code written for Fe-5%Cr alloys equilibrated at 50 K mention in appendix II.

4.6.1.1 VMD snapshots

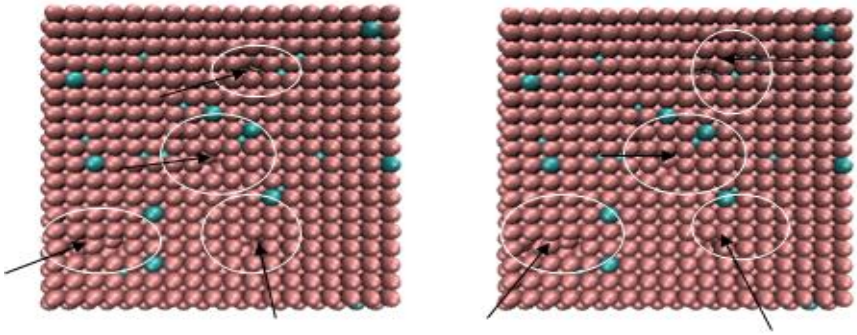

Fig.4.6.1.1 (a) Fig.4.6.1.1 (b)

Fig.4.6.1.1 (a) & Fig.4.6.1.1 (b) shows the VMD snapshots of Fe-5%Cr alloys at temp. 50 K

In the above VMD snapshots circle region show the vacancy created by MD code and arrow indicates the movement of atoms during running the MD code. Purple color indicates Fe atoms and blue color indicates Cr atoms.

4.6.1.2 MSD calculation

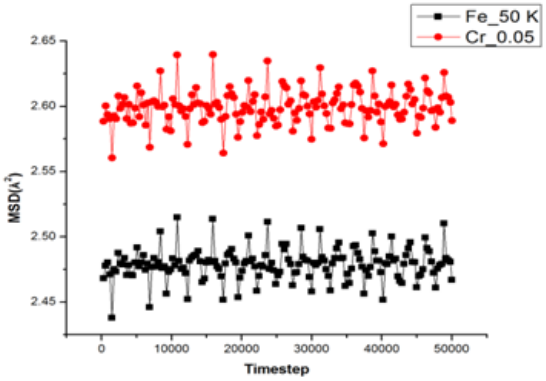

Fig.4.6.1.2 (a) MSD vs Timestep plot of Fe-5%Cr alloys at temp. 50 K

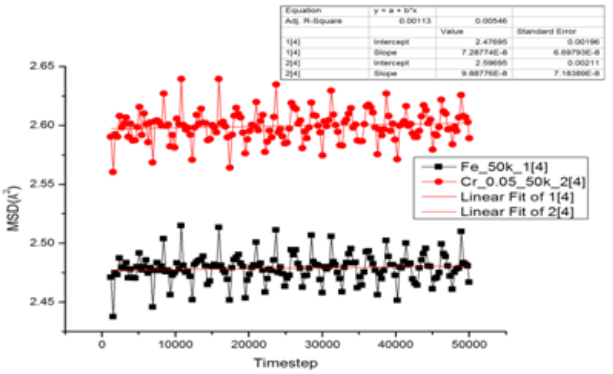

Fig.4.6.1.2 (b) MSD vs Timestep (self-diffusivity value of Fe-5%Cr alloys at temp. 50 K)

Self diffusivity of Fe & Cr has been calculated from MSD vs. time step plot at temperature 50 K. Fig.4.6.1.2 (a) shows MSD vs. time step. The value of self diffusivity calculated from the diffusive region of the plot is shown in Fig. 4.6.1.2. (b)

4.6.2 Creation of Fe-5%Cr alloys at temperature 100 K

Simulation box size of dimension 50 $Å^3$ containing 11,600 atoms were generated by running MD code. The pattern of writing the code for creating Fe-5%Cr alloys sample equilibrated at 100 K is same as code written for Fe-5%Cr alloys equilibrated at 50 K mention in appendix II.

4.6.2.1 VMD snapshots

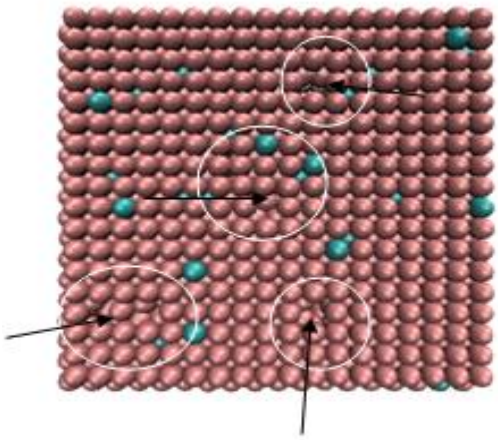

Fig.4.6.2.1 (a)

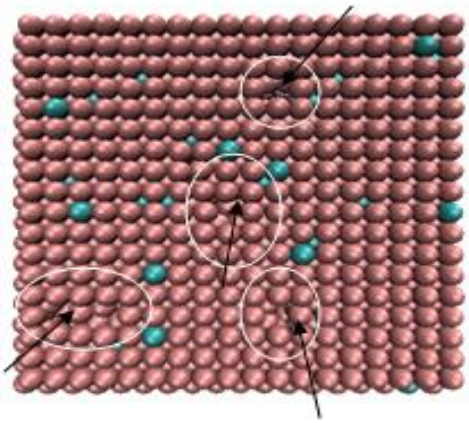

Fig.4.6.2.1 (b)

Fig.4.6.2.1 (a) & Fig.4.6.2.1 (b) shows VMD snapshots of Fe-5%Cr alloys at temp. 100 K

In the above VMD snapshots circle region show the vacancy created by MD code and arrow indicates the movement of atoms during running the MD code. Purple color indicates Fe atoms and blue color indicates Cr atoms.

4.6.2.2 MSD calculation

Self diffusivity of Fe & Cr has been calculated from MSD vs. time step plots at temperature 100 K as shown in below Fig. Fig.4.6.2.2 (a) shows MSD vs. time step. The value of self diffusivity calculated from the diffusive region of the plot is shown in Fig. 4.6.2.2. (b)

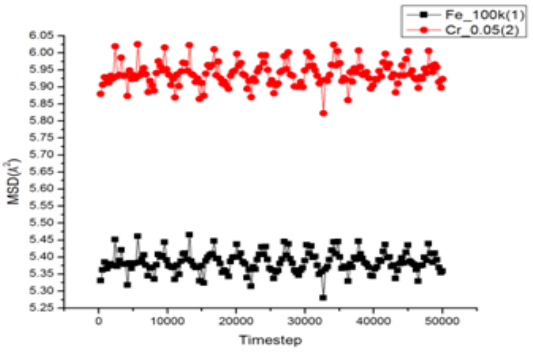

Fig.4.6.2.2 (a) MSD vs Timestep plot of Fe-5%Cr alloys at temp. 100 K

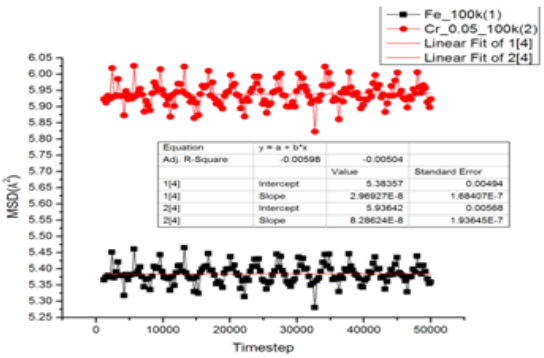

Fig.4.6.2.2 (b) MSD vs Timestep (self-diffusivity value of Fe-5%Cr alloys at temp. 100 K)

4.6.3 Creation of Fe-5%Cr alloys at temperature 300 K

Simulation box size of dimension 50 $Å^3$ containing 11,600 atoms were generated by running MD code. The pattern of writing the code for creating Fe-5%Cr alloys sample equilibrated at 300 K is same as code written for Fe-5%Cr alloys equilibrated at 50 K mention in appendix II.

4.6.3.1 VMD snapshots

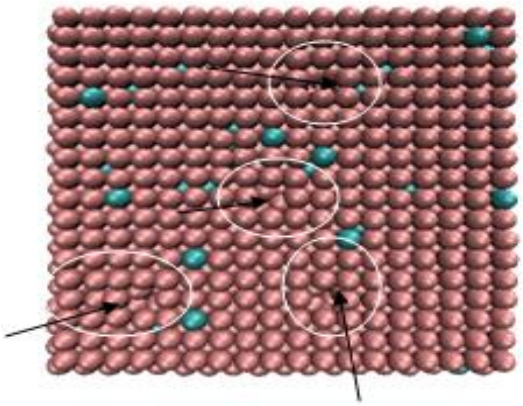

Fig.4.6.3.1 (a)

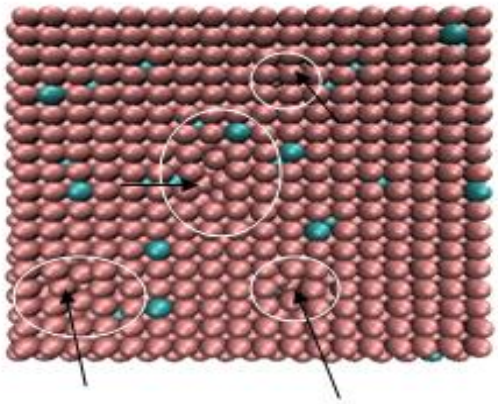

Fig.4.6.3.1 (b)

Fig.4.6.3.1 (a) & Fig.4.6.3.1 (b) shows VMD snapshots of Fe-5%Cr alloys at temp. 300 K

In the above VMD snapshots circle region show the vacancy created by MD code and arrow indicates the movement of atoms during running the MD code. Purple color indicates Fe atoms and blue color indicates Cr atoms.

4.6.3.2 MSD calculation

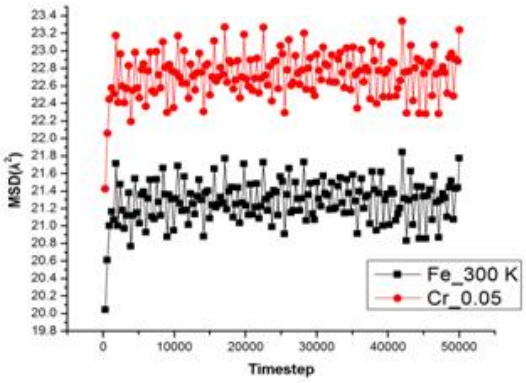

Fig.4.6.3.2 (a) MSD vs Timestep plot of Fe-5%Cr alloys at temp. 300 K

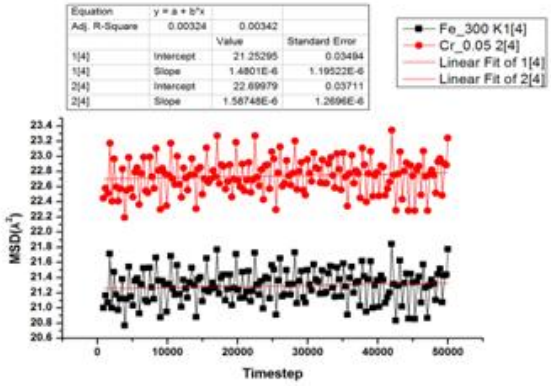

Fig.4.6.3.2 (b) MSD vs Timestep (self-diffusivity value of Fe-5%Cr alloys at temp.300 K)

Self diffusivity of Fe & Cr has been calculated from MSD vs. time step plots at temperature 300 K. Fig.4.6.3.2 (a) shows MSD vs. time step. The value of self diffusivity calculated from the diffusive region of the plot is shown in Fig. 4.6.3.2. (b)

4.6.4 Creation of Fe-5%Cr alloys at temperature 500 K

Simulation box size of dimension 50 $Å^3$ containing 11,600 atoms were generated by running MD code. The pattern of writing the code for creating Fe-5%Cr alloys sample equilibrated at 500 K is same as code written for Fe-5%Cr alloys equilibrated at 50 K mention in appendix II.

4.6.4.1 VMD snapshots

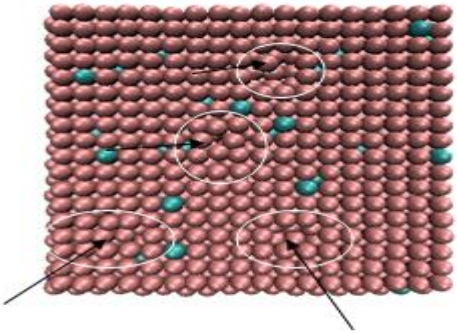

Fig.4.6.4.1 (a)

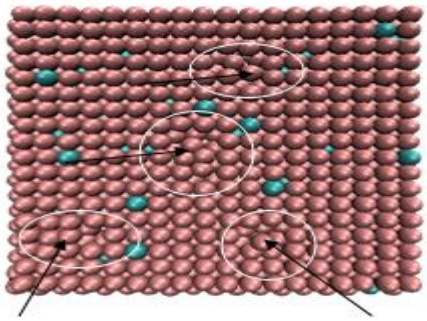

Fig.4.6.4.1 (b)

Fig.4.6.4.1 (a) & Fig.4.6.4.1 (b) shows VMD snapshots of Fe-5%Cr alloys at temp. 500 K

In the above VMD snapshots circle region show the vacancy created by MD code and arrow indicates the movement of atoms during running the MD code. Purple color indicates Fe atoms and blue color indicates Cr atoms.

4.6.4.2 MSD calculation

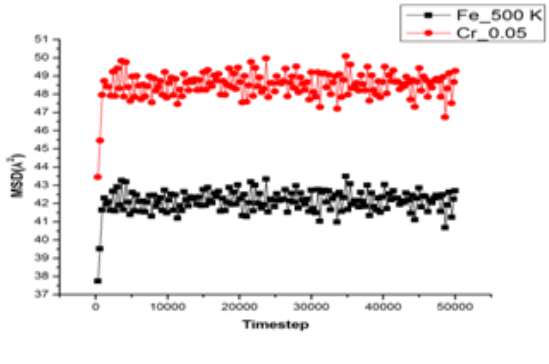

Fig.4.6.4.2 (a) MSD vs Timestep plot of Fe-5%Cr alloys at temp. 500 K

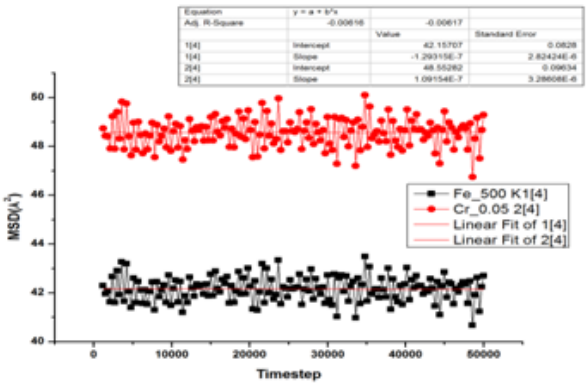

Fig.4.6.4.2 (b) MSD vs Timestep (self-diffusivity value of Fe-5%Cr alloys at temp.500 K)

Self diffusivity of Fe & Cr has been calculated from MSD vs. time step plots at temperature 500 K. Fig. Fig.4.6.4.2 (a) shows MSD vs. time step. The value of self diffusivity calculated from the diffusive region of the plot is shown in Fig. 4.6.4.2. (b)

4.6.5 Creation of Fe-5%Cr alloys at temperature 700 K

Simulation box size of dimension 50 $Å^3$ containing 11,600 atoms were generated by running MD code. The pattern of writing the code for creating Fe-5%Cr alloys sample equilibrated at 700 K is same as code written for Fe-5%Cr alloys equilibrated at 50 K mention in appendix II.

4.6.5.1 VMD snapshots

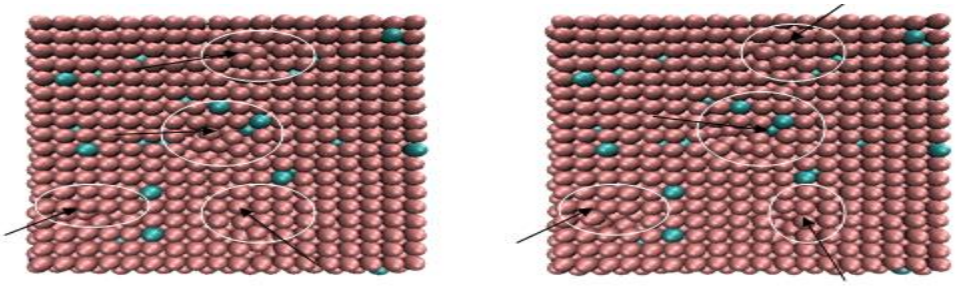

Fig.4.6.5.1 (a)

Fig.4.6.5.1 (b)

Fig.4.6.5.1 (a) & Fig.4.6.5.1 (b) shows VMD snapshots of Fe-5%Cr alloys at temp. 700 K

In the above VMD snapshots circle region show the vacancy created by MD code and arrow indicates the movement of atoms during running the MD code. Purple color indicates Fe atoms and blue color indicates Cr atoms.

4.6.5.2 MSD calculation

Self diffusivity of Fe & Cr has been calculated from MSD vs. time step plots at temperature 700 K. Fig.4.6.3.2 (a) shown below is MSD vs. time step. The value of self diffusivity calculated from the diffusive region of the plot is shown in Fig. 4.6.3.2. (b)

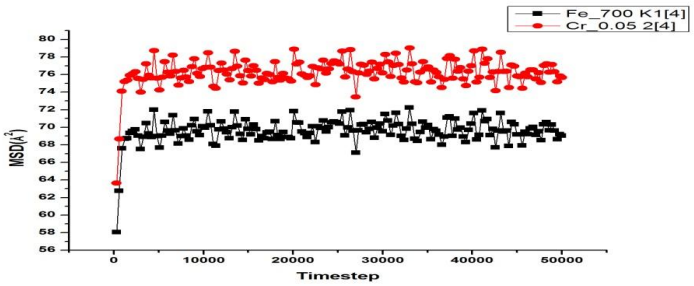

Fig.4.6.5.2 (a) MSD vs. Time step plot of Fe-5%Cr alloys at temp. 700 K

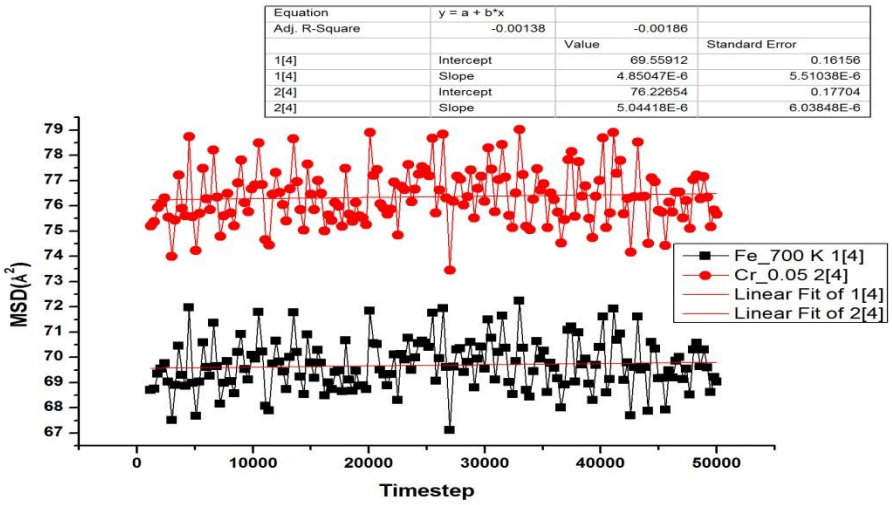

Fig.4.6.5.2 (b) MSD vs. Time step (self-diffusivity value of Fe-5%Cr alloys at temp.700 K)

4.6.6 Creation of Fe-5%Cr alloys at temperature 1000 K

Simulation box size of dimension 50 $Å^3$ containing 11,600 atoms were generated by running MD code. The pattern of writing the code for creating Fe-5%Cr alloys sample equilibrated at 1000 K is same as code written for Fe-5%Cr alloys equilibrated at 50 K mention in appendix II.

4.6.6.1 VMD snapshots

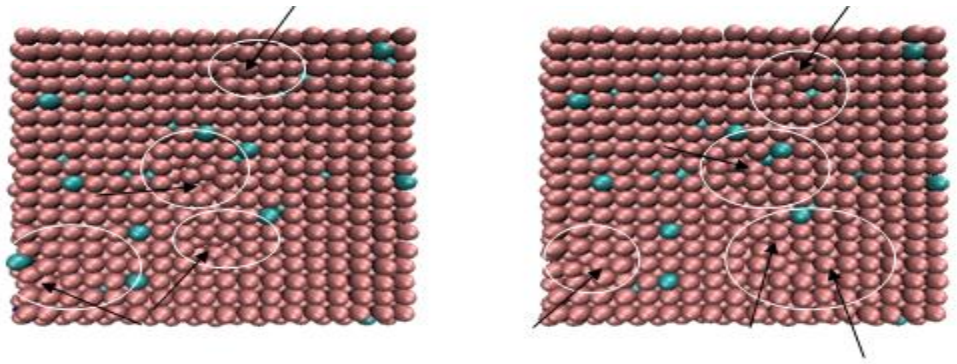

Fig.4.6.6.1 (a) Fig.4.6.6.1 (b)

Fig.4.6.6.1 (a) & Fig.4.6.6.1 (b) shows VMD snapshots of Fe-5%Cr alloys at temp. 1000 K

In the above VMD snapshots circle region show the vacancy created by MD code and arrow indicates the movement of atoms during running the MD code. Purple color indicates Fe atoms and blue color indicates Cr atoms.

4.6.6.2 MSD calculation

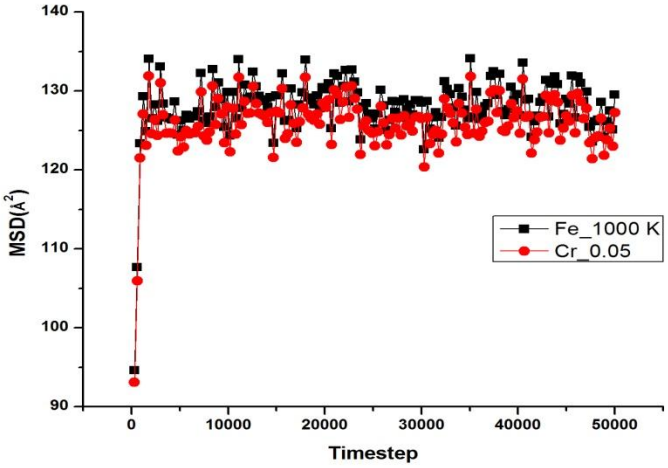

Fig.4.6.6.2 (a) MSD vs. Time step plot of Fe-5%Cr alloys at temp. 1000 K

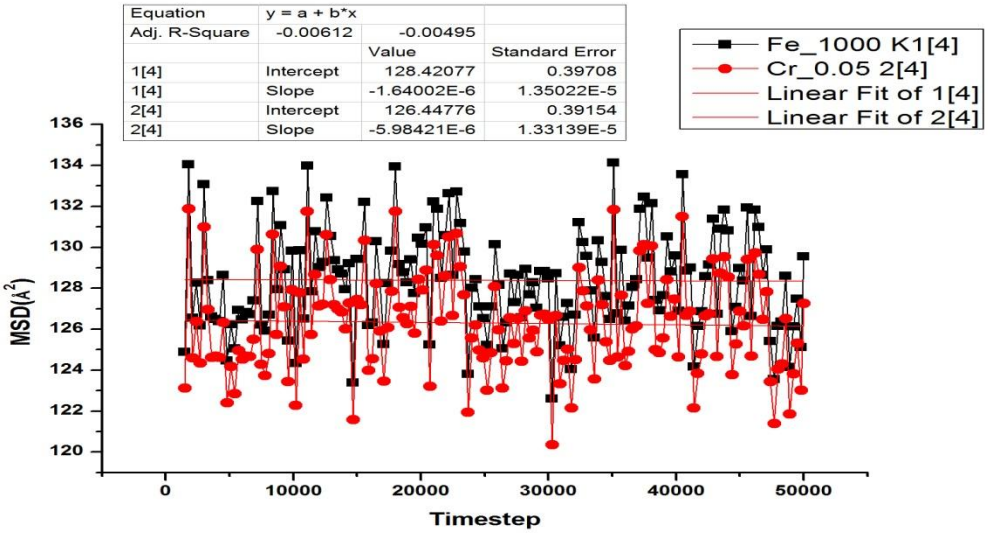

Fig.4.6.6.2 (b) MSD vs. Time step (self-diffusivity value of Fe-5%Cr alloys at temp.1000 K)

Self diffusivity of Fe & Cr has been calculated from MSD vs. time step plots at temperature 1000 K. Fig.4.6.6.2 (a) shows MSD vs. time step. The value of self diffusivity calculated from the diffusive region of the plot is shown in Fig. 4.6.6.2. (b)

4.7 Creation of Fe-10%Cr alloys

4.7.1 Creation of Fe-10%Cr alloys at temperature 50 K

Simulation box size of dimension 50 $Å^3$ containing 11,600 atoms were generated by running MD code. The pattern of writing the code for creating Fe-10%Cr alloys sample equilibrated at 50 K is same as code written for Fe-5%Cr alloys equilibrated at 50 K mention in appendix II.

4.7.1.1 VMD snapshots

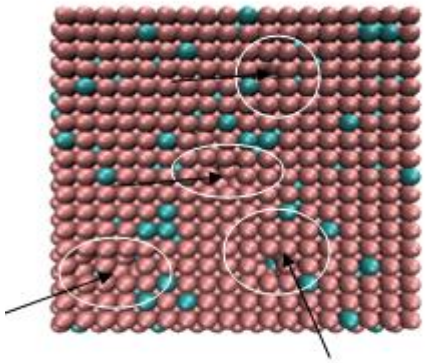

Fig.4.7.1.1 (a)

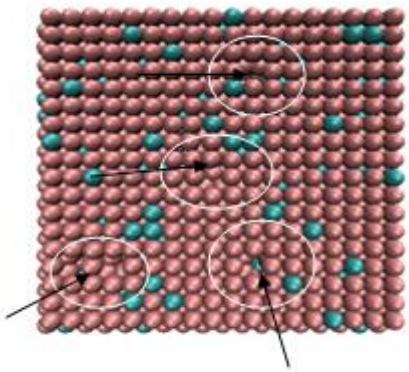

Fig.4.7.1.1 (b)

Fig.4.7.1.1 (a) & Fig.4.7.1.1 (b) shows VMD snapshots of Fe-10%Cr alloys at temp. 50 K

In the above VMD snapshots circle region show the vacancy created by MD code and arrow indicates the movement of atoms during running the MD code. Purple color indicates Fe atoms and blue color indicates Cr atoms.

4.7.1.2 MSD calculation

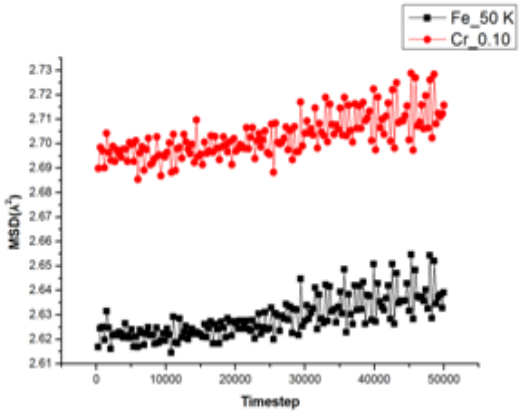

Fig.4.7.1.2 (a) MSD vs Timestep plot of Fe-10%Cr alloys at temp. 50 K

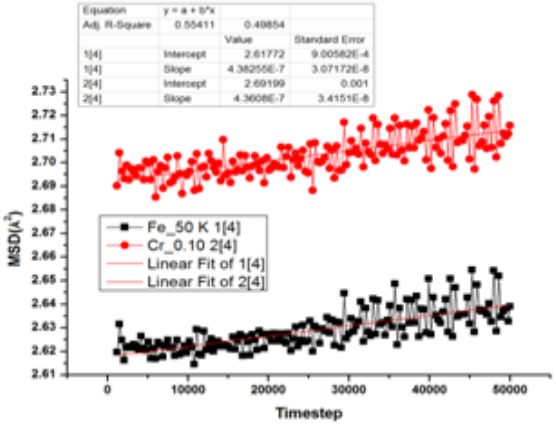

Fig.4.7.1.2 (b) MSD vs Timestep (self-diffusivity value of Fe-10%Cr alloys at temp.50 K)

Self diffusivity of Fe & Cr has been calculated from MSD vs. time step plots at temperature 50 K. Fig.4.7.1.2 (a) shows MSD vs. time step. The value of self diffusivity calculated from the diffusive region of the plot is shown in Fig. 4.7.1.2. (b)

4.7.2 Creation of Fe-10%Cr alloys at temperature 100 K

Simulation box size of dimension 50 $Å^3$ containing 11,600 atoms were generated by running MD code. The pattern of writing the code for creating Fe-10%Cr alloys sample equilibrated at 100 K is same as code written for Fe-5%Cr alloys equilibrated at 50 K mention in appendix II.

4.7.2.1 VMD snapshots

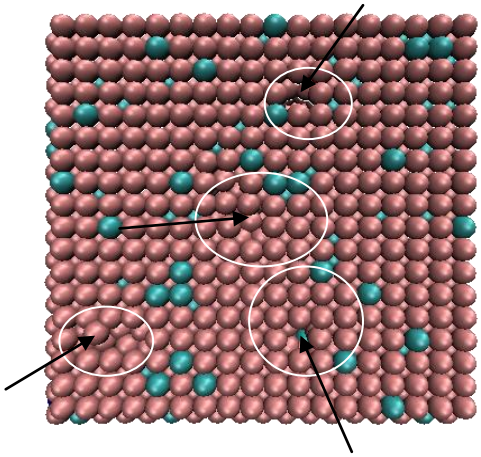

Fig.4.7.2.1 (a)

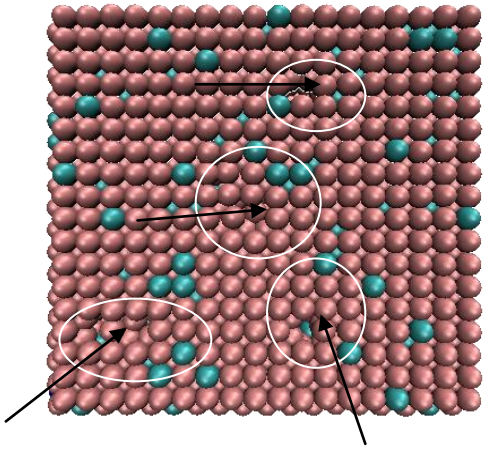

Fig.4.7.2.1 (b)

Fig.4.7.2.1 (a) & Fig.4.7.2.1 (b) shows VMD snapshots of Fe-10%Cr alloys at temp.100 K.

In the above VMD snapshots circle region show the vacancy created by MD code and arrow indicates the movement of atoms during running the MD code. Purple color indicates Fe atoms and blue color indicates Cr atoms.

4.7.2.2 MSD calculation

Self diffusivity of Fe & Cr has been calculated from MSD vs. time step plots at temperature 100 K. Fig.4.7.2.2 (a) shows MSD vs. time step. The value of self diffusivity calculated from the diffusive region of the plot is shown in Fig. 4.7.2.2. (b)

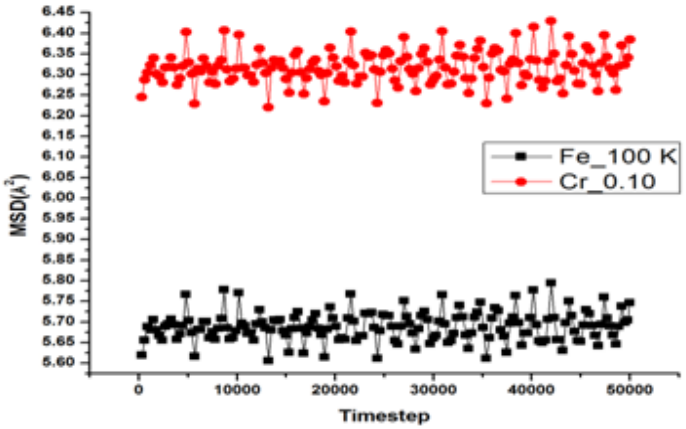

Fig.4.7.2.2 MSD vs. Time step plot of Fe-10%Cr alloys at temp.100 K

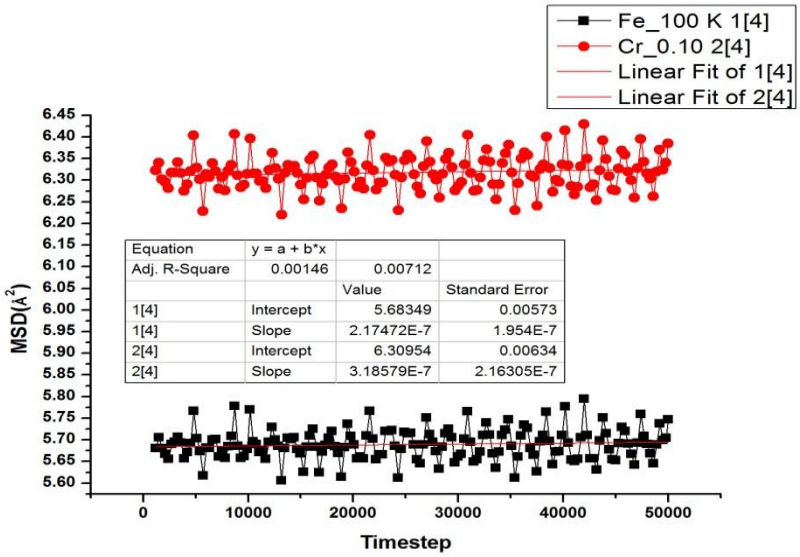

Equation	y = a + b*x		
Adj. R-Square	0.00146	0.00712	
		Value	Standard Error
1[4]	Intercept	5.68349	0.00573
1[4]	Slope	2.17472E-7	1.954E-7
2[4]	Intercept	6.30954	0.00634
2[4]	Slope	3.18579E-7	2.16305E-7

Fig.4.7.2.2 MSD vs. Time step (self-diffusivity value of Fe-10%Cr alloys at temp.100 K)

4.7.3 Creation of Fe-10%Cr alloys at temperature 300 K

Simulation box size of dimension 50 $Å^3$ containing 11,600 atoms were generated by running MD code. The pattern of writing the code for creating Fe-10%Cr alloys sample equilibrated at 300 K is same as code written for Fe-5%Cr alloys equilibrated at 50 K mention in appendix II.

4.7.3.1 VMD snapshots

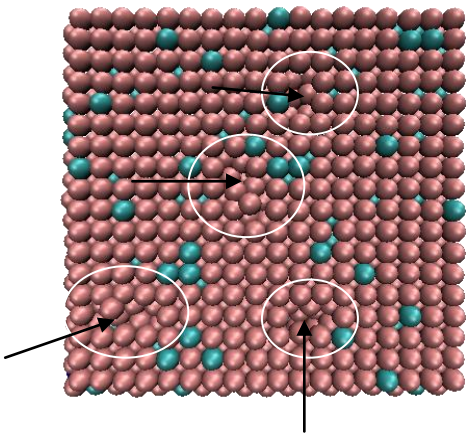

Fig.4.7.3.1 (a)

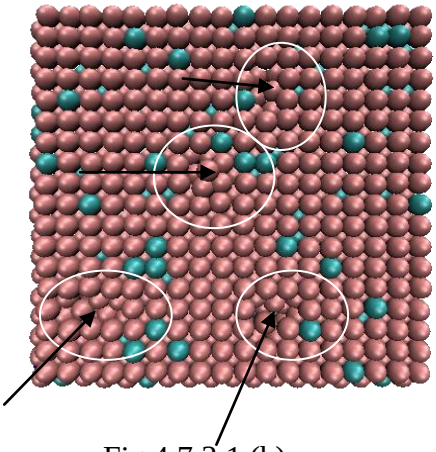

Fig.4.7.3.1 (b)

Fig.4.7.3.1 (a) & Fig.4.7.3.1 (b) shows VMD snapshots of Fe-10%Cr alloys at temp.300 K.

In the above VMD snapshots circle region show the vacancy created by MD code and arrow indicates the movement of atoms during running the MD code. Purple color indicates Fe atoms and blue color indicates Cr atoms.

4.7.3.2 MSD calculation

Self diffusivity of Fe & Cr has been calculated from MSD vs. time step plots at temperature 300 K. Fig.4.7.3.2 (a) shows MSD vs. time step. The value of self diffusivity calculated from the diffusive region of the plot is shown in Fig. 4.7.3.2. (b)

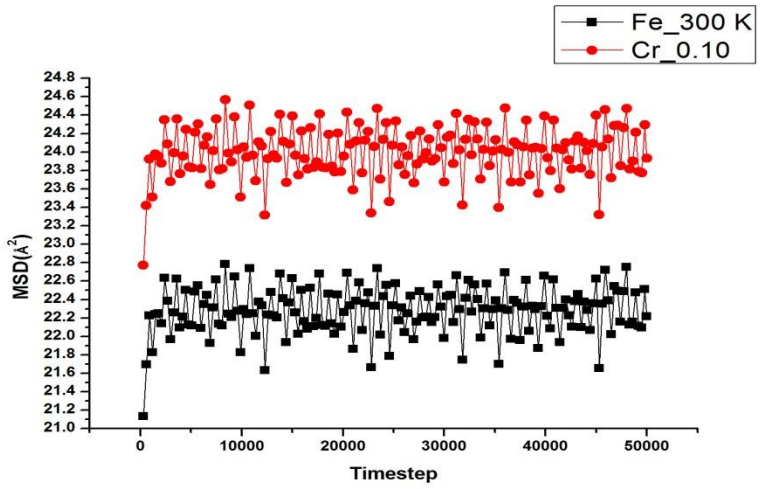

Fig.4.7.3.2 (a) MSD vs. Time step plot of Fe-10%Cr alloys at temp.300 K

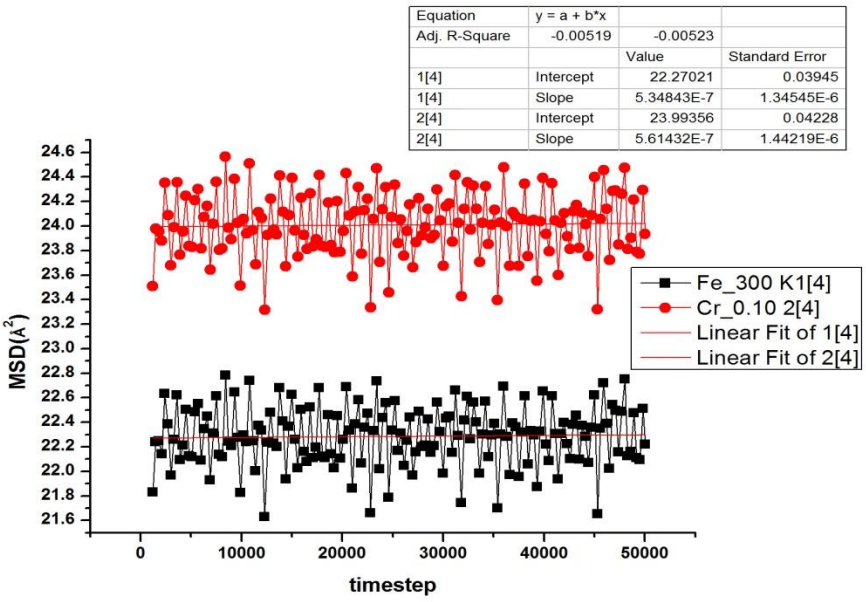

Fig.4.7.3.2 (b) MSD vs. Time step (self-diffusivity value of Fe-10%Cr alloys at temp.300 K)

4.7.4 Creation of Fe-10%Cr alloys at temperature 500 K

Simulation box size of dimension 50 $Å^3$ containing 11,600 atoms were generated by running MD code. The pattern of writing the code for creating Fe-10%Cr alloys sample equilibrated at 500 K is same as code written for Fe-5%Cr alloys equilibrated at 50 K mention in appendix II.

4.7.4.1 VMD snapshots

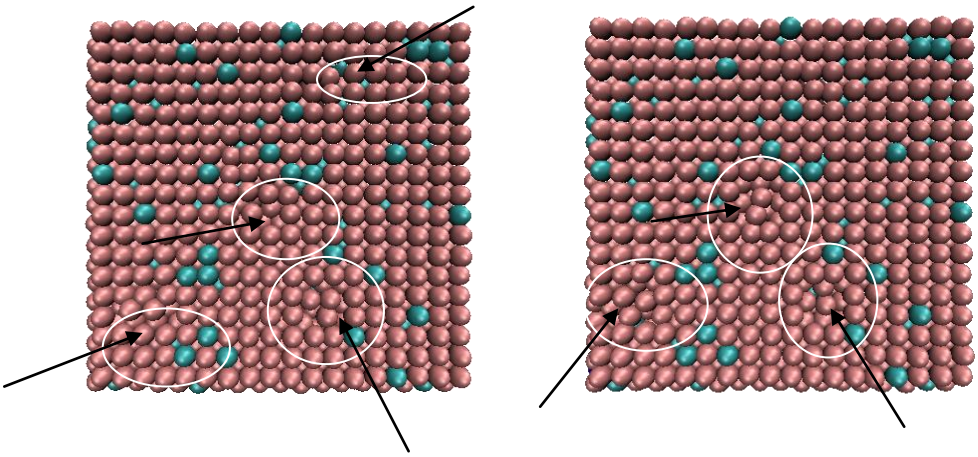

Fig.4.7.4.1 (a) Fig.4.7.4.1 (b)

Fig.4.7.4.1 (a) & Fig.4.7.4.1 (b) shows VMD snapshots of Fe-10%Cr alloys at temp.500 K.

In the above VMD snapshots circle region show the vacancy created by MD code and arrow indicates the movement of atoms during running the MD code. Purple color indicates Fe atoms and blue color indicates Cr atoms.

4.7.4.2 MSD calculation

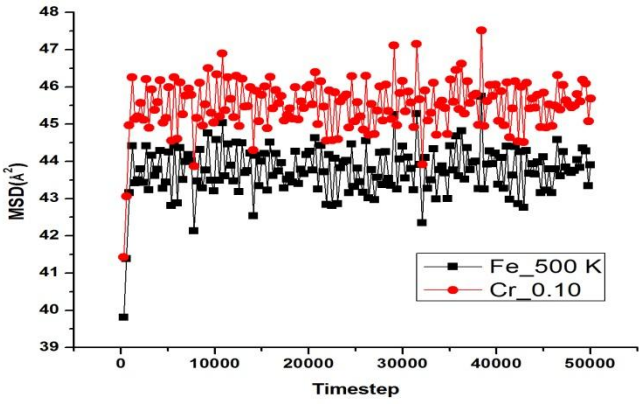

Fig.4.7.4.2 MSD vs. Time step plot of Fe-10%Cr alloys at temp.500 K

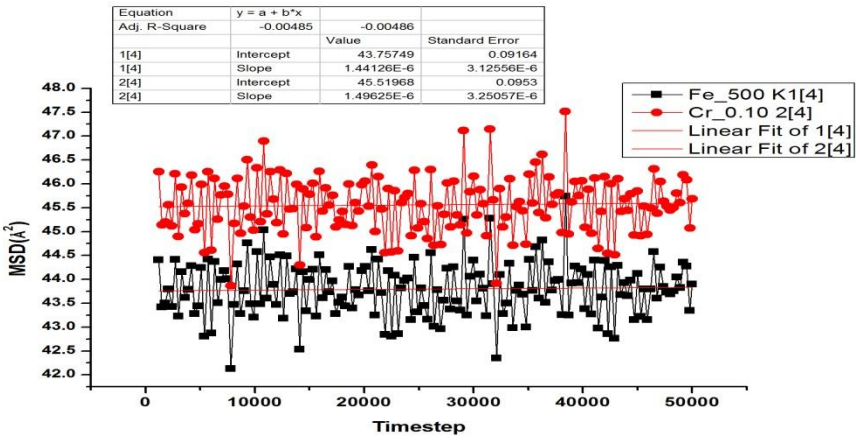

Fig.4.7.4.2 MSD vs. Time step (self-diffusivity value of Fe-10%Cr alloys at temp.500 K)

Self diffusivity of Fe & Cr has been calculated from MSD vs. time step plots at temperature 500 K. Fig.4.7.4.2 (a) shows MSD vs. time step. The value of self diffusivity calculated from the diffusive region of the plot is shown in Fig. 4.7.4.2. (b)

4.7.5 Creation of Fe-10%Cr alloys at temperature 700 K

Simulation box size of dimension 50 $Å^3$ containing 11,600 atoms were generated by running MD code. The pattern of writing the code for creating Fe-10%Cr alloys sample equilibrated at 700 K is same as code written for Fe-5%Cr alloys equilibrated at 50 K mention in appendix II.

4.7.5.1 VMD snapshots

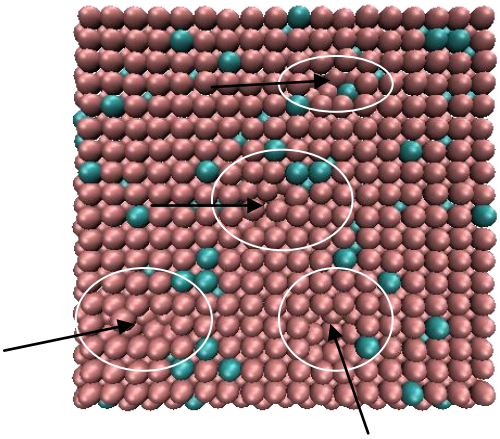

Fig.4.7.5.1 (a)

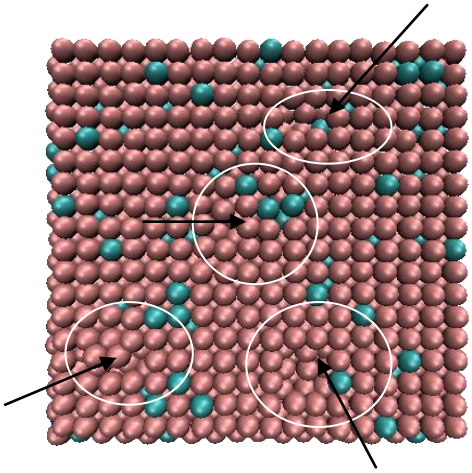

Fig.4.7.5.1 (b)

Fig.4.7.5.1 (a) & Fig.4.7.5.1 (b) shows VMD snapshots of Fe-10%Cr alloys at temp.500 K.

In the above VMD snapshots circle region show the vacancy created by MD code and arrow indicates the movement of atoms during running the MD code. Purple color indicates Fe atoms and blue color indicates Cr atoms.

4.7.5.2 MSD calculation

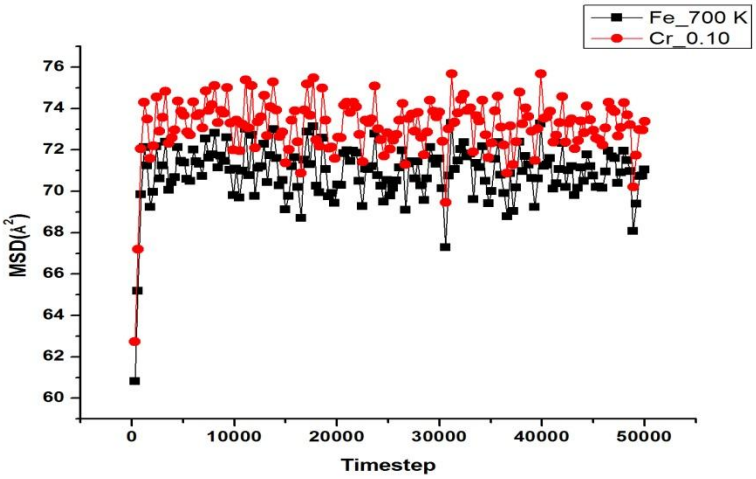

Fig.4.7.5.2 (a) MSD vs. Time step plot of Fe-10%Cr alloys at temp.700 K

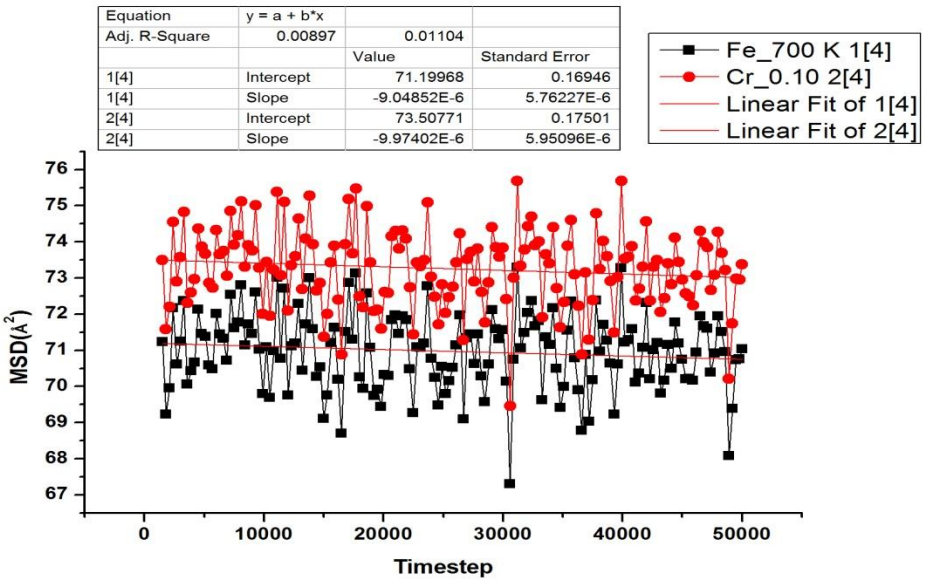

Fig.4.7.5.2 (b) MSD vs. Time step (self-diffusivity value of Fe-10%Cr alloys at temp.700 K)

Self diffusivity of Fe & Cr has been calculated from MSD vs. time step plots at temperature 700 K. Fig.4.7.5.2 (a) shows MSD vs. time step. The value of self diffusivity calculated from the diffusive region of the plot is shown in Fig. 4.7.5.2. (b)

4.7.6 Creation of Fe-10%Cr alloys at temperature 1000 K

Simulation box size of dimension 50 $Å^3$ containing 11,600 atoms were generated by running MD code. The pattern of writing the code for creating Fe-10%Cr alloys sample equilibrated at 1000 K is same as code written for Fe-5%Cr alloys equilibrated at 50 K mention in appendix II.

4.7.6.1 VMD snapshots

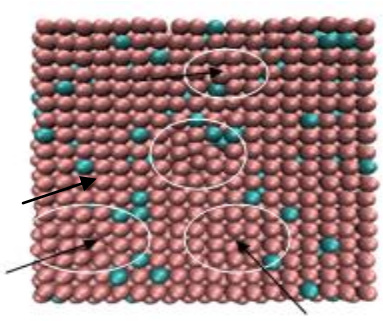

Fig.4.7.6.1 (a)

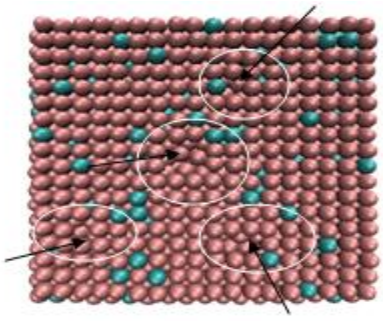

Fig.4.7.6.1 (b)

Fig.4.7.6.1 (a) & Fig.4.7.6.1 (b) shows VMD snapshots of Fe-10%Cr alloys at temp.1000 K.

In the above VMD snapshots circle region show the vacancy created by MD code and arrow indicates the movement of atoms during running the MD code. Purple color indicates Fe atoms and blue color indicates Cr atoms.

4.7.6.2 MSD calculation

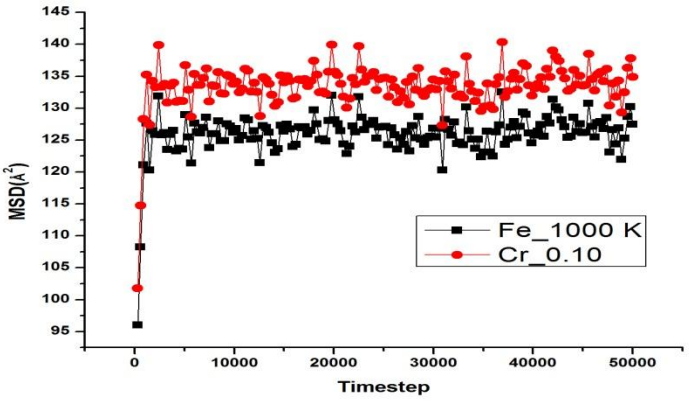

Fig.4.7.6.2 (a) MSD vs. Time step plot of Fe-10%Cr alloys at temp.1000 K

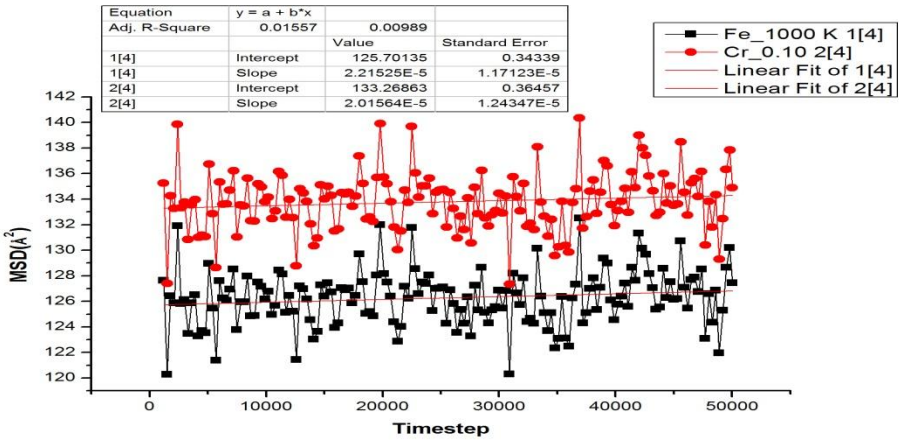

Fig.4.7.6.2 (b) MSD vs. Time step (self-diffusivity value of Fe-10%Cr alloys at temp.1000 K)

Self diffusivity of Fe & Cr has been calculated from MSD vs. time step plots at temperature 1000 K. Fig.4.7.6.2 (a) shows MSD vs. time step. The value of self diffusivity calculated from the diffusive region of the plot is shown in Fig. 4.7.6.2. (b)

4.8 Creation of Fe-15%Cr alloys

4.8.1 Creation of Fe-15%Cr alloys at temperature 50 K

Simulation box size of dimension 50 $Å^3$ containing 11,600 atoms were generated by running MD code. The pattern of writing the code for creating Fe-15%Cr alloys sample equilibrated at 50 K is same as code written for Fe-5%Cr alloys equilibrated at 50 K mention in appendix II.

4.8.1.1 VMD snapshots

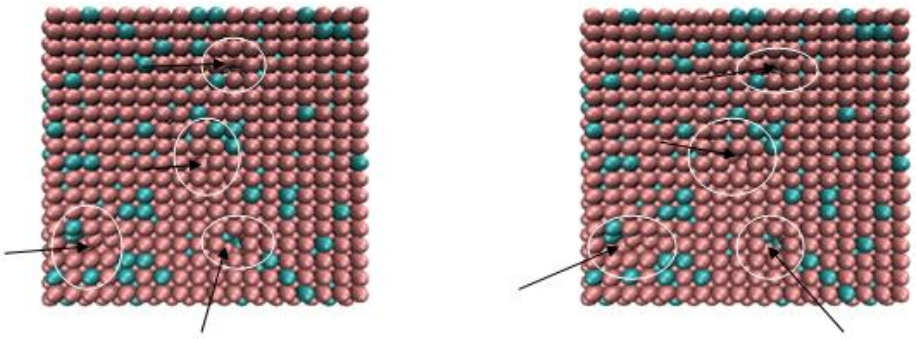

Fig.4.8.1.1 (a)

Fig.4.8.1.1 (b)

Fig.4.8.1.1 (a) & Fig.4.8.1.1 (b) shows VMD snapshots of Fe-15%Cr alloys at temp.50 K.

In the above VMD snapshots circle region show the vacancy created by MD code and arrow indicates the movement of atoms during running the MD code. Purple color indicates Fe atoms and blue color indicates Cr atoms.

4.8.1.2 MSD calculation

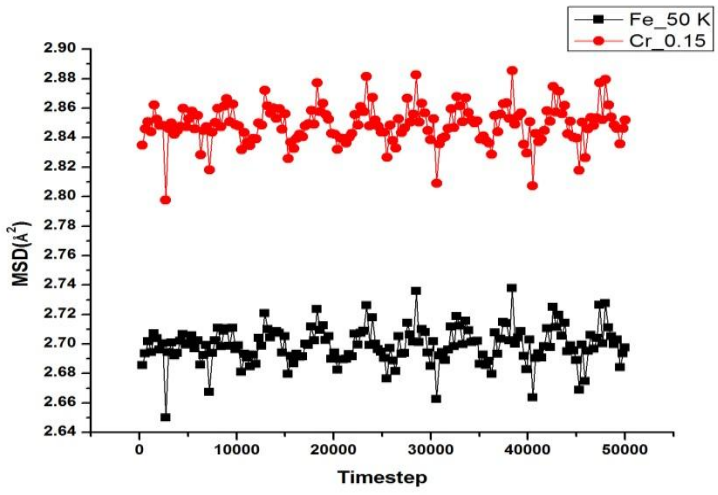

Fig .4.8.1.2 (a) MSD vs. Time step plot of Fe-15%Cr alloys at temp.50 K

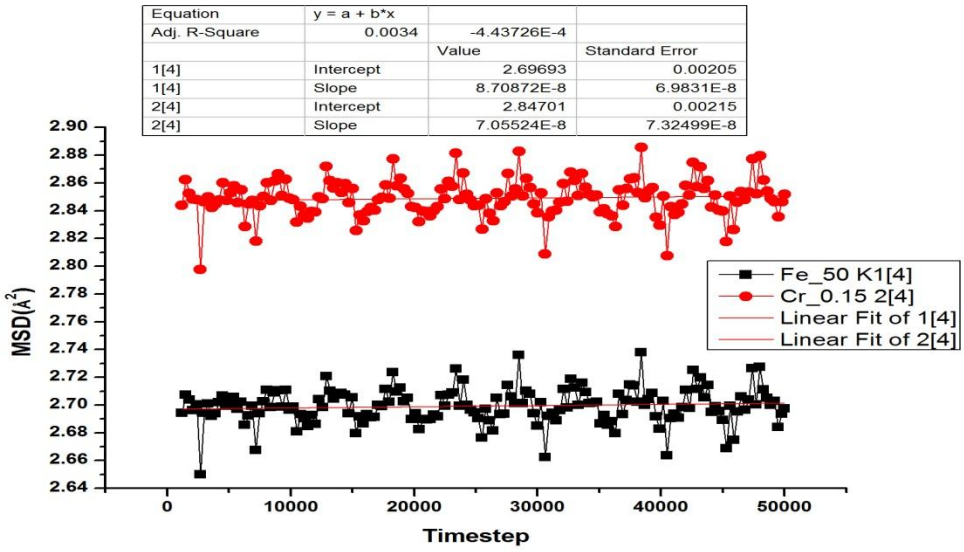

Fig .4.8.1.2 (b) MSD vs. Time step (self-diffusivity value of Fe-10%Cr alloys at temp.50 K)

Self diffusivity of Fe & Cr has been calculated from MSD vs. time step plots at temperature 50 K. Fig.4.8.1.2 (a) shows MSD vs. time step. The value of self diffusivity calculated from the diffusive region of the plot is shown in Fig. 4.8.1.2. (b)

4.8.2 Creation of Fe-15%Cr alloys at temperature 100 K

Simulation box size of dimension 50 $Å^3$ containing 11,600 atoms were generated by running MD code. The pattern of writing the code for creating Fe-15%Cr alloys sample equilibrated at 100 K is same as code written for Fe-5%Cr alloys equilibrated at 50 K mention in appendix II.

4.8.2.1 VMD snapshots

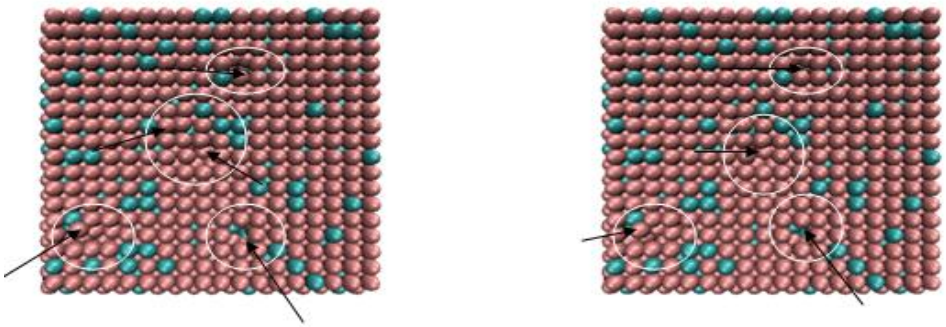

Fig.4.8.2.1 (a) Fig.4.8.2.1 (b)

Fig.4.8.2.1 (a) & Fig.4.8.2.1 (b) shows VMD snapshots of Fe-15%Cr alloys at temp.100 K.

In the above VMD snapshots circle region show the vacancy created by MD code and arrow indicates the movement of atoms during running the MD code. Purple color indicates Fe atoms and blue color indicates Cr atoms.

4.8.2.2 MSD calculation

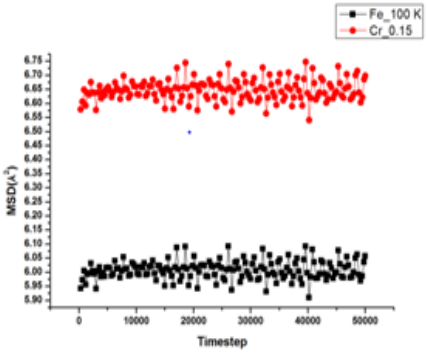

Fig.4.8.2.2 (a) MSD vs Timestep plot of Fe-15%Cr alloys at temp.100 K

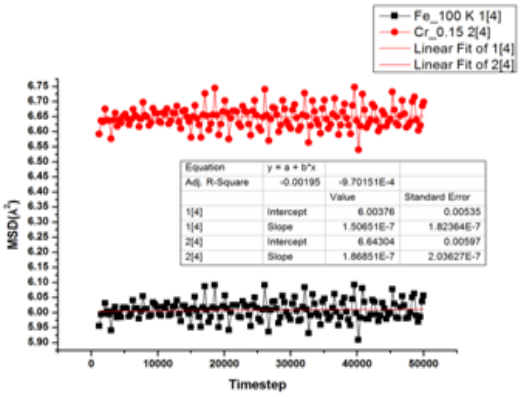

Fig.4.8.2.2 (b) MSD vs Timestep (self-diffusivity value of Fe-15%Cr alloys at temp.100 K)

Self diffusivity of Fe & Cr has been calculated from MSD vs. time step plot at temperature 100 K. Fig.4.8.2.2 (a) shows MSD vs. time step. The value of self diffusivity calculated from the diffusive region of the plot is shown in Fig. 4.8.2.2. (b)

4.8.3 Creation of Fe-15%Cr alloys at temperature 300 K

Simulation box size of dimension 50 $Å^3$ containing 11,600 atoms were generated by running MD code. The pattern of writing the code for creating Fe-15%Cr alloys sample equilibrated at 300 K is same as code written for Fe-5%Cr alloys equilibrated at 50 K mention in appendix II.

4.8.3.1 VMD snapshots

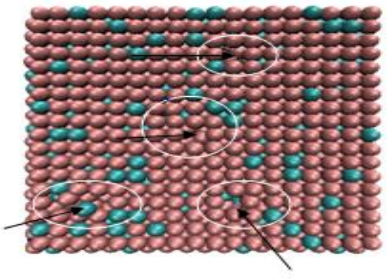

Fig.4.8.3.1 (a)

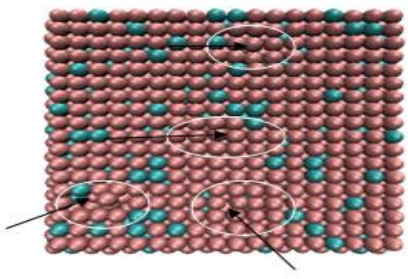

Fig.4.8.3.1 (b)

Fig.4.8.3.1 (a) & Fig.4.8.3.1 (b) shows VMD snapshots of Fe-15%Cr alloys at temp.300 K.

In the above VMD snapshots circle region show the vacancy created by MD code and arrow indicates the movement of atoms during running the MD code. Purple color indicates Fe atoms and blue color indicates Cr atoms.

4.8.3.2 MSD calculation

Self diffusivity of Fe & Cr has been calculated from MSD vs. time step plots at temperature 300 K. Fig.4.8.3.2 (a) shows MSD vs. time step. The value of self diffusivity calculated from the diffusive region of the plot is shown in Fig. 4.8.3.2. (b)

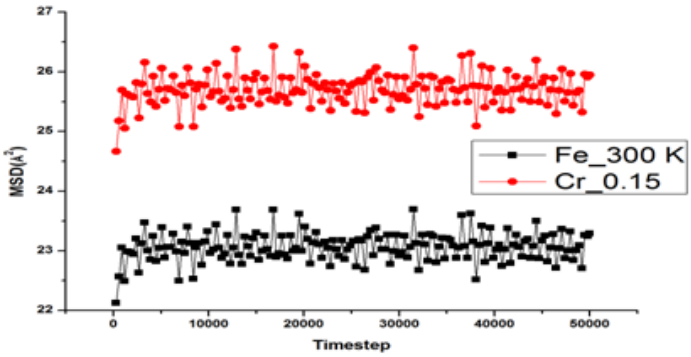

Fig.4.8.3.2 (a) MSD vs. Time step plot of Fe-15%Cr alloys at temp.300 K

Equation	y = a + b*x		
Adj. R-Square	-0.00108	-0.00268	
		Value	Standard Error
1[4]	Intercept	23.0417	0.0375
1[4]	Slope	1.16118E-6	1.27911E-6
2[4]	Intercept	25.68496	0.04174
2[4]	Slope	1.06997E-6	1.42354E-6

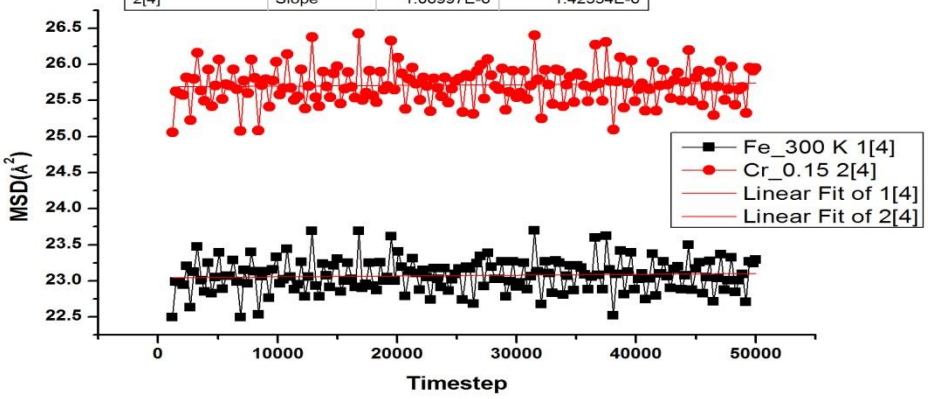

Fig.4.8.3.2 (b) MSD vs. Time step (self-diffusivity value of Fe-15%Cr alloys at temp.300 K)

4.8.4 Creation of Fe-15%Cr alloys at temperature 500 K

Simulation box size of dimension 50 $Å^3$ containing 11,600 atoms were generated by running MD code. The pattern of writing the code for creating Fe-15%Cr alloys sample equilibrated at 500 K is same as code written for Fe-5%Cr alloys equilibrated at 50 K mention in appendix II.

4.8.4.1 VMD snapshots

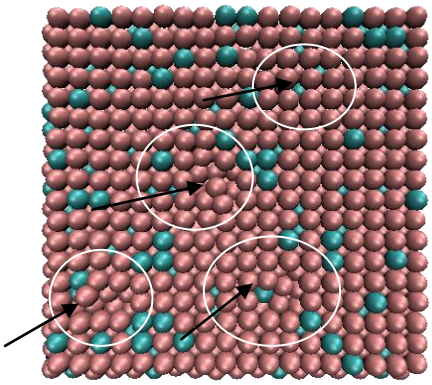

Fig.4.8.4.1 (a)

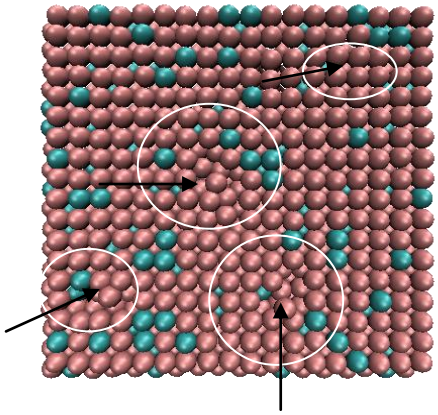

Fig.4.8.4.1 (b)

Fig.4.8.4.1 (a) & Fig.4.8.4.1 (b) shows VMD snapshots of Fe-15%Cr alloys at temp.500 K.

In the above VMD snapshots circle region show the vacancy created by MD code and arrow indicates the movement of atoms during running the MD code. Purple color indicates Fe atoms and blue color indicates Cr atoms.

4.8.4.2 MSD calculation

Self diffusivity of Fe & Cr has been calculated from MSD vs. time step plots at temperature 500 K. Fig.4.8.4.2 (a) shows MSD vs. time step. The value of self diffusivity calculated from the diffusive region of the plot is shown in Fig. 4.8.4.2. (b)

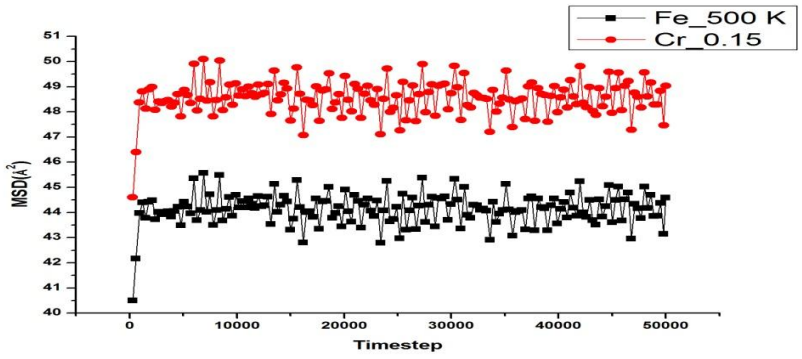

Fig.4.8.4.2 (a) MSD vs. Time step plot of Fe-15%Cr alloys at temp.500 K

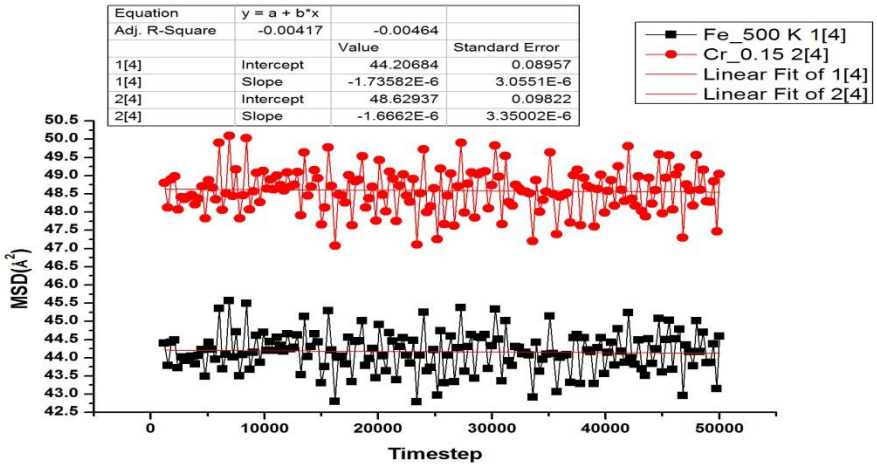

Fig.4.8.4.2 (b) MSD vs. Time step (self-diffusivity value of Fe-15%Cr alloys at temp.500 K)

4.8.5 Creation of Fe-15%Cr alloys at temperature 700 K

Simulation box size of dimension 50 $Å^3$ containing 11,600 atoms were generated by running MD code. The pattern of writing the code for creating Fe-15%Cr alloys sample equilibrated at 700 K is same as code written for Fe-5%Cr alloys equilibrated at 50 K mention in appendix II.

4.8.5.1 VMD snapshots

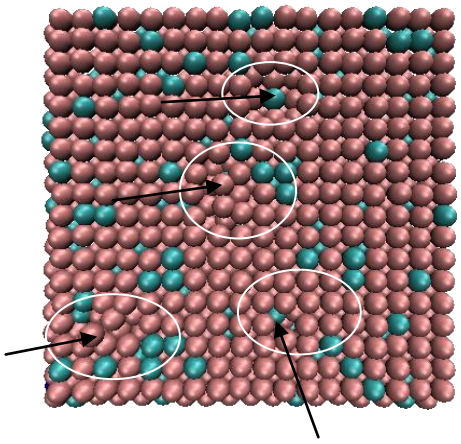

Fig. 4.8.5.1 (a)

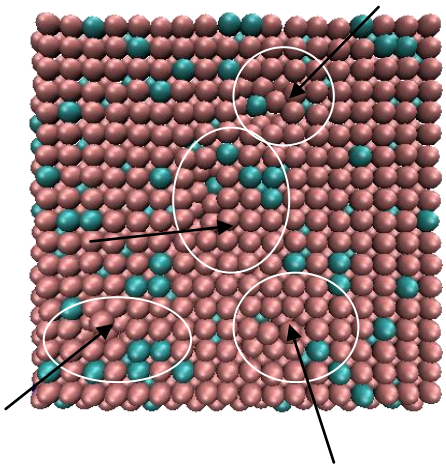

Fig.4.8.5.1 (b)

Fig.4.8.5.1 (a) & Fig.4.8.5.1 (b) shows VMD snapshots of Fe-15%Cr alloys at temp.700 K.

In the above VMD snapshots circle region show the vacancy created by MD code and arrow indicates the movement of atoms during running the MD code. Purple color indicates Fe atoms and blue color indicates Cr atoms.

4.8.5.2 MSD calculation

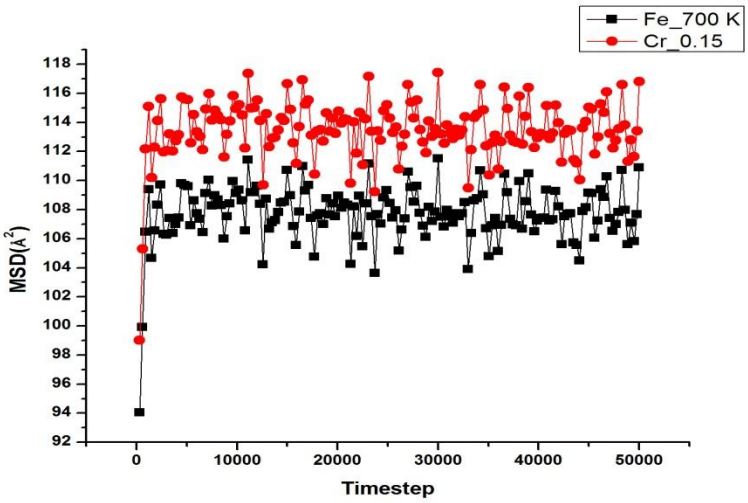

Fig.4.8.5.2 (a) MSD vs. Time step plot of Fe-15%Cr alloys at temp.700 K

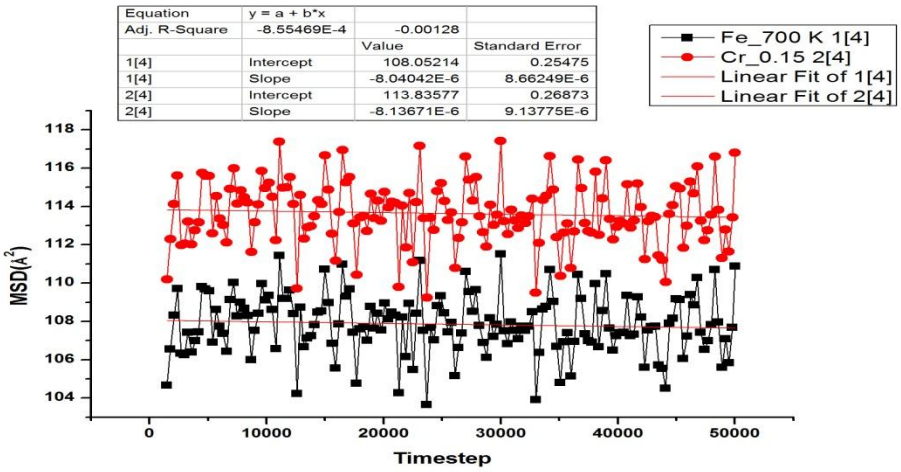

Fig.4.8.5.2 (b) MSD vs. Time step (self-diffusivity value of Fe-15%Cr alloys at temp.700 K)

Self diffusivity of Fe & Cr has been calculated from MSD vs. time step plots at temperature 700 K. Fig.4.8.5.2 (a) shows MSD vs. time step. The value of self diffusivity calculated from the diffusive region of the plot is shown in Fig. 4.8.5.2. (b)

4.8.6 Creation of Fe-15%Cr alloys at temperature 1000 K

Simulation box size of dimension 50 $Å^3$ containing 11,600 atoms were generated by running MD code. The pattern of writing the code for creating Fe-15%Cr alloys sample equilibrated at 1000 K is same as code written for Fe-5%Cr alloys equilibrated at 50 K mention in appendix II.

4.8.6.1 VMD snapshots

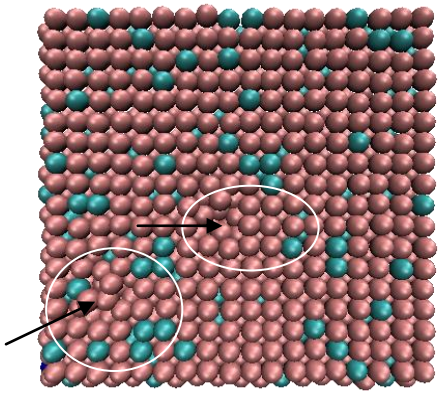

Fig.4.8.6.1 (a)

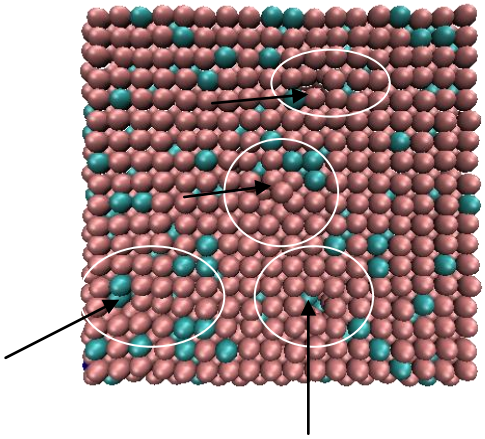

Fig.4.8.6.1 (b)

Fig.4.8.6.1 (a) & Fig.4.8.6.1 (b) shows VMD snapshots of Fe-15%Cr alloys at temp.1000 K.

In the above VMD snapshots circle region show the vacancy created by MD code and arrow indicates the movement of atoms during running the MD code. Purple color indicates Fe atoms and blue color indicates Cr atoms.

4.8.6.2 MSD calculation

Self diffusivity of Fe & Cr has been calculated from MSD vs. time step plots at temperature 1000 K. Fig.4.8.6.2 (a) shows MSD vs. time step. The value of self diffusivity calculated from the diffusive region of the plot is shown in Fig. 4.8.6.2. (b)

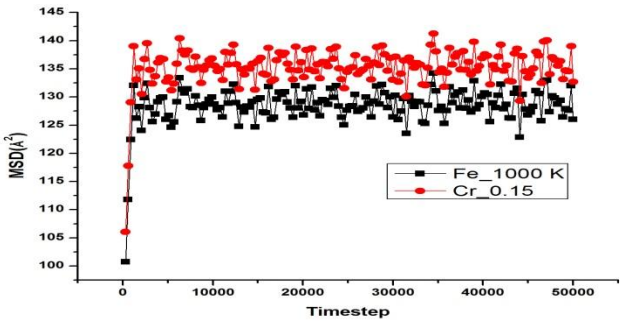

Fig.4.8.6.2 (a) MSD vs. Time step plot of Fe-15%Cr alloys at temp.1000 K

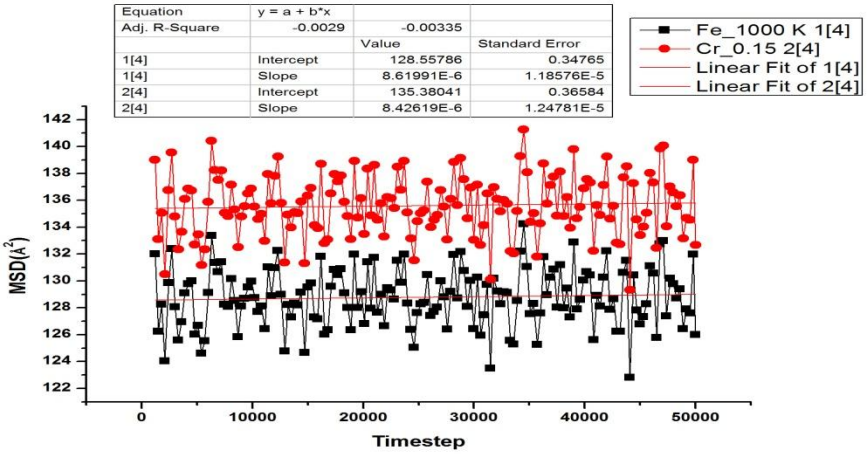

Fig.4.8.6.2 (b) MSD vs. Time step (self-diffusivity value of Fe-15%Cr alloys at temp.1000 K)

4.9 Creation of Fe-20%Cr alloys

4.9.1 Creation of Fe-20%Cr alloys at temperature 50 K

Simulation box size of dimension 50 $Å^3$ containing 11,600 atoms were generated by running MD code. The pattern of writing the code for creating Fe-20%Cr alloys sample equilibrated at 50 K is same as code written for Fe5%-Cr alloys equilibrated at 50 K mention in appendix II.

4.9.1.1 VMD snapshots

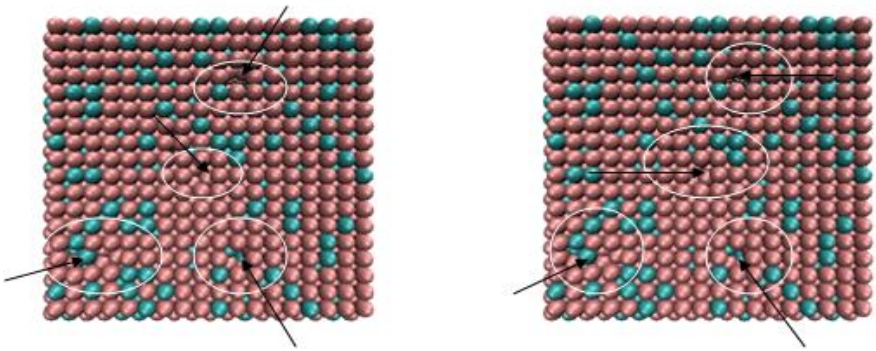

Fig.4.9.1.1 (a)

Fig.4.9.1.1 (b)

Fig.4.9.1.1 (a) & Fig.4.9.1.1 (b) shows VMD snapshots of Fe-20%Cr alloys at temp.50 K.

In the above VMD snapshots circle region show the vacancy created by MD code and arrow indicates the movement of atoms during running the MD code. Purple color indicates Fe atoms and blue color indicates Cr atoms.

4.9.1.2 MSD calculation

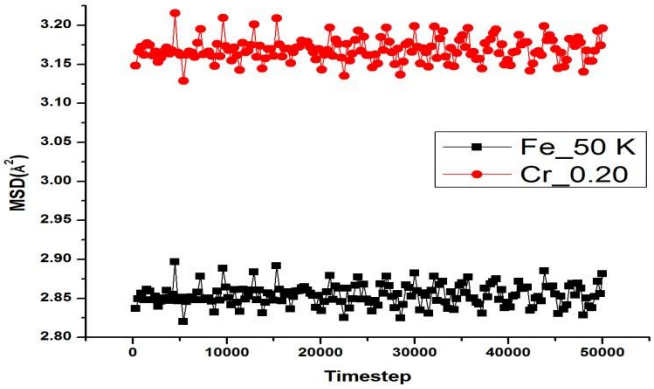

Fig.4.9.1.2 (a) MSD vs. Time step plot of Fe-20%Cr alloys at temp.50 K

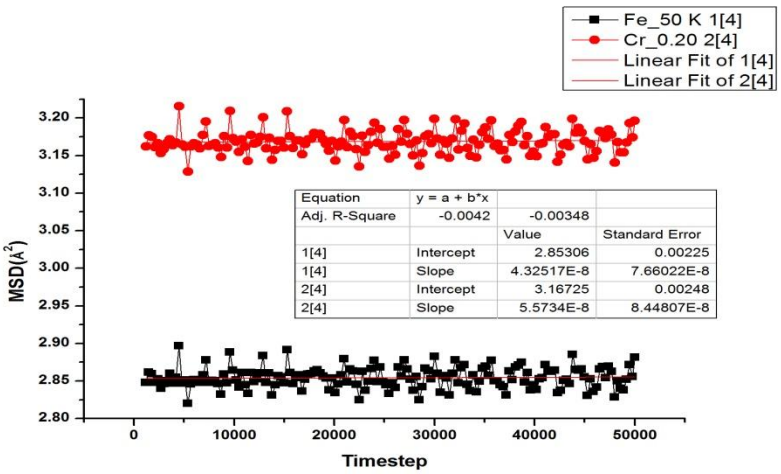

Fig.4.9.1.2 (b) MSD vs. Time step (self-diffusivity value of Fe-20%Cr alloys at temp.50 K)

Self diffusivity of Fe & Cr has been calculated from MSD vs. time step plots at temperature 50 K. Fig.4.9.1.2 (a) shows MSD vs. time step. The value of self diffusivity calculated from the diffusive region of the plot is shown in Fig. 4.9.1.2. (b)

4.9.2 Creation of Fe-20%Cr alloys at temperature 100 K

Simulation box size of dimension 50 $Å^3$ containing 11,600 atoms were generated by running MD code. The pattern of writing the code for creating Fe-20%Cr alloys sample equilibrated at 100 K is same as code written for Fe-5%Cr alloys equilibrated at 50 K mention in appendix II.

4.9.2.1 VMD snapshots

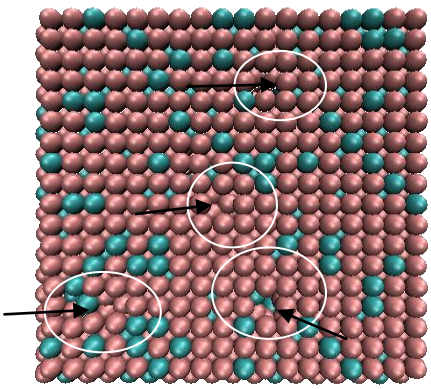

Fig.4.9.2.1 (a)

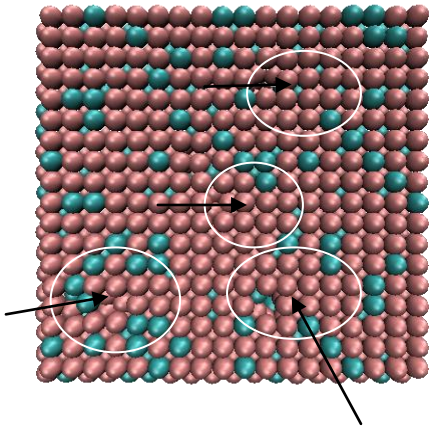

Fig.4.9.2.1 (b)

Fig.4.9.2.1 (a) & Fig.4.9.2.1 (b) shows VMD snapshots of Fe-20%Cr alloys at temp.100 K.

In the above VMD snapshots circle region show the vacancy created by MD code and arrow indicates the movement of atoms during running the MD code. Purple color indicates Fe atoms and blue color indicates Cr atoms.

4.9.2.2 MSD calculation

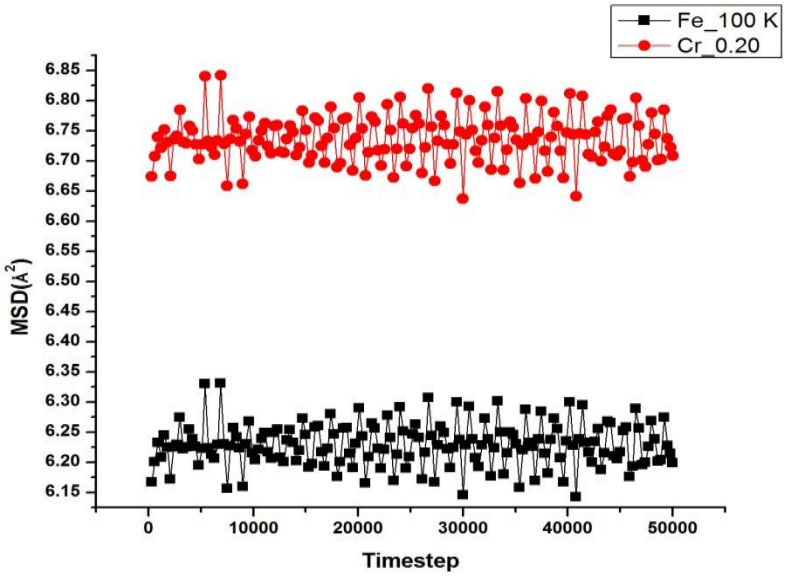

Fig.4.9.2.2 (a) MSD vs. Time step plot of Fe-20%Cr alloys at temp.100 K

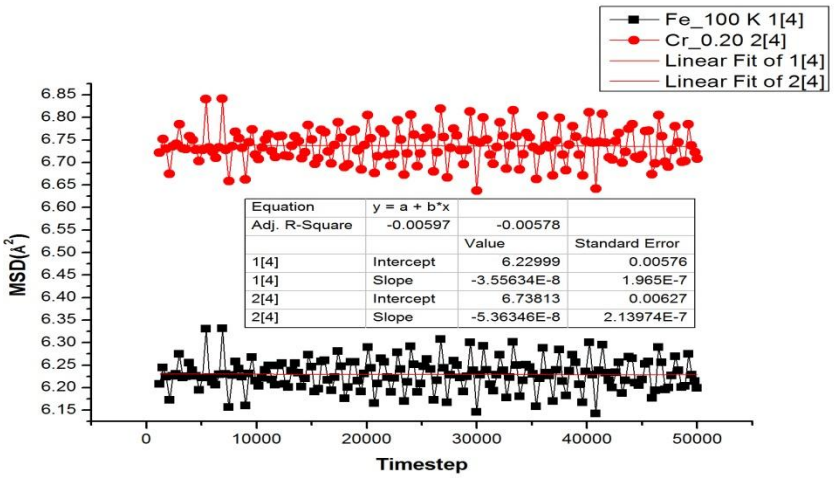

Fig.4.9.2.2 (b) MSD vs. Time step (self-diffusivity value of Fe-20%Cr alloys at temp.100 K)

Self diffusivity of Fe & Cr has been calculated from MSD vs. time step plots at temperature 100 K. Fig.4.9.2.2 (a) shows MSD vs. time step. The value of self diffusivity calculated from the diffusive region of the plot is shown in Fig. 4.9.2.2. (b)

4.9.3 Creation of Fe-20%Cr alloys at temperature 300 K

Simulation box size of dimension 50 $Å^3$ containing 11,600 atoms were generated by running MD code. The pattern of writing the code for creating Fe-20%Cr alloys sample equilibrated at 300 K is same as code written for Fe-5%Cr alloys equilibrated at 50 K mention in appendix II.

4.9.3.1 VMD snapshots

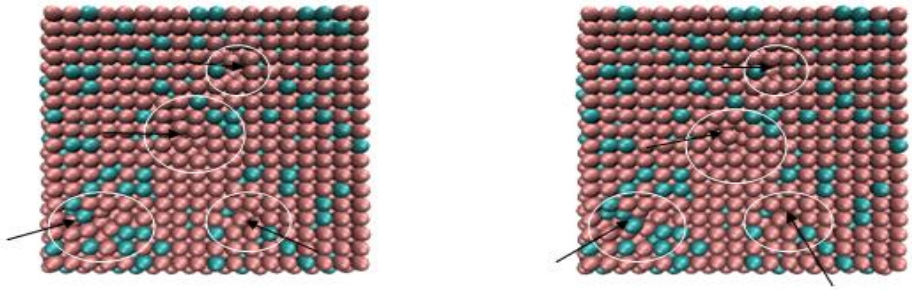

Fig.4.9.3.1 (a)

Fig.4.9.3.1 (b)

Fig.4.9.3.1 (a) & Fig.4.9.3.1 (b) shows VMD snapshots of Fe-20%Cr alloys at temp.300 K.

In the above VMD snapshots circle region show the vacancy created by MD code and arrow indicates the movement of atoms during running the MD code. Purple color indicates Fe atoms and blue color indicates Cr atoms.

4.9.3.2 MSD calculation

Self diffusivity of Fe & Cr has been calculated from MSD vs. time step plots at temperature 300 K. Fig.4.9.3.2 (a) shows MSD vs. time step. The value of self diffusivity calculated from the diffusive region of the plot is shown in Fig. 4.9.3.2. (b)

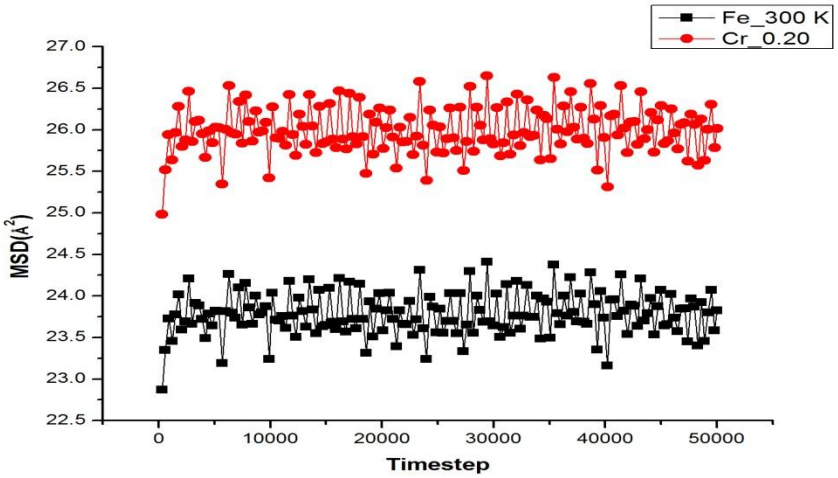

Fig.4.9.3.2 (a) MSD vs. Time step plot of Fe-20%Cr alloys at temp.300 K

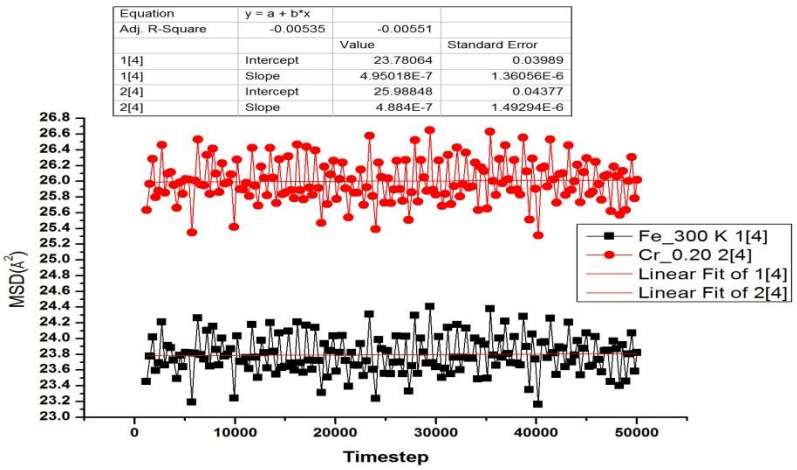

Fig.4.9.3.2 (b) MSD vs. Time step (self-diffusivity value of Fe-20%Cr alloys at temp.300 K)

4.9.4 Creation of Fe-20%Cr alloys at temperature 500 K

Simulation box size of dimension 50 $Å^3$ containing 11,600 atoms were generated by running MD code. The pattern of writing the code for creating Fe-20%Cr alloys sample equilibrated at 500 K is same as code written for Fe-5%Cr alloys equilibrated at 50 K mention in appendix II.

4.9.4.1 VMD snapshots

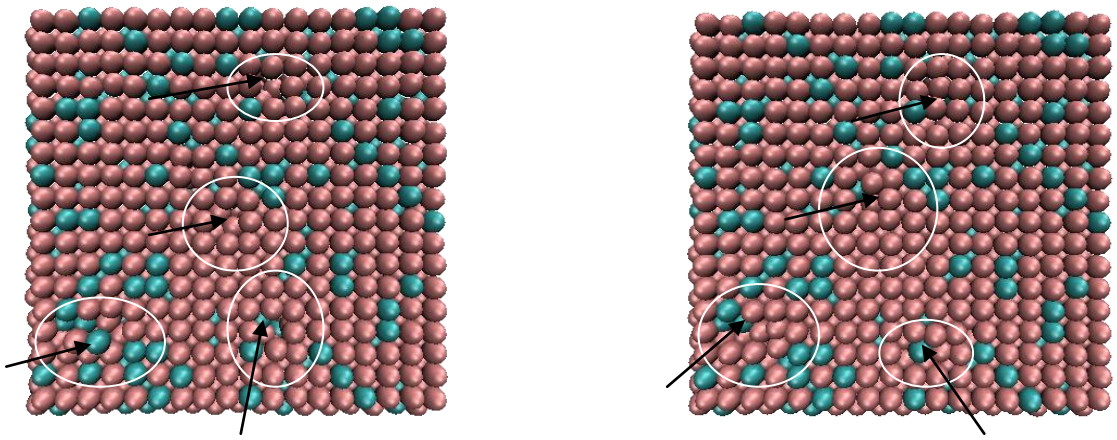

Fig.4.9.4.1 (a)

Fig.4.9.4.1 (b)

Fig.4.9.4.1 (a) & Fig.4.9.4.1 (b) shows VMD snapshots of Fe-20%Cr alloys at temp.500 K.

In the above VMD snapshots circle region show the vacancy created by MD code and arrow indicates the movement of atoms during running the MD code. Purple color indicates Fe atoms and blue color indicates Cr atoms.

4.9.4.2 MSD calculation

Self diffusivity of Fe & Cr has been calculated from MSD vs. time step plots at temperature 500 K. Fig.4.9.4.2 (a) shows MSD vs. time step. The value of self diffusivity calculated from the diffusive region of the plot is shown in Fig. 4.9.4.2. (b)

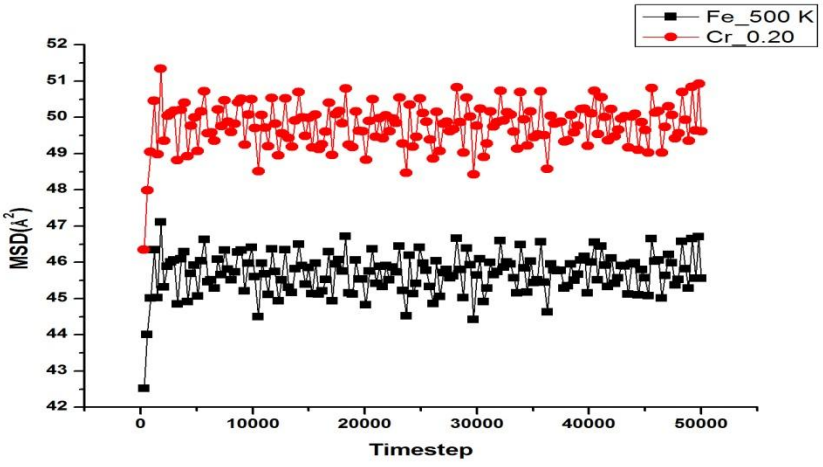

Fig.4.9.4.2 (a) MSD vs. Time step plot of Fe-20%Cr alloys at temp.500 K

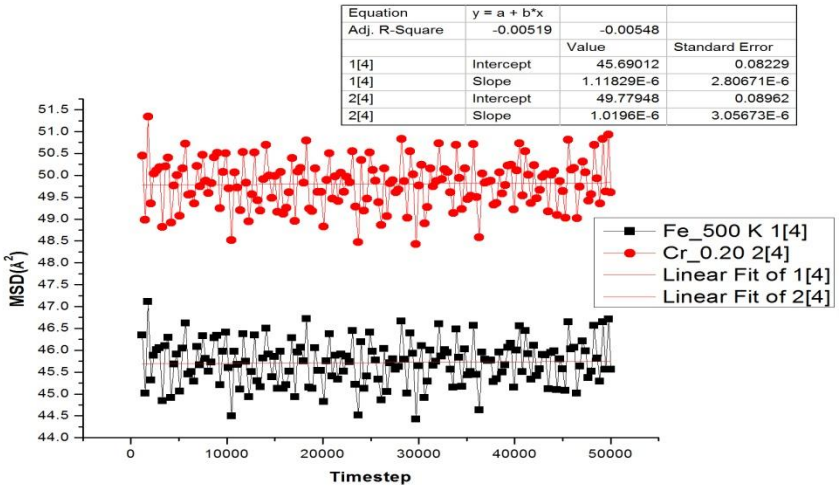

Fig.4.9.4.2 (b) MSD vs. Time step (self-diffusivity value of Fe-20%Cr alloys at temp.500 K)

4.9.5 Creation of Fe-20%Cr alloys at temperature 700 K

Simulation box size of dimension 50 $Å^3$ containing 11,600 atoms were generated by running MD code. The pattern of writing the code for creating Fe-20%Cr alloys sample equilibrated at 700 K is same as code written for Fe-5%Cr alloys equilibrated at 50 K mention in appendix II.

4.9.5.1 VMD snapshots

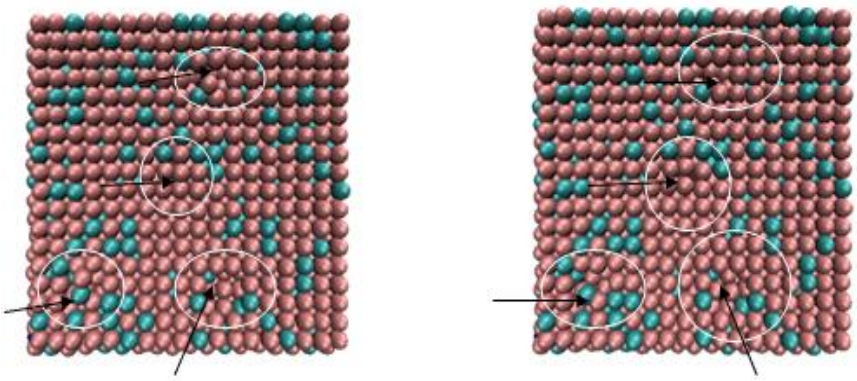

Fig.4.9.5.1 (a) Fig.4.9.5.1 (b)

Fig.4.9.5.1 (a) & Fig.4.9.5.1 (b) shows VMD snapshots of Fe-20%Cr alloys at temp.700 K.

In the above VMD snapshots circle region show the vacancy created by MD code and arrow indicates the movement of atoms during running the MD code. Purple color indicates Fe atoms and blue color indicates Cr atoms.

4.9.5.2 MSD calculation

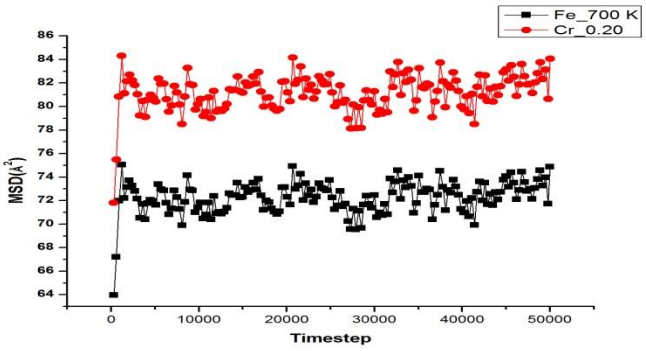

Fig.4.9.5.2 (a) MSD vs. Time step plot of Fe-20%Cr alloys at temp.700 K

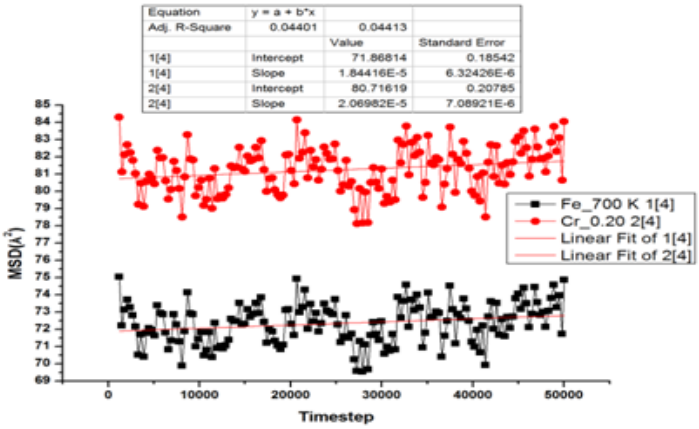

Fig.4.9.5.2 (b) MSD vs. Time step (self-diffusivity value of Fe-20%Cr alloys at temp.700 K)

Self diffusivity of Fe & Cr has been calculated from MSD vs. time step plots at temperature 700 K. Fig.4.9.5.2 (a) shows MSD vs. time step. The value of self diffusivity calculated from the diffusive region of the plot is shown in Fig. 4.9.5.2. (b)

4.9.6 Creation of Fe-20%Cr alloys at temperature 1000 K

Simulation box size of dimension 50 $Å^3$ containing 11,600 atoms were generated by running MD code. The pattern of writing the code for creating Fe-20%Cr alloys sample equilibrated at 1000 K is same as code written for Fe-5%Cr alloys equilibrated at 50 K mention in appendix II.

4.9.6.1 VMD snapshots

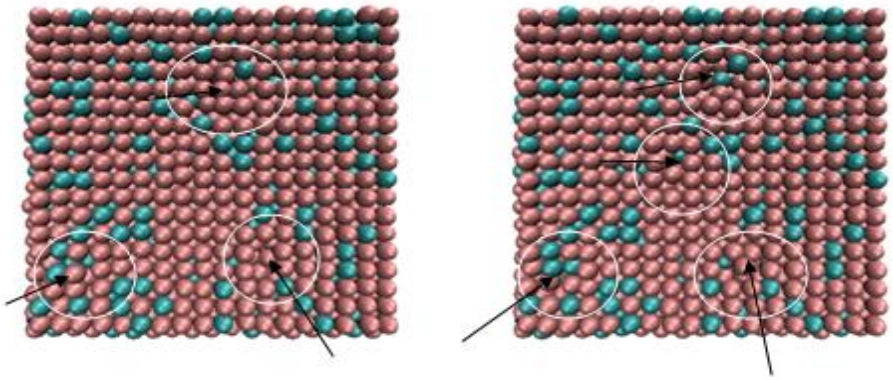

Fig.4.9.6.1 (a)

Fig.4.9.6.1 (b)

Fig.4.9.6.1 (a) & Fig.4.9.6.1 (b) shows VMD snapshots of Fe-20%Cr alloys at temp.1000 K.

In the above VMD snapshots circle region show the vacancy created by MD code and arrow indicates the movement of atoms during running the MD code. Purple color indicates Fe atoms and blue color indicates Cr atoms.

4.9.6.2 MSD calculation

Self diffusivity of Fe & Cr has been calculated from MSD vs. time step plots at temperature 700 K. Fig.4.9.6.2 (a) shows MSD vs. time step. The value of self diffusivity calculated from the diffusive region of the plot is shown in Fig. 4.9.6.2. (b)

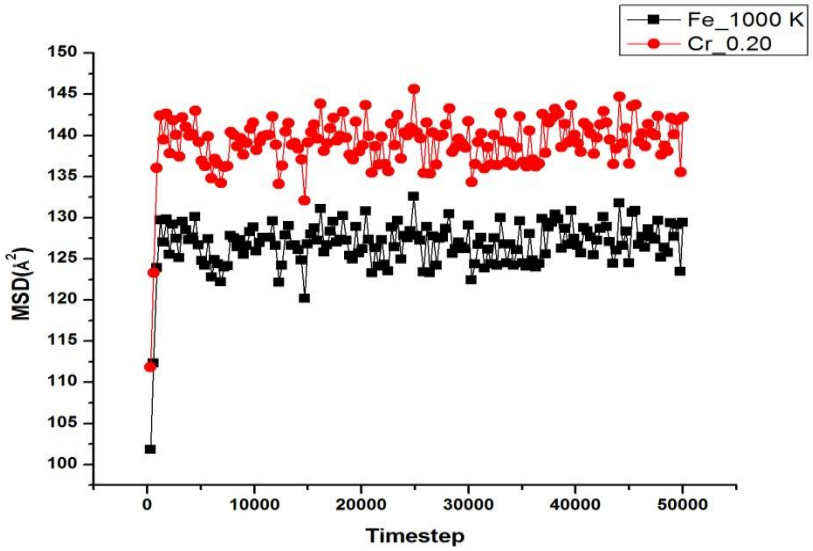

Fig.4.9.6.2 (a) MSD vs. Time step plot of Fe-20%Cr alloys at temp.1000 K

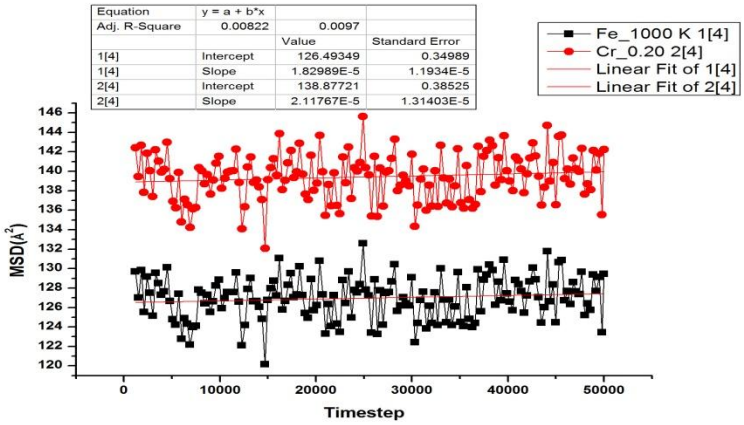

Fig.4.9.6.2 (b) MSD vs. Time step (self-diffusivity value of Fe-20%Cr alloys at temp.1000 K)

4.10 Creation of Fe-25%Cr alloys

4.10.1 Creation of Fe-25%Cr alloys at temperature 50 K

Simulation box size of dimension 50 $Å^3$ containing 11,600 atoms were generated by running MD code. The pattern of writing the code for creating Fe-25%Cr alloys sample equilibrated at 50 K is same as code written for Fe-5%Cr alloys equilibrated at 50 K mention in appendix II.

4.10.1.1 VMD snapshots

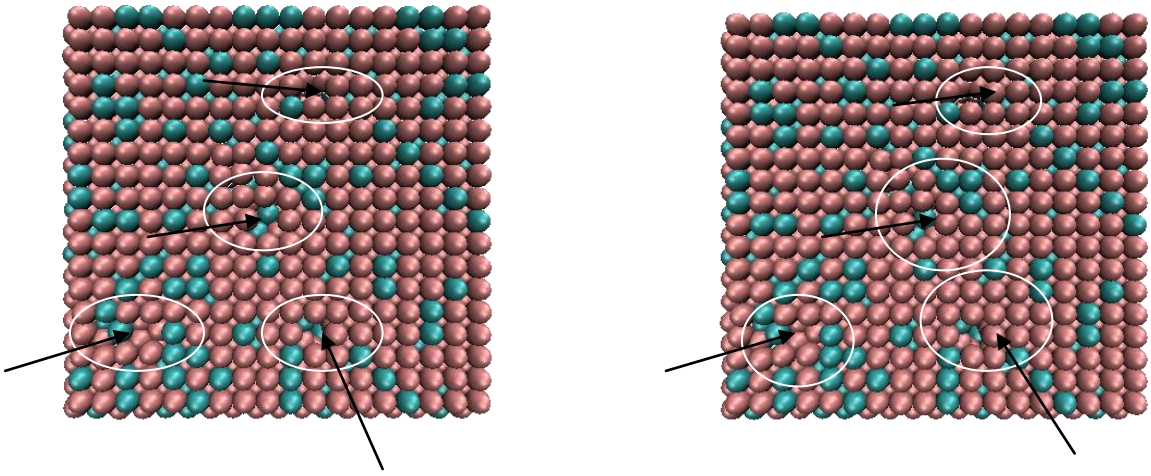

Fig.4.10.1.1 (a) Fig.4.10.1.1 (b)

Fig.4.10.1.1 (a) & Fig.4.10.1.1 (b) shows VMD snapshots of Fe-25%Cr alloys at temp.50 K.

In the above VMD snapshots circle region show the vacancy created by MD code and arrow indicates the movement of atoms during running the MD code. Purple color indicates Fe atoms and blue color indicates Cr atoms.

4.10.1.2 MSD calculation

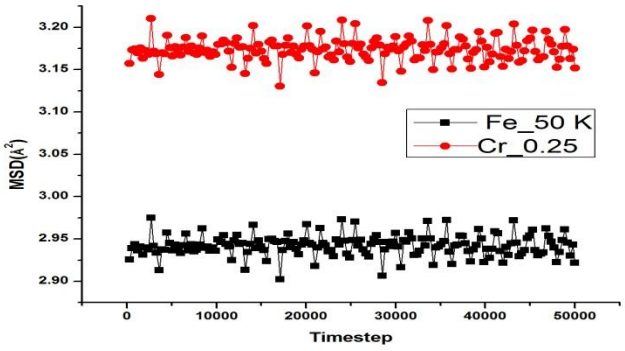

Fig.4.10.1.2 (a) MSD vs. Time step plot of Fe-25%Cr alloys at temp.50 K

Self diffusivity of Fe & Cr has been calculated from MSD vs. time step plots at temperature 50 K. Fig.4.10.1.2 (a) shows MSD vs. time step. The value of self diffusivity calculated from the diffusive region of the plot is shown in Fig. 4.10.1.2. (b)

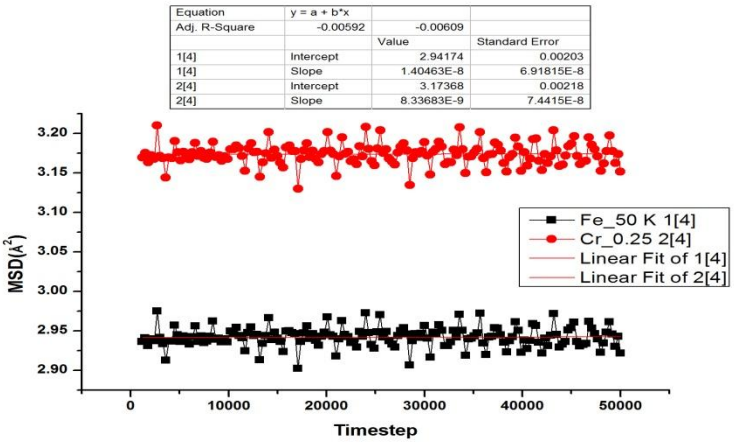

Fig.4.10.1.2 (b) MSD vs. Time step (self-diffusivity value of Fe-25%Cr alloys at temp.50 K)

4.10.2 Creation of Fe-25%Cr alloys at temperature 100 K

Simulation box size of dimension 50 $Å^3$ containing 11,600 atoms were generated by running MD code. The pattern of writing the code for creating Fe-25%Cr alloys sample equilibrated at 100 K is same as code written for Fe-5%Cr alloys equilibrated at 50 K mention in appendix II.

4.10.2.1. VMD snapshots

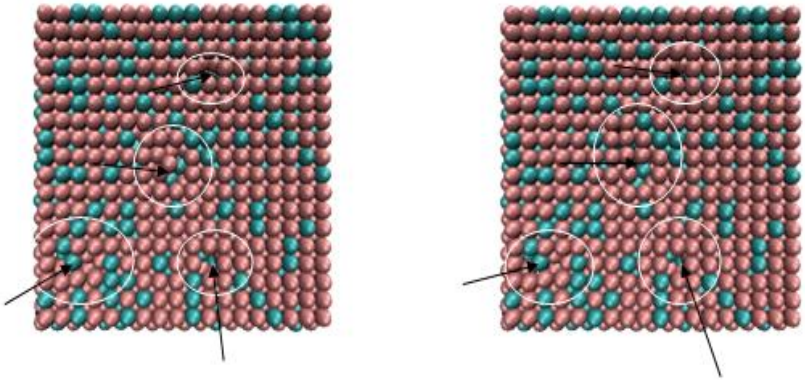

Fig.4.10.2.1 (a)

Fig.4.10.2.1 (b)

Fig.4.10.2.1 (a) & Fig.4.10.2.1 (b) shows VMD snapshots of Fe-25%Cr alloys at temp.100 K.

In the above VMD snapshots circle region show the vacancy created by MD code and arrow indicates the movement of atoms during running the MD code. Purple color indicates Fe atoms and blue color indicates Cr atoms.

4.10.2.2 MSD calculation

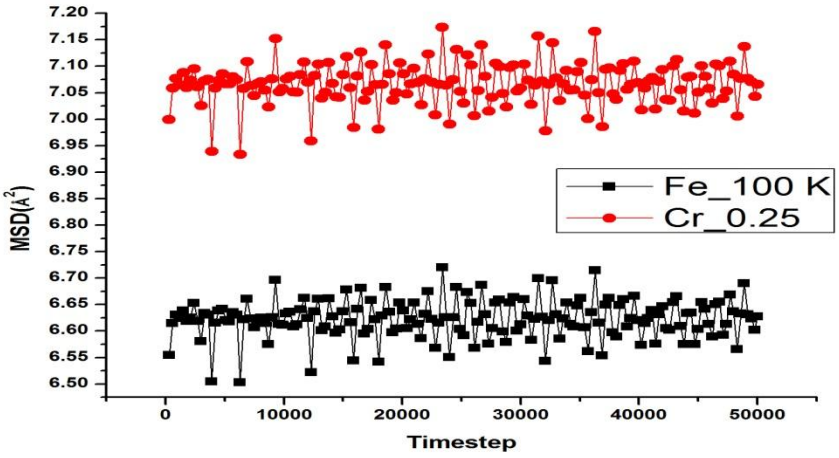

Fig.4.10.2.2 (a) MSD vs. Time step plot of Fe-25%Cr alloys at temp.100 K

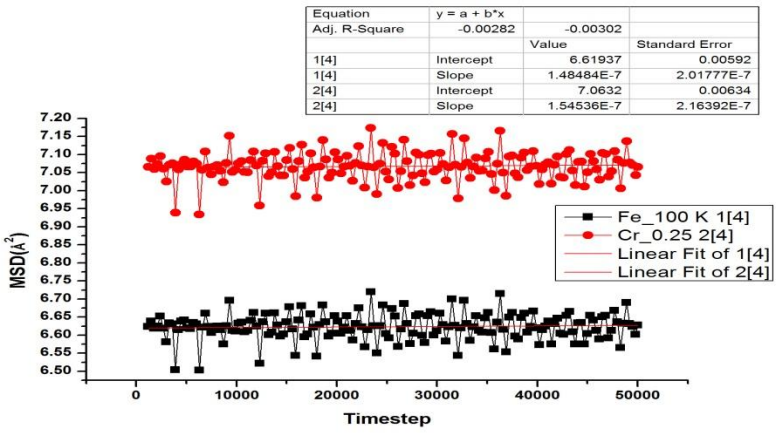

Fig.4.10.2.2 (b) MSD vs. Time step (self-diffusivity value of Fe-25%Cr alloys at temp.100 K)

Self diffusivity of Fe & Cr has been calculated from MSD vs. time step plots at temperature 100 K. Fig.4.10.2.2 (a) shows MSD vs. time step. The value of self diffusivity calculated from the diffusive region of the plot is shown in Fig. 4.10.2.2. (b)

4.10.3 Creation of Fe-25%Cr alloys at temperature 300 K

Simulation box size of dimension 50 $Å^3$ containing 11,600 atoms were generated by running MD code. The pattern of writing the code for creating Fe-25%Cr alloys sample equilibrated at 300 K is same as code written for Fe-5%Cr alloys equilibrated at 50 K mention in appendix II.

4.10.3.1 VMD snapshots

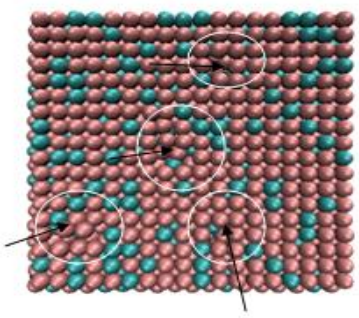

Fig.4.10.3.1 (a)

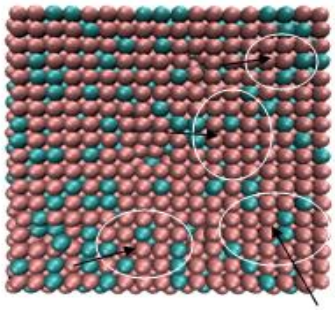

Fig.4.10.3.1 (b)

Fig.4.10.3.1 (a) & Fig.4.10.3.1 (b) shows VMD snapshots of Fe-25%Cr alloys at temp.300 K.

In the above VMD snapshots circle region show the vacancy created by MD code and arrow indicates the movement of atoms during running the MD code. Purple color indicates Fe atoms and blue color indicates Cr atoms.

4.10.3.2 MSD calculation

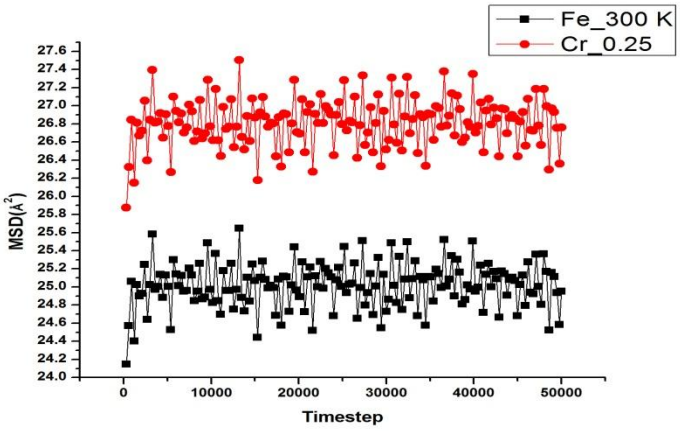

Fig.4.10.3.2 (a) MSD vs. Time step plot of Fe-25%Cr alloys at temp.300 K

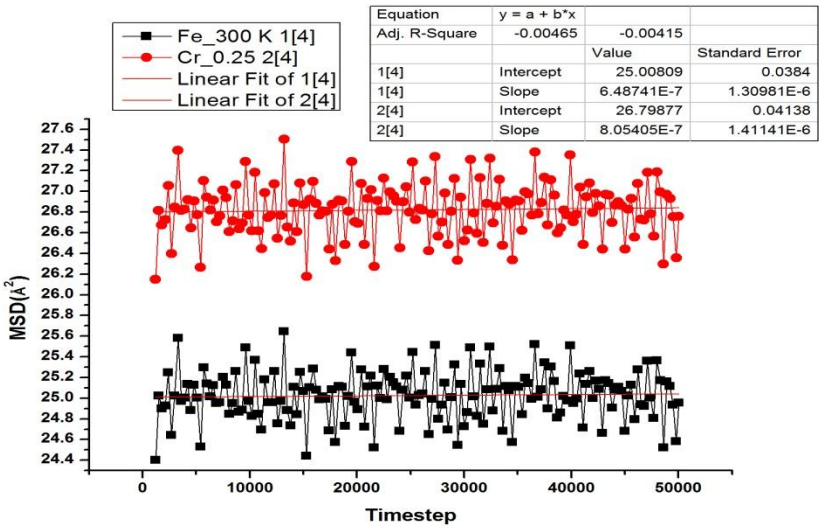

Fig.4.10.3.2 (b) MSD vs. Time step (self-diffusivity value of Fe-25%Cr alloys at temp.300 K)

Self diffusivity of Fe & Cr has been calculated from MSD vs. time step plots at temperature 300 K. Fig.4.10.3.2 (a) shows MSD vs. time step. The value of self diffusivity calculated from the diffusive region of the plot is shown in Fig. 4.10.3.2. (b)

4.10.4 Creation of Fe-25%Cr alloys at temperature 500 K

Simulation box size of dimension 50 $Å^3$ containing 11,600 atoms were generated by running MD code. The pattern of writing the code for creating Fe-25%Cr alloys sample equilibrated at 500 K is same as code written for Fe-5%Cr alloys equilibrated at 50 K mention in appendix II.

4.10.4.1 VMD snapshots

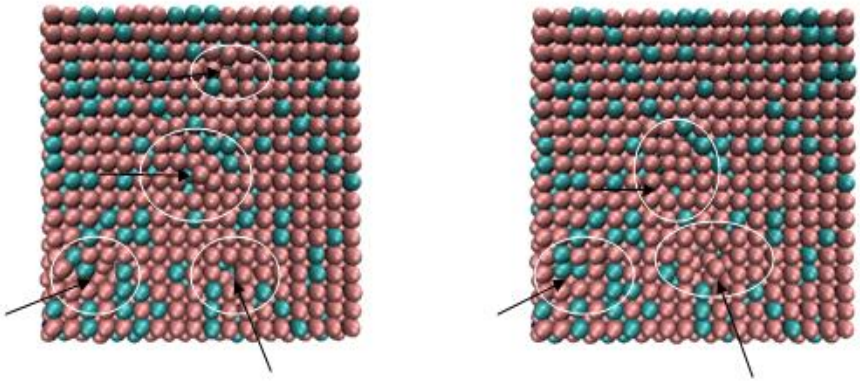

Fig.4.10.4.1 (a) Fig.4.10.4.1 (b)

Fig.4.10.4.1 (a) & Fig.4.10.4.1 (b) shows VMD snapshots of Fe-25%Cr alloys at temp.500 K.

In the above VMD snapshots circle region show the vacancy created by MD code and arrow indicates the movement of atoms during running the MD code. Purple color indicates Fe atoms and blue color indicates Cr atoms.

4.10.4.2 MSD calculation

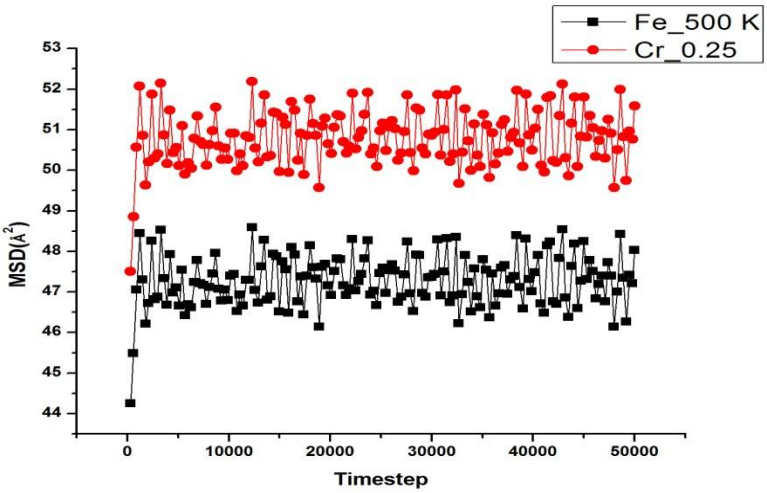

Fig.4.10.4.2 (a) MSD vs. Time step plot of Fe-25%Cr alloys at temp.500 K

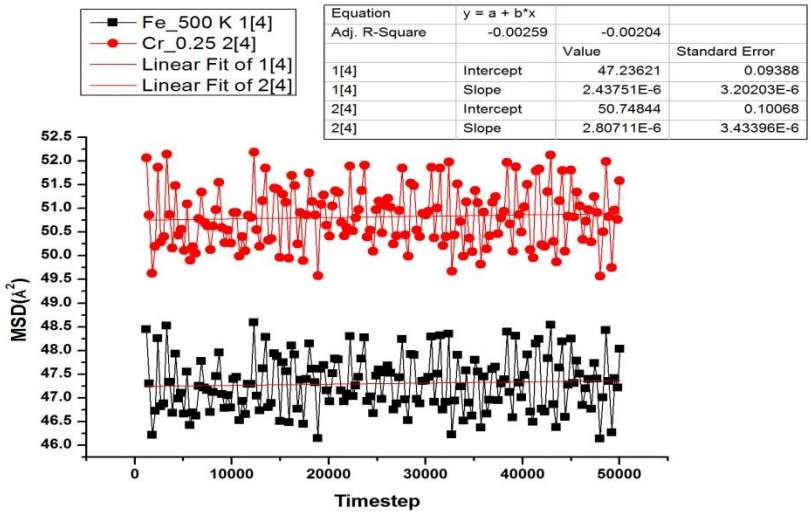

Fig.4.10.4.2 (b) MSD vs. Time step (self-diffusivity value of Fe-25%Cr alloys at temp.500 K)

Self diffusivity of Fe & Cr has been calculated from MSD vs. time step plots at temperature 500 K. Fig.4.10.4.2 (a) shows MSD vs. time step. The value of self diffusivity calculated from the diffusive region of the plot is shown in Fig. 4.10.4.2. (b)

4.10.5 Creation of Fe-25%Cr alloys at temperature 700 K

Simulation box size of dimension 50 $Å^3$ containing 11,600 atoms were generated by running MD code. The pattern of writing the code for creating Fe-25%Cr alloys sample equilibrated at 700 K is same as code written for Fe-5%Cr alloys equilibrated at 50 K mention in appendix II.

4.10.5.1 VMD snapshots

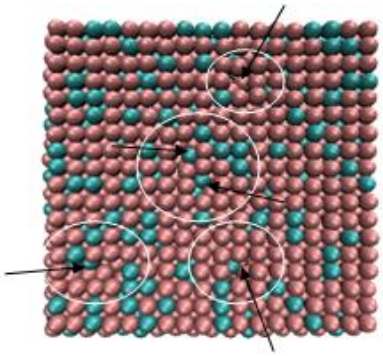

Fig.4.10.5.1 (a)

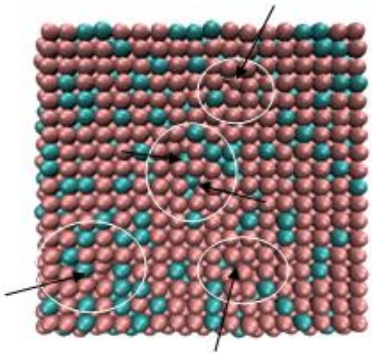

Fig.4.10.5.1 (b)

Fig.4.10.5.1 (a) & Fig.4.10.5.1 (b) shows VMD snapshots of Fe-25%Cr alloys at temp.700 K.

In the above VMD snapshots circle region show the vacancy created by MD code and arrow indicates the movement of atoms during running the MD code. Purple color indicates Fe atoms and blue color indicates Cr atoms.

4.10.5.2 MSD calculation

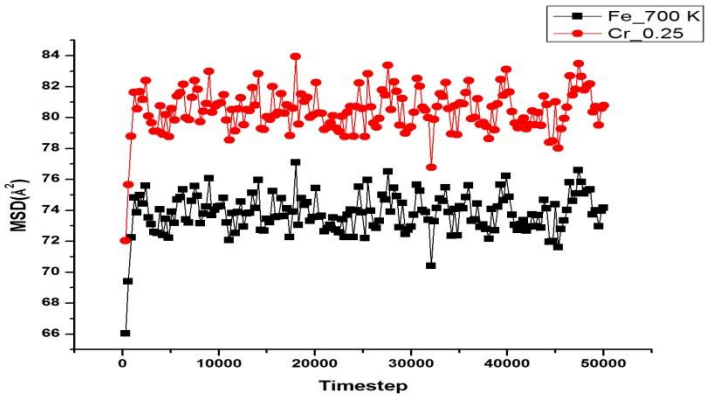

Fig.4.10.5.2 (a) MSD vs. Time step plot of Fe-25%Cr alloys at temp.700 K

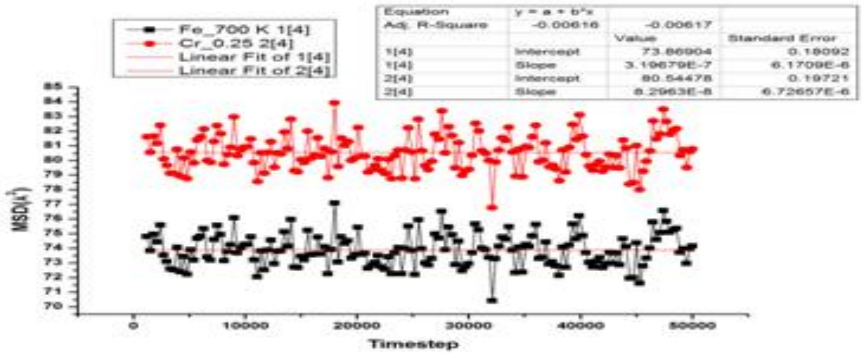

Fig.4.10.5.2 (b) MSD vs. Time step (self-diffusivity value of Fe-25%Cr alloys at temp.700 K)

Self diffusivity of Fe & Cr has been calculated from MSD vs. time step plots at temperature 700 K. Fig.4.10.5.2 (a) shows MSD vs. time step. The value of self diffusivity calculated from the diffusive region of the plot is shown in Fig. 4.10.5.2. (b)

4.10.6 Creation of Fe-25%Cr alloys at temperature 1000 K

Simulation box size of dimension 50 $Å^3$ containing 11,600 atoms were generated by running MD code. The pattern of writing the code for creating Fe-25%Cr alloys sample equilibrated at 1000 K is same as code written for Fe-5%Cr alloys equilibrated at 50 K mention in appendix II.

4.10.6.1 VMD snapshots

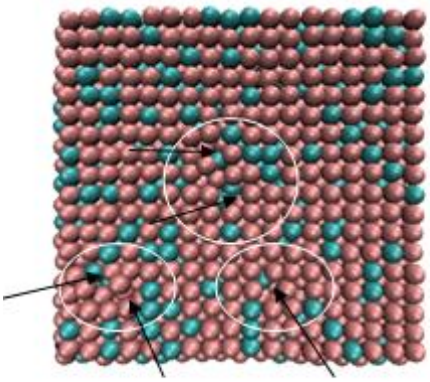

Fig.4.10.6.1 (a)

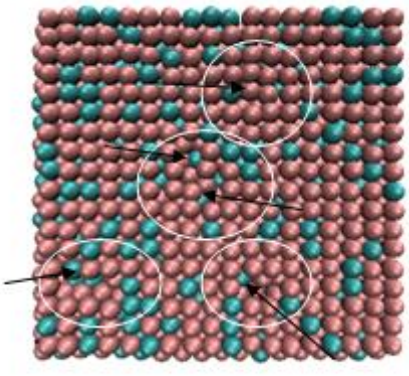

Fig.4.10.6.1 (b)

Fig.4.10.6.1 (a) & Fig.4.10.6.1 (b) shows VMD snapshots of Fe-25%Cr alloys at temp.1000 K.

In the above VMD snapshots circle region show the vacancy created by MD code and arrow indicates the movement of atoms during running the MD code. Purple color indicates Fe atoms and blue color indicates Cr atoms.

4.10.6.2 MSD calculation

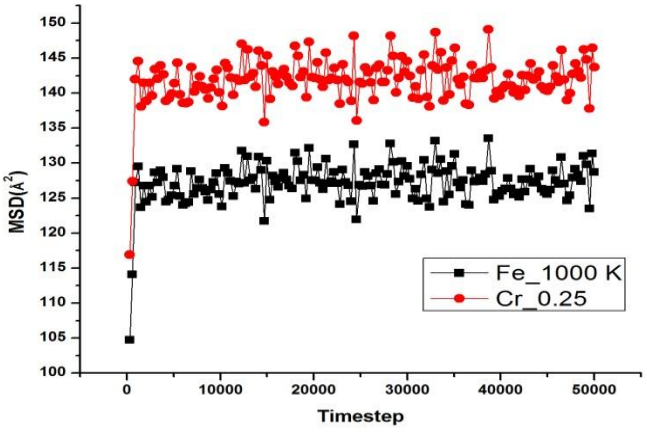

Fig.4.10.6.2 (a) MSD vs. Time step plot of Fe-25%Cr alloys at temp.1000 K

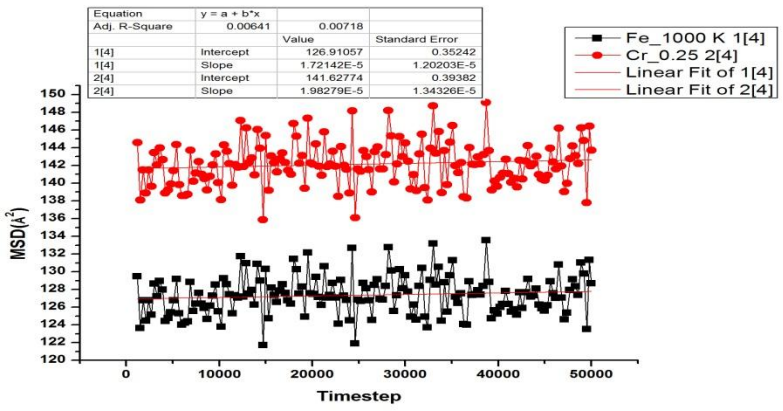

Fig.4.10.6.2 (a) MSD vs. Time step (self-diffusivity value of Fe-25%Cr alloys at temp.1000 K)

Self diffusivity of Fe & Cr has been calculated from MSD vs. time step plots at temperature 1000 K. Fig.4.10.6.2 (a) shows MSD vs. time step. The value of self diffusivity calculated from the diffusive region of the plot is shown in Fig. 4.10.6.2. (b)

All the diffusivity value calculated from MSD plots are tabulated shown in Table 4.2

Table 4.2: MSD values of Fe-Cr alloys with varying composition at various temperature

Temp. (in K)	MSD (m^2/s) value		MSD (m^2/s) value		MSD (m^2/s) value		MSD (m^2/s) value		MSD (m^2/s) value	
	Fe	5% Cr	Fe	10% Cr	Fe	15% Cr	Fe	20%Cr	Fe	25% Cr
50	7.28774 $\times10^{-16}$	9.88776 $\times10^{-16}$	4.38255 $\times10^{-15}$	4.3608 $\times10^{-15}$	8.70872 $\times10^{-16}$	7.05524 $\times10^{-16}$	4.32517 $\times10^{-16}$	5.5734 $\times10^{-16}$	1.40463 $\times10^{-16}$	8.33683 $\times10^{-17}$
100	2.96927 $\times10^{-16}$	8.28624 $\times10^{-16}$	2.17472 $\times10^{-15}$	3.18579 $\times10^{-15}$	1.50651 $\times10^{-15}$	1.86851 $\times10^{-15}$	-3.55634 $\times10^{-16}$	-5.3634 $\times10^{-16}$	1.48484 $\times10^{-15}$	1.54536 $\times10^{-15}$
300	1.4801 $\times10^{-14}$	1.58748 $\times10^{-14}$	5.34843 $\times10^{-15}$	5.61432 $\times10^{-15}$	1.16118 $\times10^{-14}$	1.006997 $\times10^{-14}$	4.95018 $\times10^{-15}$	4.884 $\times10^{-15}$	6.48741 $\times10^{-15}$	8.05405 $\times10^{-15}$
500	-1.2931 $\times10^{-15}$	1.09154 $\times10^{-15}$	1.44126 $\times10^{-14}$	1.49625 $\times10^{-14}$	-1.73582 $\times10^{-14}$	-16662 $\times10^{-14}$	1.11829 $\times10^{-14}$	1.0196 $\times10^{-14}$	2.43751 $\times10^{-14}$	2.80711 $\times10^{-14}$
700	4.85047 $\times10^{-14}$	5.04418 $\times10^{-16}$	-9.0485 $\times10^{-16}$	-9.9740 $\times10^{-14}$	-8.04042 $\times10^{-14}$	-8.13671 $\times10^{-14}$	1.84416 $\times10^{-13}$	2.06982 $\times10^{-13}$	3.19679 $\times10^{-15}$	8.2963× 10^{-16}
1000	-1.6400 $\times10^{-14}$	-5.9842 $\times10^{-14}$	2.21525 $\times10^{-13}$	2.01564 $\times10^{-13}$	8.61991 $\times10^{-14}$	8.42619 $\times10^{-14}$	1.82989 $\times10^{-13}$	2.11767 $\times10^{-13}$	1.72142 $\times10^{-13}$	1.98279 $\times10^{-13}$

CHAPTER 5

Conclusions

5.1. Conclusions

- Diffusivity value of pure Fe is lower at lower temperature (50 K,100 K), but diffusivity value increases linearly above 100 K temperature

- Diffusivity value of Fe-Cr alloys is also increases with increasing the Cr percentage at 300 K

- In some composition MSD value are coming negative, it is due to condition setup that are not fully adjustable

- Diffusivity value in Fe-25%Cr alloys Cr diffusivity value are increasing with respect to the Fe diffusivity values

5.2. Suggested research for future work

- Those diffusivity value are coming negative will be corrected by setting different condition

- Some of the mechanical properties will be investigated that are responsible for wear and damage through radiation

References

[1] M. A. Steicher, Stainless Steel: Past, Present, and Future, in Stainless Steel'77, R.Q. Barr, Ed., Climax Molybdenum Co., 1977, p 1-34

[2] Source book of Stainless Steels, American Society for Metals, 1976, p 107

[3] Metals Handbook, 8th ed., American Society for Metals, 1973

[4] I. Kaur, Y. Mishin, and W. Gust, Fundamentals of Grain and Interphase Boundary Diffusion (John Wiley & Sons, Chichester, New York, 1995).

[5] Y. Mishin, in Diffusion Processes in Advanced Technological Materials, edited by D. Gupta (William Andrew, Norwich, NY, 2005), p. 113.

[6] P. G. Lucasson and R. M. Walker, Phys. Rev. 127 (1962) 485–500.

[7] R. A. Johnson: Phys. Rev. 134 (1964) A1329–A1336.

[8] Katsuyuki Kusunoki, Materials Transactions, Vol. 47, No. 8 (2006) pp. 1906 -1909

[9] United States Subcommittee on Generation IV Technology Planning on a Technology Roadmap for Generation IV Nuclear Energy Systems. Report to Nuclear Energy Research Advisory Committee. Washington: Technical Roadmap Report, 2003.

[10] Ustinovshikov, Y., B. Pushkarev, and I. Igumnov. "Fe---rich portion of the Fe---Cr phase diagram: electron microscopy study." Journal of Materials Science 37: 2031---42 (2002).

[11] Iron--Chromium (Fe--Cr) Phase Diagram. 2009. http://www.calphad.com/iron---chromium.html (accessed 10 April 2010).

[12] A. Einstein, Ann. Phys. 17 (1905) 549.

[13] P.G. Shewmon, Diffusion in Solids, McGraw Hill, New York, 1963.

[14] Mikhail I. Mendelev *et al* PHYSICAL REVIEW B 80, 144111 (2009)

[15] G. J. Ackland, M. I. Mendelev, D. J. Srolovitz, S. Han, and A. V. Barashev, J. Phys.: Condens. Matter 16, S2629 _2004_

.

[16] Katsuyuki Kusunoki, Materials Transactions, Vol. 47, No. 8 (2006) pp. 1906 to 1909

[17] M. I. Haftel, T. D. Andreadis, J. V. Lill and M. Eridon: Phys. Rev. B42 (1990) 11540–11552.

[18] H. Chamati *et al* received 11 October 2005; accepted for publication 8 February 2006

[19] Y.Iijima and K.Hirano: Diffusion Process in Nuclear Materials, ed. By R.P.Agarwala, Elsevier Science Publisher B.V., (1992), 169-200.

[20] L. Malerba, D. Terentyev, P. Olsson, R. Chakarova,J. Wallenius, J. Nucl. Mater. 329 (2004) 1156.

[21] J.-H. Shim, H.-J. Lee, B.D. Wirth, J. Nucl. Mater. 351(2006) 56.

[22] D. Terentyev, L. Malerba, J. Nucl. Mater. 329(2004)1161.

[23] R. Chakarova, V. Pontikis, J. Wallenius, Delivery report WP6, SPIRE project, EC contract no. FIKW-CT-2000-00058 (June 2002), available at http:// www.neutron.kth.se/publications

[24] P. Olsson, L. Malerba, A. Almazouzi, SCK-CEN Report, BLG-950 (June 2003).

[25] R.A. Wolfe, H.W. Paxton, Trans. Metall. Soc. AIME 230(1964) 1426

[26] L.I.Ivanov and N.P.Ivanchev: Izvest.Akad.Nauk,Otdel.Tekh.Nauk, No.8(1958), 15-18

[27] D.Terentyev, L.Malerba, J. Nucl. Mater. 329-333 (2004) 1161-1165

[28] K.L. Wong, J. H. Shim, B.D. Wirth, J.Nucl. Mater.367-370 (2007) 276-281.

[29] Motohide Sugihara, Yoshihiro Yamazaki, Seiichi, Takaki, Kenji Abiko and Yoshiaki Iijima, Mat. Trans. JIM vol.41 No. 1(2000) 87-90.

[30] Rahman, A. Phys. Rev. (1964) A136, 405.

[31] Stillinger, F.H. and Rahman, (1974) A.J.Chem.Phys.60, 1545

[32] Kazutaka Fujita, Junji Ohgi, Vitek, Tao Zhang and Akihisa Inoue, Molecular Dynamics Simulation on Anelasticity under Tensile and Shearing Stresses in single Component Amorphous Metal, Materials Transactions. 2005,46: 2875-2879.

[33] Arthur F. Voter, Robert Averback, Stephen Foiles, Atomistic Simulation Methods, DOE panel on computational methods for fusion materials, march 31, 2004

[34] Wilfred Gunsteren and Herman Berendsen, Computer Simulation of Molecular Dynamics: Methodology, Applications, and Perspectives in Chemistry

[35] Michael P. Allen, Introduction to Molecular Dynamics Simulation, John von Neumann Institute for Computing, J ulich, NIC Series. 2004, 23: 1-28,

[36] Q. Spreiter and M Walter, Classical molecular dynamics simulation with the velocity verlet algorithm at strong external magnetic field

[37] M.S. Daw, M.I. Baskes. Phys. Rev. Lett. 50, 1285 (1983)

[38] M. S. Daw, M. I. Baskes. Embedded-atom method: Derivation and application to impurities, surfaces, and other defects in metals. Phys. Rev. B 29, 6443 - 6453 (1984)

[39] Mayur Suri, Phase-Transition Assisted Deposition of Passivated Nanospheres, Master thesis, Graduate School of the University of Minnesota.

[40] http://www.etomica.org/app/modules/sites/Ljmd/Background2.html

[41] http://people.cst.cmich.edu/petko1vg/isaacs/phys/msd.html

[42] www.matdl.org

[43] Haile, J.M., "Molecular Dynamics Simulation", John Wiley & Sons, Inc., New York, 1992.

[44] www.lammps. Sandia.gov

[45] Humphrey, W., Dalke, A., Schulten, VMD: Visual molecular dynamics, Journal of Molecular Graphics & Modelling.1996, 14: 33-38.

Appendix I

MD code written for Pure Fe-lattice & its MSD calculation

```
# this MD code is for obtaining 3d-crystal lattice of Fe at temperature 50k
units                   metal
echo                    both
atom_style              atomic
dimension               3
boundary                p p p
region                  box block 0 50 0 50 0 50  units box
create_box              1 box

lattice                 bcc 2.851
region                  Fe block 0 50 0 50  0 50 units box
create_atoms            1 region Fe units box
region                  Fe1  sphere 25.0   25.0   48.44   2  units box
group                   void1  region Fe1
delete_atoms            group void1
region                  Fe2  sphere 10.0   10.0   48.44   2  units box
group                   void2  region Fe2
delete_atoms            group void2
region                  Fe3  sphere 20.0   30.0   48.44   2  units box
group                   void3  region Fe3
delete_atoms            group void3
region                  Fe4  sphere 30.0   10.0   48.44   2  units box
```

```
group           void4  region Fe4
delete_atoms    group void4
region          Fe5  sphere 30.0   40.0   48.44   2  units box
group           void5  region Fe5
delete_atoms     group void5
region          Fe6  sphere 5.0   10.0   48.44   2  units box
group           void6  region Fe6
delete_atoms    group void6
timestep        0.002
pair_style      eam/fs
pair_coeff      * * Fe_mm.eam.fs Fe

# Energy Minimization
minimize        1.0e-7 1.0e-8 1000 10000

thermo          100
thermo_style    custom step temp  vol press pe ke etotal
dump            1 all custom 20 Fe_50k_crystal_void_dump.lammpstrj id type x y z vx vy vz
log             log2Fe_50k_crystal_void_s.data
velocity        all create 50 873847 rot yes mom yes dist gaussian
#fixes
fix             1 all nvt  temp  50  50  0.01
run             10000
unfix           1
```

After creating simulation box with Fe atoms filled inside it we go for calculating MSD value running the code given below:

 # msd calculation in Fe crystal at 50k file

```
units           metal
boundary        p p p
atom_style      atomic
read_data       Fe50k_void_data.txt
group           Fe type 1
timestep        0.002
pair_style      eam/fs
pair_coeff      * * Fe_mm.eam.fs Fe
# Energy Minimization
minimize        1.0e-4 1.0e-6 10000 1000000
velocity        all create 50 5812775 rot yes mom yes dist gaussian
# MSD Calculation
compute         1 Fe msd

dump            1 all atom 1000 dump.Fe_msd_50K_11643_3d.dump.lammpstrj
log             logFe_msd_50k_11643.data
fix             1 all npt temp 50.0 50.0 0.2 iso -1000.0 -1000.0 0.2
thermo          300
thermo_style    custom step temp press vol pe ke etotal c_1[4]
run             50000
```

****

Appendix II

MD code written for Fe-Cr alloy system & its MSD calculation

This MD code is for obtaining 3d-crystal lattice of Fe0.05Cr alloys with void at temperature 50k

```
units           metal
echo            both
atom_style      atomic
dimension       3
boundary        p p p
region          box block 0 50 0 50 0 50  units box
create_box      2 box
lattice         bcc 2.851
region          Fe block 0 50 0 50  0 50 units box
create_atoms    1 region Fe units box
set             region Fe type/fraction 2 0.05 12393

region          Fe1  sphere 25.0   25.0   48.44   2  units box
group           void1  region Fe1
delete_atoms    group void1
region          Fe2  sphere 10.0   10.0   48.44   2  units box
group           void2  region Fe2
delete_atoms    group void2
region          Fe3  sphere 20.0   30.0   48.44   2  units box
group           void3  region Fe3
delete_atoms    group void3
```

```
region          Fe4  sphere 30.0   10.0   48.44   2  units box
group           void4  region Fe4
delete_atoms    group void4
region          Fe5  sphere 30.0   40.0   48.44   2  units box
group           void5  region Fe5
delete_atoms     group void5
region          Fe6  sphere 5.0   10.0   48.44   2  units box
group           void6  region Fe6
delete_atoms    group void6
timestep        0.002
pair_style      eam/cd
pair_coeff      * * FeCr.cdeam Fe Cr

# Energy Minimization
minimize        1.0e-7 1.0e-8 1000 10000
thermo          100
thermo_style    custom step temp vol press pe ke etotal

dump            1 all custom 20 Fe5Cr_void_50k_s_dump.lammpstrj id type x y z vx vy vz
log             logFe5Cr_void_50k_s.data
velocity        all create 50 873847 rot yes mom yes dist gaussian
#fixes
compute         1 all rdf 100
fix             1 all ave/time 100 1 100 c_1 file FeCr.rdf mode vector
```

```
fix             2 all nvt temp 50 50 0.01
run             10000
unfix           2
```

After creating simulation box with Fe-Cr alloy atoms filled inside it we go for calculating MSD value running the code given below:

 # msd calculation of Fe0.05Cr crystal at temperature 50k in file

```
units           metal
boundary        p p p
atom_style      atomic
read_data       Fe5Cr_crystal_50k_data.txt
group           Fe type 1
group           Cr type 2
timestep        0.002
pair_style      eam/cd
pair_coeff      * * FeCr.cdeam Fe Cr

# Energy Minimization
minimize        1.0e-4 1.0e-6 10000 1000000

velocity        all create 50.0 5812775 rot yes mom yes dist gaussian

# MSD Calculation
compute         1 Fe msd
compute         2 Cr msd
```

dump	1 all atom 1000 dump.Fe5Cr_50k_3d_11643_msd.dump.lammpstrj
log	logFe5Cr_50k_crystal_msd_11643.data
fix	1 all npt temp 50.0 50.0 0.2 iso -1000.0 -1000.0 0.2
thermo	300
thermo_style	custom step temp press vol pe ke etotal c_1[4] c_2[4]
run	50000

****